

AD-A095 566

NEW MEXICO STATE UNIV LAS CRUCES PHYSICAL SCIENCE LAB

F/G 4/1

D-REGION ELECTRON DENSITY MEASUREMENTS OBTAINED BY PARTIAL REFL--ETC(U)

NOV 80 D MOTT, W GAMMILL, R VALDEZ

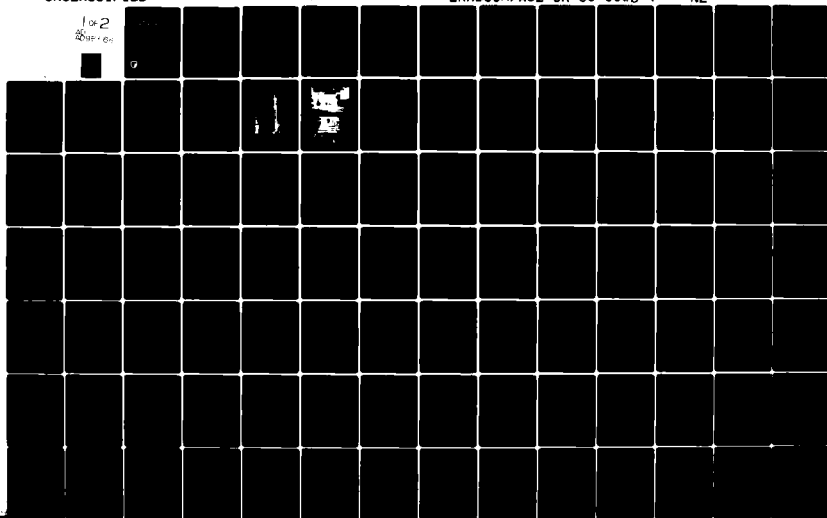
DAAD07-79-C-0008

UNCLASSIFIED

ERADCOM/ASL-CR-80-0008-4

NL

1 of 2
20 SEP 80



ASL-CR-80-0008-4

LEVEL

12

AD

Reports Control Symbol
OSD 1366

D-REGION ELECTRON DENSITY MEASUREMENTS OBTAINED BY PARTIAL REFLECTION TECHNIQUES

NOVEMBER 1980

Prepared by

D. MOTT
W. GAMMILL
R. VALDEZ

Physical Science Laboratory
New Mexico State University
Las Cruces, New Mexico 88003

UNDER CONTRACT: DAAD07-79-C0008

Contract Monitor: Robert Olsen

Approved for public release; distribution unlimited

DDC FILE COPY



US Army Electronics Research and Development Command
ATMOSPHERIC SCIENCES LABORATORY
White Sands Missile Range, NM 88002

81 2 26 047

NOTICES

Disclaimers

The findings in this report are not to be construed as an official Department of the Army position, unless so designated by other authorized documents.

The citation of trade names and names of manufacturers in this report is not to be construed as official Government indorsement or approval of commercial products or services referenced herein.

Disposition

Destroy this report when it is no longer needed. Do not return it to the originator.

1. REF ID: A5L

SECURITY CLASSIFICATION OF THIS PAGE (When Data Entered)

19 REPORT DOCUMENTATION PAGE		READ INSTRUCTIONS BEFORE COMPLETING FORM
1. REPORT NUMBER ASL-CR-80-0008-4	2. GOVT ACCESSION NO. AD-A095 566 (9)	3. RECIPIENT'S CATALOG NUMBER
4. TITLE (and Subtitle) D-REGION ELECTRON DENSITY MEASUREMENTS OBTAINED BY PARTIAL REFLECTION TECHNIQUES.	5. TYPE OF REPORT & PERIOD COVERED R&D Final Report	6. PERFORMING ORG. REPORT NUMBER
7. AUTHOR(s) D. Mott / W. Gammill / R. Valdez	8. CONTRACT OR GRANT NUMBER(s)	
9. PERFORMING ORGANIZATION NAME AND ADDRESS Physical Sciences Laboratory New Mexico State University Las Cruces, New Mexico 88003	10. PROGRAM ELEMENT, PROJECT, TASK AREA & WORK UNIT NUMBERS DA Task DAAD07-79-C0008	
11. CONTROLLING OFFICE NAME AND ADDRESS US Army Electronics Research and Development Command Adelphi, MD 10783	12. REPORT DATE November 1980	13. NUMBER OF PAGES 125
14. MONITORING AGENCY NAME & ADDRESS (if different from Controlling Office) Atmospheric Sciences Laboratory White Sands Missile Range, NM 88002	15. SECURITY CLASS. (of this report) UNCLASSIFIED	15a. DECLASSIFICATION/DOWNGRADING SCHEDULE
16. DISTRIBUTION STATEMENT (of this Report) Approved for public release; distribution unlimited.		
17. DISTRIBUTION STATEMENT (of the abstract entered in Block 20, if different from Report)		
18. SUPPLEMENTARY NOTES Robert Olsen, Contract Monitor		
19. KEY WORDS (Continue on reverse side if necessary and identify by block number) D-region HE propagation Electron densities Refractive index Partial reflection sounder Ionosphere		
20. ABSTRACT (Continue on reverse side if necessary and identify by block number) D-region electron densities are derived utilizing a ground based partial reflection sounder. The sounder frequency is approximately 2 MHz, with right-hand and left-hand polarized pulses transmitted vertically. This report describes the sounder system hardware and the necessary software to derive electron densities from the returned vertical pulses. A complete set of		

20. ABSTRACT (cont)

schematics of the electronics, antenna array and operational are included. A total of 604 electron density profiles have been reduced with the sounder located at White Sands Missile Range (WSMR) and at Red Lake, Canada, as part of the 1979 solar eclipse field program. The WSMR profiles have been summarized into monthly profiles. The electron densities derived from utilizing the partial reflection technique appear to be within the expected ranges for D-region profiles.

Accession For	<input checked="" type="checkbox"/>
NTIS GPO	<input type="checkbox"/>
DTIC TAB	<input type="checkbox"/>
Unannounced	<input type="checkbox"/>
Justification	<input type="checkbox"/>
By	
Distribution	
Availability	
Dist	A

CONTENTS

SECTION

1.	Theory of the partial reflection experiment.	7
2.	Experimental procedure	12
3.	System description	14
4.	Antenna installation	25
5.	System operation	29
6.	Data processing.	35
7.	An alternate procedure for data processing	49
8.	Results.	53

REFERENCES	76
----------------------	----

APPENDIX

I.	Circuit diagrams	77
II.	Data averaging computer program	107
III.	Solar Zenith angle	115
IV.	Receiver calibration	120
V.	Polynomial approximations for $C_{3/2}(x)$ and $C_{5/2}(x)$	124

LIST OF FIGURES

3.1	Partial reflection sounder, block diagram	15
3.2A	Exterior photograph of van.	16
3.2B	Interior photographs of van	17
3.3	Phases for transmitting with circular polarization.	19
3.4	Phases for receiving with circular polarization	21
4.1	Dipole antenna element.	25
4.2	Antenna array, plan view.	26
4.3	Antenna matching calibration setup.	28
5.1	Receiver calibration setup.	33
6.1	Accumulation logic for data averaging	36
6.2	Output of averaging program	39
6.3	Procedures used in standard data processing	44
6.4	Example result, standard data processing.	48
7.1	Example result, non-standard data processing.	52
8.1	Key to electron density profiles.	54
8.2	WSMR data averages, September 1977.	65
8.3	WSMR data averages, October 1977.	66
8.4	WSMR data averages, November 1977	67
8.5	WSMR data averages, December 1977	68
8.6	WSMR data averages, January 1978.	69
8.7	WSMR data averages, February 1978	70
8.8	WSMR data averages, March 1978.	71
8.9	WSMR data averages, April 1978.	72
8.10	WSMR data averages, August 1978	73
8.11	WSMR data averages, July 1978	74
8.12	Electron density vs. time; solar eclipse of February 1979 . . .	75
AIII-1	Solar zenith angle triangle	115
AIII-2	Solar zenith angle computer program	116

LIST OF TABLES

5.1	Computer bootstrap procedure.	31
6.1	Amplitude calculations.	42
6.2	Tabulated functions $R(h)$ and $G(h)$	45
6.3	Specifications for Table 6.2.	46
7.1	Tabulated functions $E(h)$ and $U(h)$	51
8.1	Run index for WSMR, 1975.	56
8.2	Run index for WSMR, 1977-1979	57
8.3	Run index for Balmertwon, Canada, 1979.	63
AIII-1	Base values for zenith angle calculations	119
AIV-1	Typical receiver calibration data	121
AIV-2	Tabulated receiver calibration.	123

SECTION 1

Theory of the Partial Reflection Experiment

This experiment is designed to measure the density of free electrons in the ionosphere as a function of altitude, in the D region below 100 kilometers.* A radar operating at a frequency of several megahertz transmits short pulses of radiation vertically, and echoes are partially reflected (backscattered) from the free electrons in the lower ionosphere. Echo strength vs. time (with time a measure of altitude) is digitized and recorded on magnetic tape.

Circular polarization of the electromagnetic radiation, both right-hand and left-hand polarization, is utilized. Several pulses are transmitted and received in right-hand polarization, and the next several pulses are transmitted and received in left-hand polarization.

Because of the earth's magnetic field, the index of refraction of the ionosphere is different for the two polarization modes. This difference leads to different coefficients of reflection and absorption of the radio waves. The mode for which absorption and reflection is less is called the ordinary mode, while the other is called the extraordinary mode. The differences in the absorption and reflection provide the key to measuring electron density.

It is assumed that the amplitude A_m (m is an index to identify polarization mode) of an echo partially reflected from the ionosphere, from altitude h above the station, is related to an ionospheric reflection coefficient R_m and absorption coefficient K_m as follows:

$$A_m(h) \propto R_m(h) e^{-2 \int_0^h K_m(y) dy}$$

As shown below, K_m at any altitude is proportional to the density N of free electrons at that altitude; i.e., $K_m = F_m N$, where F_m is the proportionality factor.

*It is also known as the differential absorption experiment. Reference (1) contains an excellent review of the theory.

When circularly polarized waves of both the ordinary (o) mode and the extraordinary (x) mode are transmitted at equal power, then

$$\left[\frac{A_x}{A_o} \right]_h = \left[\frac{R_x}{R_o} \right]_h e^{-2 \int_0^h [F_x - F_o]_y N(y) dy}$$

This equation is solved for N:

$$N(h) = \frac{1}{2[F_x - F_o]_h} \frac{d}{dh} \left[\ln \frac{R_x/R_o}{A_x/A_o} \right] \quad (1.1)$$

Equation (1.1) may serve as the basis for reducing data from the partial reflection experiment. In this case, the function A_x/A_o vs. altitude is the input data, while functions R_x/R_o and $[F_x - F_o]$ are precomputed from theoretical relationships. The reader should note that, in Equation (1.1), the mathematical operations performed on the data are such that, under some conditions, a small fractional uncertainty in A_x or A_o may result in a large fractional uncertainty in N.

According to Sen and Wyller (2), and in the longitudinal approximation (direction of propagation parallel to the earth's magnet field lines), the square of the ionosphere's index of refraction, as a function of altitude, is this:

$$n_{\pm}^2 = 1 - \frac{\omega_p^2}{\omega^2} \left[y_{\pm} C_{\frac{3}{2}}(y_{\pm}) + i \frac{5}{2} C_{\frac{5}{2}}(y_{\pm}) \right] \quad (1.2)$$

'+' corresponding to ordinary circular polarization of the electromagnetic radiation, and '-' to the extraordinary polarization. Equation (1.2) contains these terms:

$$y_{\pm} \equiv \frac{\omega \pm \omega_H}{\nu}$$

$$\omega_N = \sqrt{\frac{Ne^2}{\epsilon_0 m}}$$

plasma frequency, radians/sec

$N(h)$

density of free electrons at altitude h

e

electron charge

m

electron mass

ϵ_0

permittivity of free space

ω

signal frequency, radians/sec

$$\omega_H = \frac{eB}{m}$$

gyromagnetic frequency, radians/sec (assumed constant over altitudes of interest)

B

earth's magnetic field intensity

$\nu(h)$

rate, in collisions per second, at which free electrons at altitude h , having the most probable energy, collide with other particles

$$C_p(\alpha) \equiv \frac{1}{p!} \int_0^{\infty} \frac{\epsilon^p e^{-\epsilon}}{\alpha^2 + \epsilon^2} d\epsilon$$

See Appendix V for numerical approximations of this integral.

It is well known that the reflection coefficient for the ionosphere is proportional to the fractional variation in n , i.e., $R \propto \delta n/n$. There is general agreement among investigators that variations in n are proportional to variations in electron density, and that n is relatively independent of variations in other parameters of the ionosphere. Accordingly, $\delta n \propto \delta N$ is assumed. From Equation (1.2) it then follows that

$$R_m \propto - \frac{\delta N}{n_m^2 \nu} \left[y_m C_{\frac{3}{2}}(y_m) + i \frac{5}{2} C_{\frac{5}{2}}(y_m) \right]$$

In the partial reflection experiment, only the absolute value of the reflection coefficient has physical significance. And in the D region of the ionosphere, n_+ and n_- both have approximately unit value. Thus, the function R_x/R_0 in Equation (1.1) may be evaluated from this expression:

$$R(h) \equiv \frac{|R_x|}{|R_0|} = \left\{ \frac{[y_- C_{\frac{3}{2}}(y_-)]^2 + [\frac{5}{2} C_{\frac{5}{2}}(y_-)]^2}{[y_+ C_{\frac{3}{2}}(y_+)]^2 + [\frac{5}{2} C_{\frac{5}{2}}(y_+)]^2} \right\}^{\frac{1}{2}} \quad (1.3)$$

The ionosphere's index of refraction has a real part (μ) and an imaginary part (χ); i.e., $n = \mu - i\chi$. The imaginary part is proportional to the absorption coefficient: $K = \frac{\omega}{c} \chi$. Now $n^2 = (\mu^2 - \chi^2) - i2\mu\chi$, and so by comparing this expression with Equation (1.2) we see that

$$K_m = \frac{\omega_N^2}{c\nu} \frac{5}{4} C_{\frac{5}{2}}(y_m) \equiv N F_m, \quad ,$$

where $\mu_m \sim 1$ has been assumed. Thus, the function $2(F_x - F_0)$ in Equation (1.1) may be evaluated from this equation:

$$G(h) \equiv 2(F_x - F_0) = \frac{5}{2} \frac{e^2}{\epsilon_0 m c \nu} \left[C_{\frac{5}{2}}(y_-) - C_{\frac{5}{2}}(y_+) \right] \quad (1.4)$$

Flood (3) has developed an improved approximation for index of refraction that is comparable to the Sen Wyller longitudinal approximation of Equation (1.2), but that is more accurate when the propagation is not strictly longitudinal. His expression corresponding to Equation (1.2) is this:

$$n_{\pm}^2 = 1 - \frac{\omega_N^2}{\omega\nu} \left\{ A \left[y_{\pm} C_{\frac{3}{2}}(y_{\pm}) + i \frac{5}{2} C_{\frac{5}{2}}(y_{\pm}) \right] \right. \\ + B \left[y_{\mp} C_{\frac{3}{2}}(y_{\mp}) + i \frac{5}{2} C_{\frac{5}{2}}(y_{\mp}) \right] \\ \left. + D \left[y C_{\frac{3}{2}}(y) + i \frac{5}{2} C_{\frac{5}{2}}(y) \right] \right\} \quad (1.2A)$$

where

$$y = \frac{\omega}{\nu}$$

$$A = \cos^2 \frac{\phi}{2} - \frac{1}{4} \sin^2 \phi$$

$$B = \sin^2 \frac{\phi}{2} - \frac{1}{4} \sin^2 \phi$$

$$D = \frac{1}{2} \sin^2 \phi, \quad ,$$

with ϕ the angle between the magnetic field lines and the direction of propagation (which is vertical in our case). All other terms here are the same as in Equation (1.2). Note that Equation (1.2A) reduces to Equation (1.2) in the special case $\phi = 0$.

One progresses from Equation (1.2A) to the corresponding new functions for $R(h)$ and $G(h)$ using the same logic as that leading from Equation (1.2) to Equations (1.3) and (1.4). Results are as follows:

$$R(h) = \left\{ \frac{[A y_- C_{\frac{3}{2}}(y_-) + B y_+ C_{\frac{3}{2}}(y_+) + D y C_{\frac{3}{2}}(y)]^2 + (\frac{s}{2})^2 [A C_{\frac{5}{2}}(y_-) + B C_{\frac{5}{2}}(y_+) + D C_{\frac{5}{2}}(y)]^2}{[A y_+ C_{\frac{3}{2}}(y_+) + B y_- C_{\frac{3}{2}}(y_-) + D y C_{\frac{3}{2}}(y)]^2 + (\frac{s}{2})^2 [A C_{\frac{5}{2}}(y_+) + B C_{\frac{5}{2}}(y_-) + D C_{\frac{5}{2}}(y)]^2} \right\}^{\frac{1}{2}} \quad (1.3A)$$

$$G(h) = \frac{s}{2} \frac{e^2}{\epsilon_0 m c \nu} \left[A C_{\frac{5}{2}}(y_-) + B C_{\frac{5}{2}}(y_+) - A C_{\frac{5}{2}}(y_+) - B C_{\frac{5}{2}}(y_-) \right] \quad (1.4A)$$

In summary, the reduction of partial-reflection data utilizes Equation (1.1) to convert the ratios (vs. altitude) of the measured amplitudes of extraordinary and ordinary echoes, A_x/A_0 , into an electron density vs. altitude profile. Equation (1.1) requires, in addition to the amplitude ratios, precomputed functions $R(h)$ and $G(h)$ from Equations (1.3A) and (1.4A). These functions are evaluated using either an experimental or theoretical profile of collision frequency $\nu(h)$, and an experimental or theoretical value of the gyromagnetic frequency ω_H at D-region altitude. Using the $R(h)$ and $G(h)$ notation from Equations (1.3) and (1.4), Equation (1.1) may be written in this form:

$$N = \frac{1}{G} \frac{d}{dh} \left[\ln \frac{R}{A_x/A_0} \right] \quad (1.5)$$

Tabulations of $R(h)$ and $G(h)$ used in this study are given in Table 6.2.

SECTION 2

Experimental Procedure

In practice, the amplitudes A_x and A_o (vs. altitude) of the extraordinary and ordinary echoes that are used in Equation (1.5) are average values. Echo amplitudes are subject to rapid, random fluctuation (4), and if one were to use in Equation (1.5) echo amplitudes from single measurements, the result would not be statistically significant. The time of a typical "run" of the experiment is 10 minutes, and the averages extend over such a time interval. Electron density in the lower ionosphere is generally a function of solar zenith angle, and the change in this angle over a 10-minute period is negligible.

The partial-reflection transmitter operates at a pulse repetition frequency of about 17 pulses per second, and so a great deal of data is accumulated in the course of a run. All of this data is recorded on magnetic tape for subsequent analysis.

Eight consecutive pulses from the transmitter form the basic pattern of system operation, which is under computer control. During the first 4 pulses, transmission and reception is done in the ordinary mode, and during the second 4 pulses, in the extraordinary mode. During each group of 4 pulses, receiver attenuation is increased in steps, with no attenuation for the first pulse, one unit of attenuation for the second pulse, two units for the third, and three units for the fourth. The operator selects the unit of attenuation here, which may be either 6, 9, or 12 dB.

Four levels of receiver attenuation are used to insure that some echoes from the altitude region of interest are in the range of receiver sensitivity; above the noise level but below the saturation level. In addition to the 4 stepped levels of attenuation, the operator can add fixed attenuation at the receiver input, and this increases the attenuation at all levels by the same amount. As an example, suppose that the unit of attenuation for the stepping is selected to be 6 dB. Then the four levels of stepped attenuation are 0,

6 dB, 12 dB, and 18 dB. But if the operator selects a fixed value of attenuation of 10 dB, then the net attenuation in the 4 steps is 10 dB, 16 dB, 22 dB, and 28 dB.

The echo from each pulse is "stretched" because of the partial reflections that occur from all altitudes in the lower ionosphere. That is, the extent in time of the echo is much greater than that of the transmitted pulse, and, in fact, the shape of the echo pulse is the information of interest. Each echo is digitized for recording on magnetic tape so that the amplitude functions $A_x(h)$ and $A_o(h)$ may be determined. The current digitizer is a 6-bit (only) device, so each value is an integer between 0 and 63.

The transmitted pulse has a time duration of 20×10^{-6} sec, making its spatial extent 6 kilometers (pulse time multiplied by the speed of light). It follows that the echoes being received at one instant may have been reflected from anywhere within a zone 3 kilometers thick, and variations in electron density with altitude that occur on a scale smaller than this will not be detected. Accordingly, each echo is digitized at a sample rate corresponding to a separation distance Δh of 2 km between samples, and 30 samples per echo are recorded. Thus echo information from an altitude interval of 60 km is recorded. The base of this altitude interval is selected by the operator so that the "leading edge" of the echoes is always sampled. The lower altitude is set typically to between 50 and 60 kilometers. If 50 km is chosen, then the first echo sample corresponds to return (if any) from 50 km (with altitude uncertainty determined by pulse width), and the 30th and last sample corresponds to return from 110 km. Results from the partial reflection experiment are generally not reliable above about 90 km due to the fact that most of the transmitted energy tends to be absorbed or reflected at lower altitudes, especially in the extraordinary mode.

SECTION 3

System Description

In this section, the components of the partial reflection sounder are described. The block diagram of the system is given in Figure 3.1. Electronic equipment is mounted in a mobile van, views of which are shown in Figure 3.2.

3.1. Power Supply and Relay Drivers

This unit supplies ± 5 Vdc and ± 15 Vdc to the control logic. The -5 V level provides a negative-logic capability not presently used. The power supply also provides -24 Vdc to the relay drivers that control antenna polarization.

3.2. Control Logic

The control logic unit is the source of all commands to the transmitter and receiver.

The following parameters are selected by the operator using the control unit:

<u>Parameter</u>	<u>Normal Value</u>
pulse repetition frequency, 17, 12, or 8 pps	17 pps
pulse width	20 microseconds
sample starting height	between 50 and 60 km
attenuation stepping unit, 6, 9, or 12 dB	6 dB
Antenna polarization	O and X mode

Switches on the control-unit panel are used to enter status information (date, time, etc.) that is recorded, along with data, on the magnetic tape.

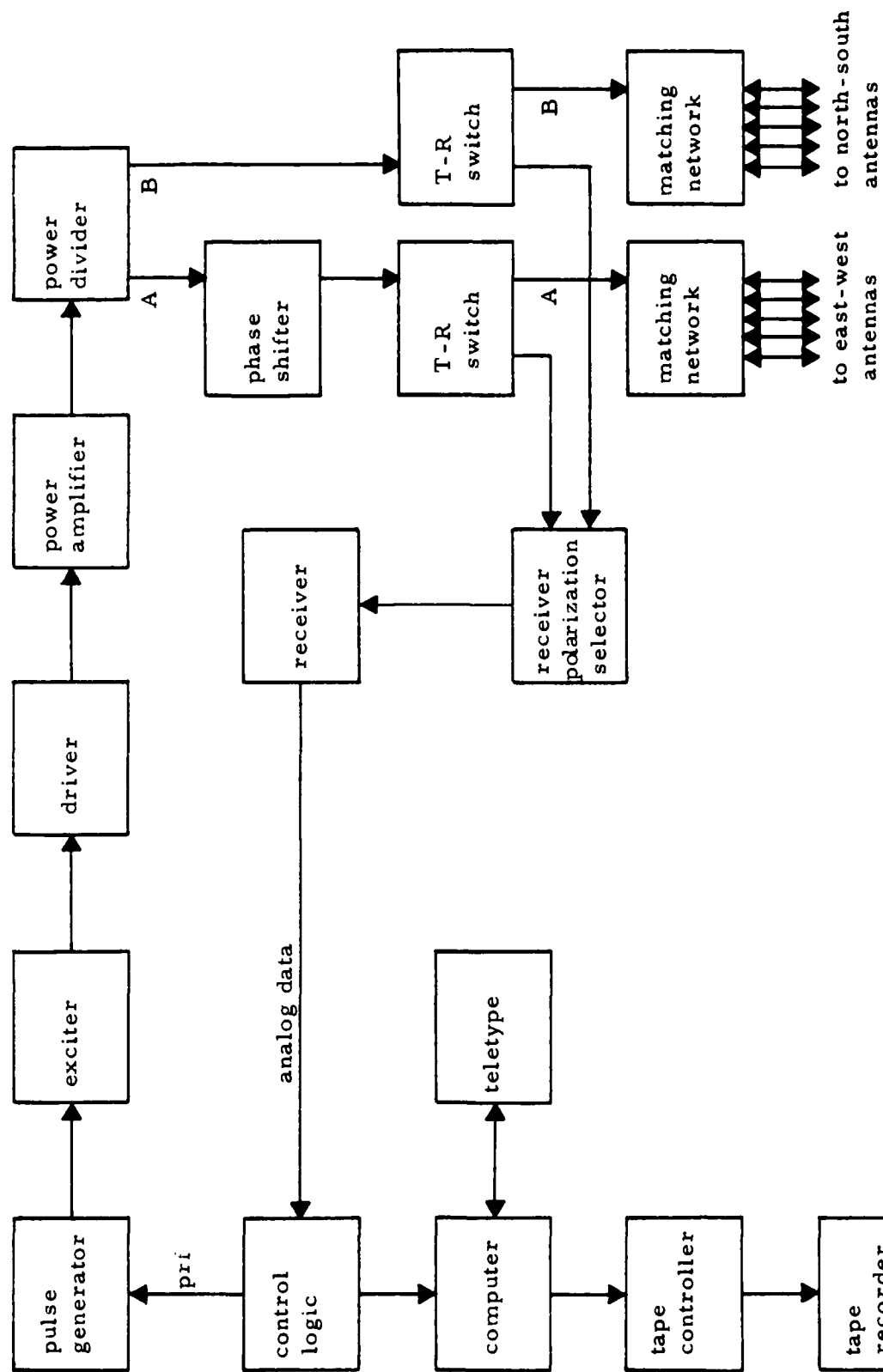


Figure 3.1. Partial reflection sounder block diagram.



Figure 3.2A. The partial reflection sonar van.



Figure 3.2B. The partial reflection sounder van. Interior views.

3.3. Pulse Generator

The pulse generator is used, under normal conditions, only to amplify the prf waveform from the control logic. Normal output level is approximately 40 volts peak to peak, which is sufficient to drive the class C exciter. The generator is manufactured by E-H Research Laboratory, model 131.

3.4. Transmitter

The transmitter is divided into three parts; exciter, driver, and power amplifier. Each part operates with class C bias. Four switches control transmitter power, as follows:

- S1 - filament voltage to exciter and driver;
- S2 - high voltage to exciter;
- S3 - filament voltage to power amplifier (P.A.);
- S4 - high voltage to driver and P.A.

Normal operating plate voltage on the P.A. is 12.5 kV. A variac is used to set this voltage level. With 12.5 kV on the plates, the P.A. screens receive 2.7 kV.

There is a 90-sec electronically-controlled delay after P.A. filaments are turned on, before the P.A. high voltage can be turned on. It is advisable to let the P.A. filaments warm up at least 3 minutes before the high voltage is applied.

Transmitter peak output is approximately 135 kW, with the 12.5 kV plate voltage.

3.5. Power Divider

This unit divides the transmitter power output into two parts, A and B, and selects between ordinary (O) and extraordinary (X) modes for transmitting with circular polarization. Mode selection is determined by the control logic. During O transmission, both the A and B components are shifted -90° with respect to the signal from the P.A. During X transmission, the shifts are $+90^\circ$ for A and -90° for B. See Figure 3.3.

O Polarization

transmitter output



X Polarization

transmitter output

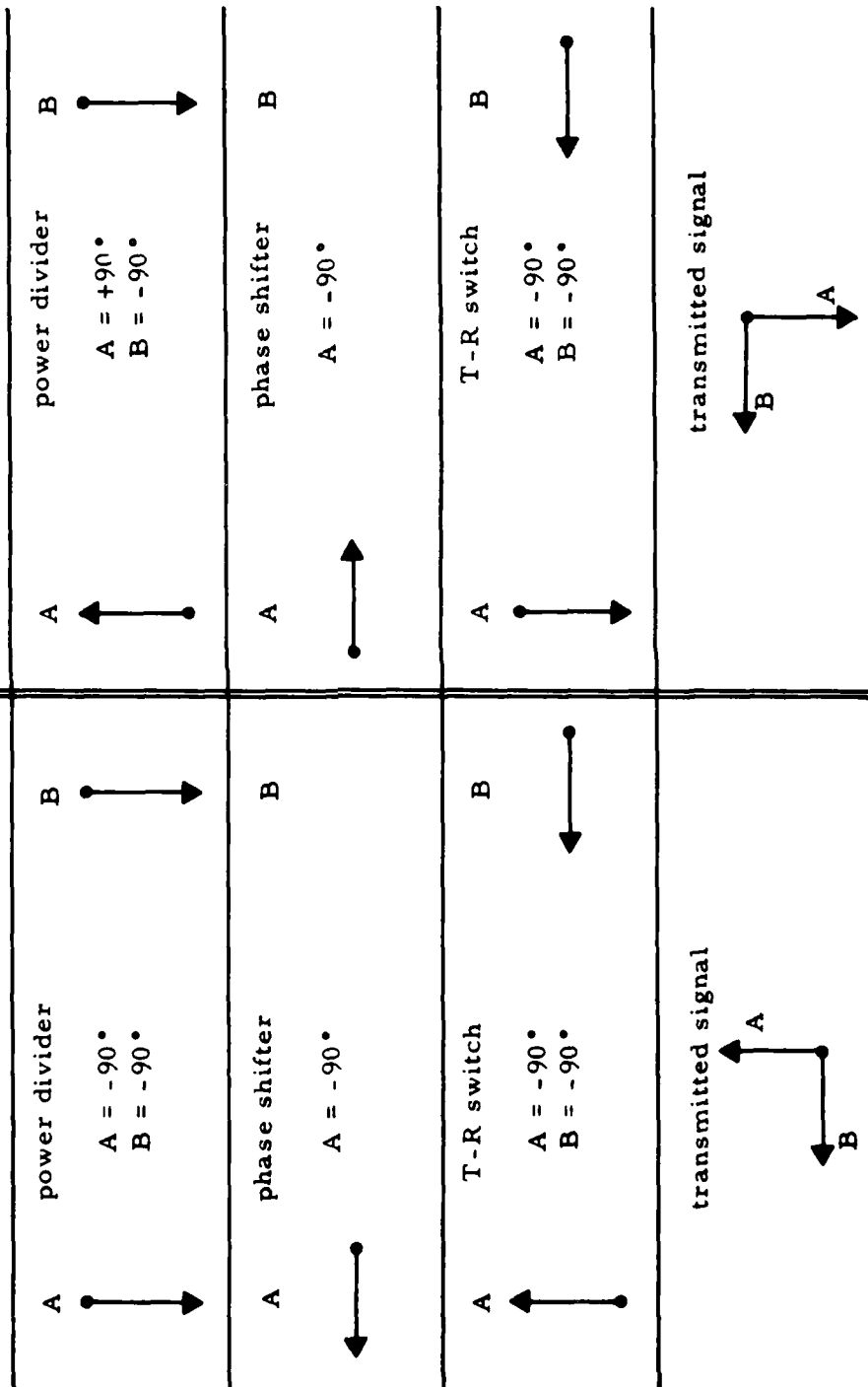


Figure 3.3. Phases for transmitting with circular polarization.

3.6. Phase Shifter

The phase shifter acts only on the A component from the power divider. For transmitting in either the O or X modes of circular polarization, it shifts the A component by another -90° . For transmitting with linear polarization, it gives no shift to the A component. See Figure 3.3 for details. Mode selection is determined by the control logic.

3.7. Transmit and Receive (T-R) Switch

The T-R switch effectively connects the antennas in the array to the transmitter when it is transmitting, and to the receiver at other times. All signals thru the T-R switch are shifted in phase by -90° . As noted, the T-R must normally pass 135 kW of power during transmission. A monitor circuit in the T-R circuit provides samples of the A and B components for monitoring transmitter performance. Monitor outputs are approximately 55 volts peak to peak.

3.8. Matching Network Box

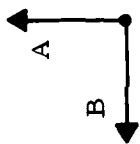
There are two matching-network boxes, one for each of the two T-R switches. The five antenna elements aligned in the east-west direction are connected to box A, and the five north-south elements are connected to box B. The antennas, with impedance 50 ohms each, are connected in parallel to the outputs of the matching network boxes, thus providing a net load impedance of 10 ohms for each of the two boxes. The matching network matches, in both cases, the 50 ohm impedance of the transmission line from the T-R switch to the 10 ohm impedance of a five-antenna load.

3.9. Receiver Polarization Selector

The echo signal received by the antennas passes thru the A and B matching network boxes and T-R switches to the receiver polarization selector. The selector has two input ports, A and B, and two output ports. As noted above, the phases of the A and B signals are both shifted by -90° in the T-R switches. If, for reception, the antenna array is to be circularly polarized, the receiver polarization selector adds a phase shift of $+90^\circ$ to signal A; and no shift for linear polarization. See Figure 3.4.

O Polarization

received signal



X Polarization

received signal

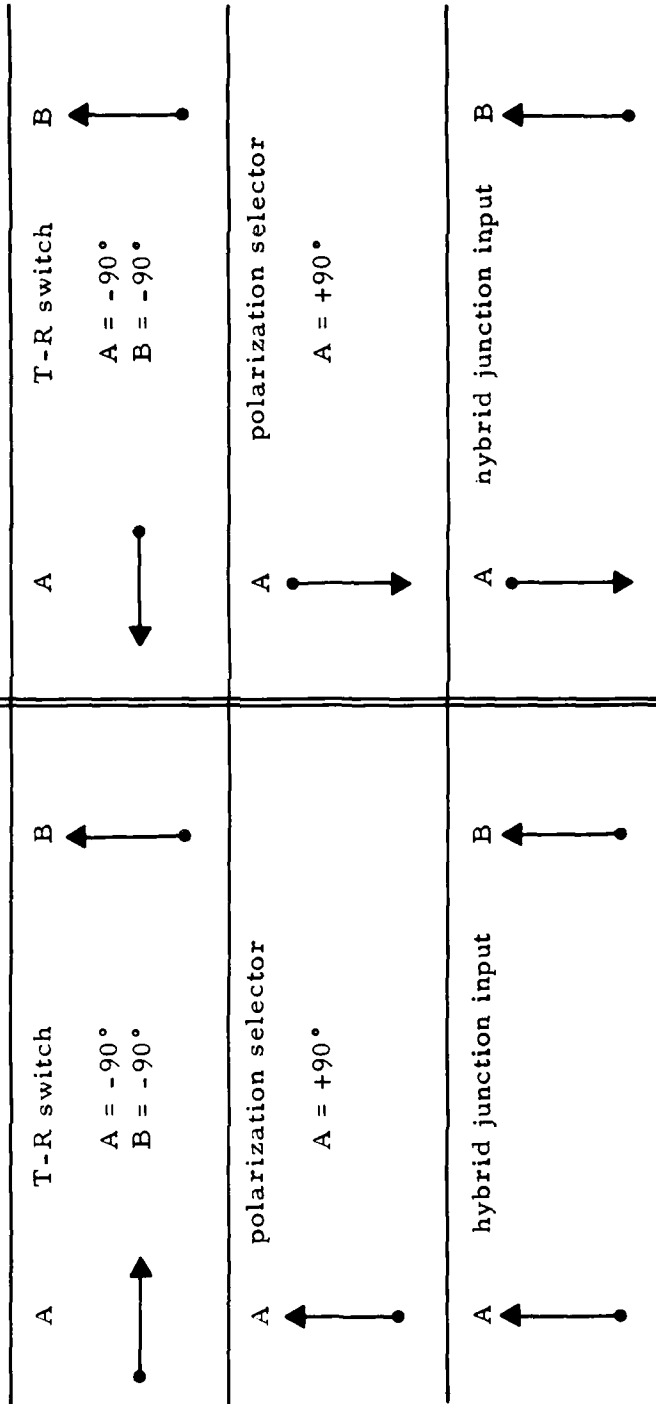
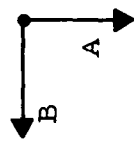


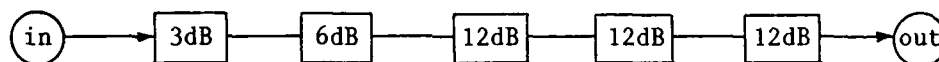
Figure 3.4. Phases for receiving with circular polarization.

The output ports are ports 2 and 4 of a 4-port hybrid junction. Signals A and B are applied to ports 3 and 1 of the hybrid, respectively. In the 0 mode of reception, signals at ports 3 and 1 are in phase, and the output is at port 2. In the X mode, signals at ports 3 and 1 are out of phase, and the output is at port 4. In either case, the non-used output port (2 or 4) is terminated with a 47 ohm resistor. Relays K3 and K4 select the appropriate output port. Control of the receiving polarization mode, circular or linear, and 0 and X selection for circular polarization, is performed by the control logic.

The output of the receiver polarization selector passes through two Hewlett-Packard attenuators in series that can be set over the ranges 0-12 dB and 0-120 dB, respectively. Appropriate values of fixed attenuation are selected during normal operation and during system calibration. (See Section 5 for details.)

3.10. Receiver

The incoming signal from the two fixed attenuators passes through a series of stepping attenuators. The potential sequence of attenuators is as shown:



Relays determine which of these attenuators is in the series at any moment, and control of the relays is performed by the control logic. The operator can select one of three patterns for the stepped attenuation. If the 6 dB pattern is selected, the net attenuation of the series is stepped through values of 0, 6, 12, and 18 dB. If the 9 dB pattern is selected, the stepped values are 0, 9, 18, and 27 dB; and for the 12 dB pattern, values are 0, 12, 24, and 36 dB. Output of the stepping attenuators is fed to the rf amplifier of the receiver.

The rf amplifier, at the front end of the receiver, has a low or high gain mode, switch controlled. The gain control switch sets the bias on the rf amplifying transistors. The gain can also be controlled remotely, via a cable connected to the back panel: Terminating the cable with either an open or a short sets the gain remotely.

Receiver i.f. is 1.50 MHz, and the local oscillator is set to 1.50 MHz below the rf frequency to be received. The i.f. gain can be controlled by a trimpot located on the front panel. Both the rf and i.f. amplifiers are blanked by the PRF control signal when the transmitter is on, to reduce ringing in the receiver.

Output of the i.f. amplifier is fed to a square-law detector that provides an output of 0 to 10 Vdc, in proportion to the power of the received signal. This analog output passes to the control logic where, at specified sample times (corresponding to sample heights), the output is converted to a 6-bit digital word.

3.11. Analog To Digital Converter

The A/D converter is located on card 8 of the control logic chassis. It is a DATEL converter model ADC-G8B1A, with 8 bits of output. However, the two least-significant bits are not used. The PDP-8 computer has a 12-bit word size, and two of the 6-bit words from the converter are packed into one computer word. All outputs from the A/D converter, plus corresponding status information, are stored (temporarily) in computer memory.

3.12. Computer

The digital computer is a Digital Equipment Corporation PDP-8/L with 12-bit words, parallel input, and 4,000 words of memory. One of its functions is to act as a data buffer for the tape recorder. Another function is to average all of the raw data in a run, with averages for each sample height and attenuation, and at the end of a run, print the results on the teletype for on-site analysis. These averages provide a field record of D-region condition and equipment operation. (Further explanations of the computer functions are given in Section 5.)

3.13. Teletype

The ARS-33 teletype prints the averages calculated by the computer, after a run and at the request of the operator, as noted in Section 3.12. It can also

print the contents of the computer memory or of any magnetic tape record, for use in trouble shooting and program analysis, or for verification or proper operation of the recording system.

3.14. Tape Recorder and Controller

The magnetic tape recorder is a Wang Co. model 10, and uses a 10½ inch reel of computer tape. Recording is on 7 tracks with a density of 200 bpi. The Datum tape controller acts as interface between the tape recorder and the computer.

SECTION 4

Antenna Installation

4.1. Antenna Elements

The partial reflection sounder has been operated at frequencies 2.2375 MHz and 2.6667 MHz. The 2.6667 MHz antenna system is discussed here, and similar concepts apply at the other frequency.

The antenna elements are made of copperweld No. 10 wire. Each element is a center-fed half-wave dipole, with quarter-wave arm length computed from the following formula:

$$\frac{\lambda}{4} = \left(\frac{3 \times 10^8 \text{ m/sec}}{f_c \text{ hertz}} \times 0.95 \right) \div 4 = 26.7 \text{ meters}$$

(end-effect factor)

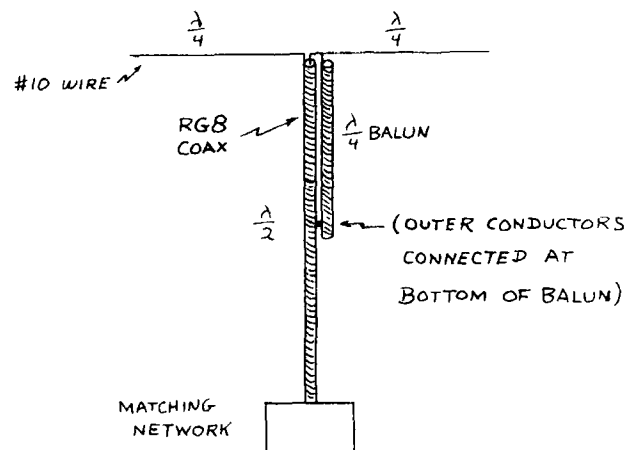
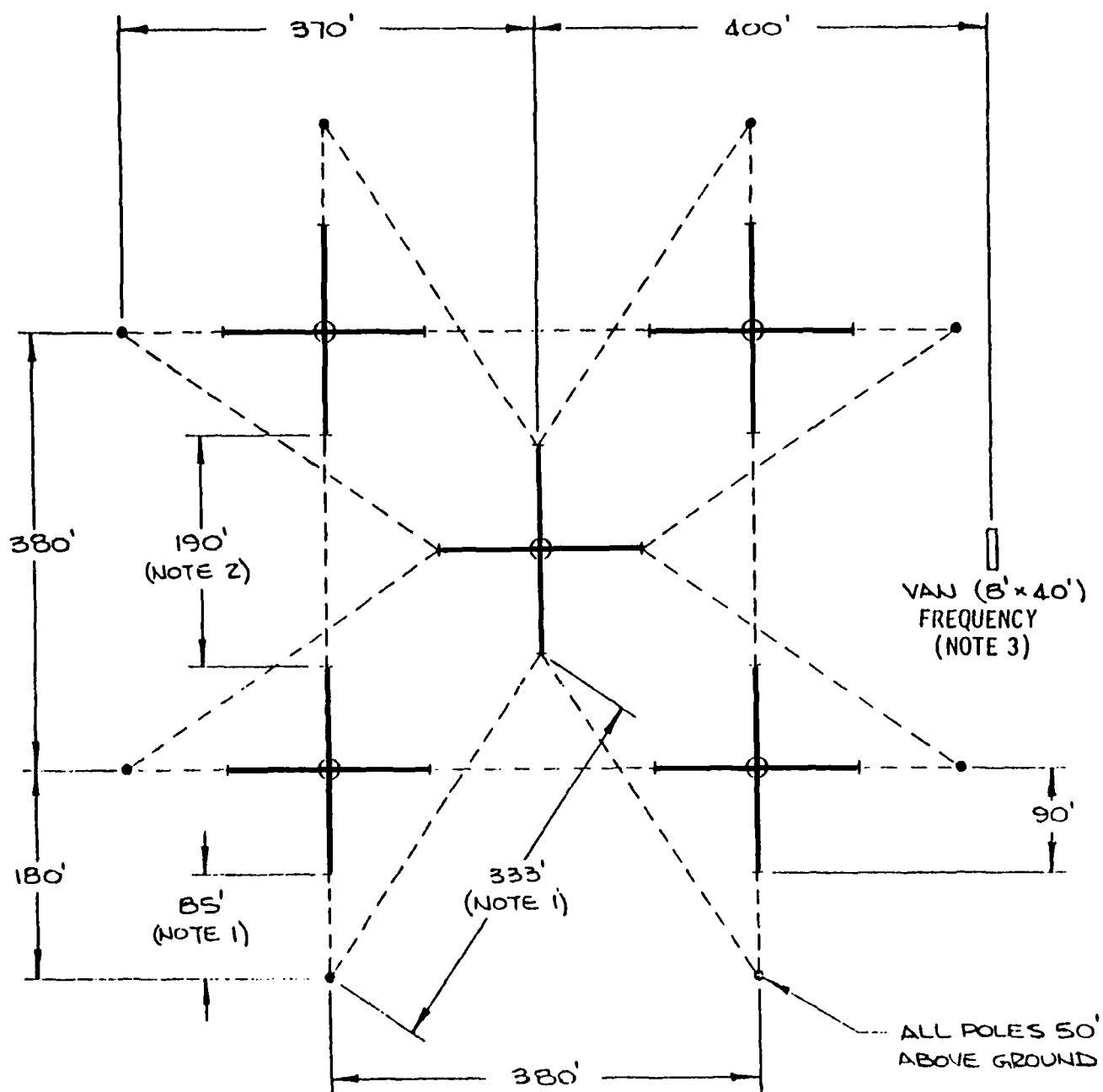


Figure 4.1. Dipole Element.

The antenna array consists of five crossed-dipole segments, for a total of 10 half-wave dipoles. Figure 4.2 gives the dimensions of the array.



- (1) Does not include 5' for pole rope
- (2) Includes length of insulator
- (3) Frequency 2.666666 MHz

Figure 4.2. Antenna array, plan view.

4.2. Feed Cables

As indicated in Figure 4.1, a feed cable and a balun are connected to the center of each dipole. Both are made from RG8 coaxial cable. Feed cables connect the dipoles to the matching network boxes, and are one-half wave, with length computed as follows:

$$\frac{\lambda}{2} = \left(\frac{3 \times 10^8 \text{ m/sec}}{f_c \text{ hertz}} \times 0.66 \right) \div 2 = 37.13 \text{ meters}$$

↑
(velocity factor for RG8)

In practice, the feed cables are cut slightly longer than the computed length, then shortened gradually until resonance is indicated on an rf bridge (RX meter, H.P. model 250). With the cable unloaded, typical readings at resonance on the RX meter are 1.2 K ohms on the R_p dial and ± 5 pf on the C_p dial.

4.3. Baluns

Balun length is computed from the formula

$$\frac{\lambda}{4} = \left(\frac{3 \times 10^8 \text{ m/sec}}{f_c \text{ hertz}} \times 0.66 \right) \div 4 = 18.57 \text{ meters}$$

As with the feed cables, baluns are cut slightly longer than the computed length, then shortened to resonance. The connection of the balun to the feed cable is shown in Figure 4.1. The feed cable and the balun should be taped together as closely as possible because gaps between the two affect the capacitive reactance of the antenna.

* The factor 0.66 in the length equations is applicable to RG8 cable.

4.4. Antenna Poles

Thirteen wooden poles, length 70 feet, are used to support the antennas. Figure 4.2 shows the distances between the poles. The antennas are mounted 50 feet above ground. Once the antennas have been calibrated, their height must be maintained constant, because height also affects the capacitive reactance.

4.5. Antenna Calibration

When the antennas are in place, the connection between feed cable and balun shields is made approximately one quarter wavelength below each antenna. The location of the connection is then varied until resonance is indicated on an RX meter attached to the feed cable. At resonance, the readings should be approximately 50 ohms R_p and ± 50 pf C_p .

4.6. Antenna Matching

After all antennas are calibrated, the two matching network boxes must be calibrated as shown in Figure 4.3 (for box A).

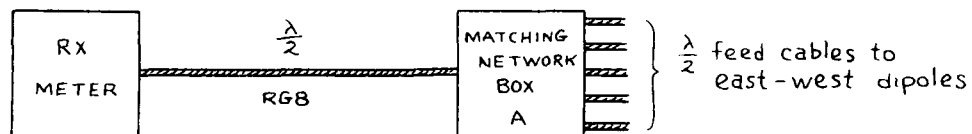


Figure 4.3. Antenna matching calibration setup.

The RX meter is set at 50 ohms R_p and 0 pf C_p , and connected to the matching network box with A calibrated at 50 ohms half-wavelength cable. The box is then adjusted to resonance using the variable capacitor and inductor within the box.

SECTION 5

System Operation

5.1. Transmitter Turn-on

To activate the transmitter and associated equipment, turn on the following in sequence:

- a. Main power (S1)
- b. Exciter high voltage (S2)
- c. P. A. filaments (S3); adjust to 7.4 Vac
- d. Pulse generator
- e. Receiver
- f. P. A. high voltage (S4); adjust to 12.5 kVdc

5.2. Logic Turn-on

To activate the logic unit and associated equipment, turn on the following in sequence:

- a. Relay power supply
- b. Logic unit power supply
- c. Tape controller
- d. Tape recorder
- e. Computer
- f. Teletype

5.3. Program Loading

To load the operating program into the computer, do the following:

- a. Thread the program tape onto the tape drive and press the "load" switch. The tape should advance to the start marker, and the "on line" status light should come on.

- b. With the computer in single-step mode, load address 7600, which is the entry address for the bootstrap loader. The contents at address 7600 will be displayed. Step thru and examine the remainder of the bootstrap, shown in Table 5.1. To see the contents of the second address, 7601, press the "examine" switch twice. Each subsequent address can then be seen via one operation of the "examine" switch. If any parts of the bootstrap program are not correct, load the correct instructions manually. This is done by re-loading the address in question, loading the correct contents on the registers, and then pressing the "deposit" switch.
- c. Go back to address 7600 and deactivate the single-step mode.
- d. Clear the registers (0000) and press the "start" switch. Execution will halt at address 7603.
- e. Load instruction 0420 on the registers and press the "continue" switch. The accumulator will then indicate 0001. If this is not the case, examine the bootstrap procedure and try the previous steps again. The accumulator must read 0001 if the operating program is to function properly.

5.4. Data Sampling Procedure

- a. Load a clean data tape and make sure the handler is "on line." An end-of-file (EOF) mark must be entered at the start of the tape and after each data run. To write the EOF mark, enter instruction 4000 at address 0200, then press the "continue" switch. The tape should advance as the EOF is written.
- b. Enter instruction 0200 (initialize) at address 0200, then press the "start" switch. The teletype will print "CN=" and the operator then types "1.0 return." This indicates the ratio between 0 and X amplitudes.

TABLE 5.1. COMPUTER BOOTSTRAP PROCEDURE

<u>Address</u>	<u>Contents</u>
7600	6711
7601	5200
7602	6706
7603	7402
7604	7300
7605	7604
7606	6716
7607	6722
7610	7300
7611	6713
7612	5211
7613	6726
7614	3623
7615	2223
7616	2222
7617	5211
7620	6723
7621	5200
* 7622	0177
* 7623	0000

* After the operating program has been loaded, the contents of address 7622 and 7623 will be 0000 and 7601, respectively.

- c. The fixed attenuators at the receiver input should now be adjusted for proper attenuation. This requires that the transmitter be in operation. Press the "start" button on the control logic unit. The transmitter will start to operate, but the received signals will not be saved either in the computer or on the data tape. The proper amount of fixed attenuation is determined by visual inspection of the receiver oscilloscope display. Normal fixed attenuation for daytime operation is the range 6 to 10 dB. To stop transmitting, it is necessary to reset the control logic. This is done by pushing the button switch on card 3 of the control unit, located behind the front panel.
- d. Enter the appropriate date, time, etc., via the thumbwheels on the front panel of the control unit. This information will be recorded on the tape, along with the data.
- e. Clear (0000) the computer registers and press the computer "continue" switch. The computer is now ready to receive the data.
- f. Press the "start" button on the control logic unit. This starts the run, with the transmitter operating, and the received signals digitized. The computer will store the digitized data, and, periodically, dump the data onto the tape. The time interval for a normal data run is 10 to 15 minutes.
- g. To terminate the run, press the "stop" button on the control unit. Then write an EOF mark on the data tape. (See step 5.4a.)
- h. (Optional) To print out the data averages on the teletype, for the run just concluded, load instruction 2000 ("computations") at address 0200 and press the "continue" switch. To stop computations, press the "stop" switch.

5.5. Receiver Calibration

The purpose of the receiver calibration is to determine the linearity and sensitivity of the receiver, and the proper functioning of the stepped attenuators. Figure 5.1 shows the calibration setup.

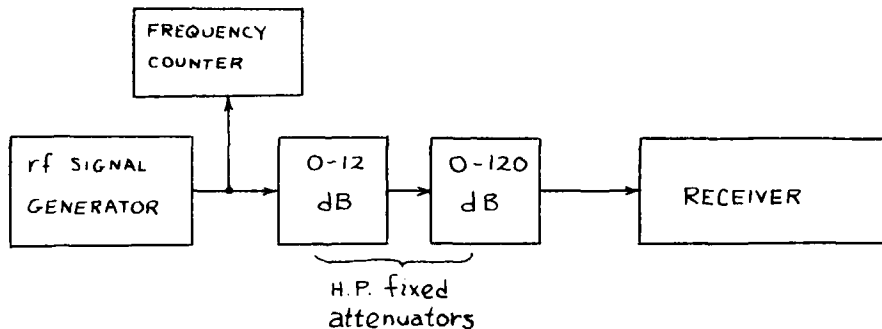


Figure 5.1. Receiver Calibration Setup.

Normal saturation threshold for the receiver is approximately -97 dBm at zero attenuation. Normal calibration levels are as follows: -90, -96, -98, -100, -102, and -108 dBm. These levels are selected using the fixed attenuators. At each level, record a "run" of (calibration) data on the tape, of several minutes duration. Note that, in addition to the fixed attenuation, the stepped attenuators will be stepping through their four levels during the run. Use a step unit of 6dB. Calibration data is written on the data tape in exactly the same format as regular data. A printout of averages on the teletype shows the operation of the stepping attenuators and the receiver linearity.

5.6. Turn-off Procedure

To shut down the station turn off the following in sequence:

- a. Teletype
- b. Computer
- c. Tape drive
- d. Tape controller
- e. Logic unit power supply
- f. Relay power supply
- g. Receiver
- h. Pulse generator
- i. Reduce P. A. high voltage to zero, then turn off (S4)
- j. Exciter high voltage (S2)
- k. Wait 5 minutes for the P. A. tubes to cool, then turn off the P.A. filaments (S3)
- l. Main power (S1)

SECTION 6

Data Processing

The first step in the data processing is to time-average the data recorded on magnetic tape during a run. This averaging is done by a computer program that runs at White Sands Missile Range on the UNIVAC 1108 system. A listing of the program, which is written in FORTRAN, is given in Appendix II. Our intention here is to summarize what this program does.

Recall that each pulse from the transmitter results in an echo that is digitized via 30 samples, and that 8 consecutive pulses form the basic operating pattern. Thus in averaging the data, 240 separate averages must be computed. We actually perform 480 averages because of the fact that the raw data is passed through two different screening procedures. (Which of the two results will be used is decided after the fact.) A slight complication arises in that each record on the data tape contains two patterns, i.e., echoes from 16 consecutive pulses, and thus yields two numbers for each running average.

Now each data-number is an integer between 0 and 63, and its value is a measure of received signal strength. "Strength" is the equivalent of signal intensity; but the information required is signal amplitude. Each data-number is converted, prior to averaging, into a corresponding measure of signal amplitude via a table-lookup procedure that is based on receiver calibration.

Appendix IV contains details regarding receiver calibration. We shall simply state here that the end-product of receiver calibration is a table of 64 numbers scaled so that the first is 0 and the last is 63. (Scaling to this range is done only for convenience. Since the end result is the amplitude ratio A_x/A_o , any constant used to scale the amplitudes cancels out in the ratio.) This table is named RX in the program. If, for example, the considered data-number is 15, then the corresponding measure of signal amplitude is the 16th value in the RX array, RX(16).

The "heart" of the averaging program is the accumulation loop, reproduced in part in Figure 6.1. Therein, the accumulations are carried out for each of the separate averaging calculations. Comments follow for each of the statements identified by number in Figure 6.1:

```

1      DO 210 J=1,8
2      K=J
3      195 K1=1
4      K2=1
5      IF (IDATA(K,IJKHT).GT.MAX1) K1=0
6      N1(J)=N1(J)+K1
7      IF (IDATA(K,IJKHT).GT.MAX2) K2=0
8      N2(J)=N2(J)+K2
9      DO 205 H=1,MM
10     IF (NSEG.EQ.1) GOTO 197
11     IF (IDATA(K,H).GT.MAXX) N3(J,H)=N3(J,H)+1
12     I=IDATA(K,H)+1
13     A1(J,H)=A1(J,H)+K1*RX(1)
14     A2(J,H)=A2(J,H)+K2*RX(1)
15     GOTO 200
16     197 A1(J,H)=IDATA(J,H)
17     A2(J,H)=IDATA(J+8,H)
18     200 CONTINUE
19     205 CONTINUE
20     K=K+8
21     IF ((K.LE.16).AND.(NSEG.NE.1)) GOTO 195
22     210 CONTINUE

```

Figure 6.1. Accumulation logic for data averaging.
These statements are from the computer
program in Appendix II.

1. J (from 1 to 8) indexes the pulses of the basic 8-pulse pattern.
2. K is initially the same as J.
- 3,4. Multipliers K1 and K2 are initially set at 1.
5. IDATA (size 16 by 30) contains the 480 data-values from one record of the data tape; 16 echoes, 30 samples per echo. Index IJKHT is a constant set by card input. If, for example, IJKHT=4, then K1 is changed to zero if IDATA(K,4) is greater than MAX1, which is another constant set by card input. The idea here is this: assume that the return from the 4th (if IJKHT=4) sampled altitude is sure to contain noise only, no partial reflections being expected from this particular altitude. Then if the noise (the data value) here exceeds the threshold value MAX1, all 30 values from this echo are not going to be included in the averages (thanks to setting K1=0).
6. N1(J) counts the number of times that K1 remains at 1, which corresponds to the number of values averaged.
7. Screening similar to that at line 5 is done here, but at a different threshold, MAX2.
8. Counting similar to that at line 6.
9. H (from 1 to MM=30) indexes the samples in each echo.
10. NSEG is a constant set by card input. It fixes the number of records to be accumulated prior to averaging. If all records in a run are to be included, any value for NSEG larger than the number of records will do. Say a run contains 800 records. If NSEG=100, then the run is effectively broken into 8 parts, and averaging will be done over each of these parts, in turn. NSEG=1 is a special case that results in the listing of all data values recorded on the tape for this run (480 values per record, and one record per page of the printout).
11. If data value IDATA(K,H) exceeds a value MAXX, counter N3(J,H) is incremented. We use MAXX=62 so that N3 counts the number of samples for which the digitizer was probably saturated. Any averages for which the N3 count is not small are suspect.
12. The data value is incremented by one and the result, I, will serve as an index for the receiver-calibration array RX (size 64).
13. Array A1 (size 8 by 30) contains the 240 accumulations corresponding to screening via MAX 1. RX(I) is the data value that will be accumulated if K1 is not zero.

14. Array A2 contains the 240 accumulations corresponding to screening via MAX2.
- 16,17. In the special case NSEG=1, the first 240 values of the record are copied into A1 (without conversion via RX), and the second 240 values are copied into A2. The A1 and A2 arrays will be printed before the next record is processed.
19. End of inner loop on sample (altitude) index H.
20. Increase K by 8.
21. If NSEG>1 and if $K \leq 16$, go back and accumulate values from the second half of the record (echoes 9 through 16).
22. End of outer loop on echo (pulse) index J.

An example of the output obtained from the averaging program is shown in Figure 6.2. A page of output similar to this is generated for every run, or for every run segment, that is averaged.

The following comments relate to Figure 6.2, and describe the material found on the lines marked, at the left of the figure, with letters A through F:

- A.
 - Tape file number.
 - Starting height; i.e., the lower limit of the altitude interval sampled.
 - Segment number (applicable to averages over parts of the run).
 - Records per segment (NSEG). Since 999 is greater than the number of records here, the entire run is processed as one segment.
 - Reference height index (IJKHR) used to select noise values from each echo to test against the screening thresholds MAX1 and MAX2.
- B.
 - Time, date, and comments -- reference information entered via cards.
 - Solar zenith angle, computed using the preceeding time and date. See Appendix III.
- C. Reference information contained on the data tape, and obtained from thumbwheels set by the operator prior to the run.

A → FILE NO. = 6 RECORDS PER SEGMENT = 999 REF. HEIGHT INDEX = 1
 B → TIME, DATE, COMMENTS: 02/20/79 0730:00 SOLAR ZENITH ANGLE = 1.366 RADJANS, OR 78.250 DEGREES

C → RECORD MONTH DAY YEAR HOUR MINUTE FILE IAPF
 1 2 32 9 15 0 6 2

D → NO OF RECORDS USED = 872 MAXI VALUE = 10 MAX2 VALUE = 5 PARITY CHECK = 872

E → 35 34 33 32 31 30 29 28 27 26 25 24 23 22 21 20 19 18 17 16 15 14 13 12 11 10 9 8 7 6 5 4 3 2 1

F →	AVERAGES USING MAX1																AVERAGES USING MAX2																	
	25	26	27	28	29	30	31	32	33	34	35	36	37	38	39	40	41	42	43	44	45	46	47	48	49	50	51	52	53	54	55			
55	11.742	6.992	3.279	.852	10.722	5.672	3.157	.985	8.892	5.394	2.281	.822	8.450	4.038	2.226	.938																		
57	16.898	8.711	3.366	.858	15.752	7.929	3.277	.849	16.735	7.889	3.010	.842	15.115	7.091	2.893	.832																		
59	19.927	9.818	3.469	.820	18.870	9.396	3.377	.820	19.831	9.980	3.541	.822	18.115	9.478	3.460	.819																		
61	19.997	9.554	3.348	.692	19.309	9.226	3.442	.769	20.991	9.831	3.514	.694	19.149	9.457	3.495	.772																		
63	19.567	9.736	3.565	.826	19.487	9.609	3.417	.873	19.656	9.952	3.640	.819	19.025	9.836	3.473	.876																		
65	18.879	8.975	3.337	.735	19.879	9.635	3.590	.814	18.699	8.948	3.375	.727	19.680	9.817	3.608	.817																		
67	21.192	9.984	3.375	.792	24.549	12.855	4.836	.978	21.230	10.166	3.373	.790	24.585	13.032	4.803	.981																		
69	24.672	12.850	4.897	1.043	33.252	20.026	9.005	2.380	24.500	12.915	4.829	1.045	32.997	19.904	8.989	2.388																		
71	29.981	16.708	7.028	1.677	37.792	25.970	12.980	4.701	29.654	16.639	6.951	1.657	38.081	26.022	13.025	4.691																		
73	30.525	17.557	7.639	1.856	37.376	25.978	13.376	5.200	30.382	17.470	7.532	1.847	36.825	25.989	13.377	5.196																		
75	29.232	16.579	6.732	1.535	35.548	21.955	10.371	3.401	29.048	16.414	6.714	1.521	35.619	21.907	10.256	3.409																		
77	38.757	27.958	14.724	5.803	40.958	33.172	19.832	8.864	39.329	27.875	14.731	5.799	40.443	32.978	19.771	8.879																		
79	39.419	33.640	20.925	9.506	43.004	36.513	24.783	12.401	39.455	33.422	20.957	9.491	44.071	36.483	24.716	12.417																		
81	44.442	37.738	25.767	12.809	45.892	39.080	28.617	15.594	43.555	37.473	25.778	12.809	45.057	39.269	28.641	15.597																		
83	43.999	38.322	28.554	15.154	43.303	37.445	29.391	16.361	44.771	38.110	28.525	15.146	43.947	37.682	29.409	16.357																		
85	46.478	39.878	29.963	16.031	40.932	33.608	20.425	9.875	46.386	40.147	29.972	16.023	41.300	33.517	20.349	9.870																		
87	46.989	39.619	32.877	20.303	37.717	26.707	13.700	5.424	47.052	39.923	32.959	20.310	37.526	26.647	13.713	5.419																		
89	47.167	40.342	31.699	18.428	37.716	26.737	13.152	4.818	47.599	40.554	31.848	18.423	37.190	26.780	13.253	4.818																		
91	51.702	45.577	39.463	27.848	42.672	33.642	20.479	9.349	51.764	45.718	39.593	27.864	42.573	33.751	20.556	9.378																		
93	52.971	45.184	42.416	27.517	44.011	38.419	28.184	15.668	56.435	45.307	42.877	37.562	43.030	38.258	28.240	15.697																		
95	52.648	47.636	41.357	34.075	40.586	35.333	25.327	13.283	51.743	46.397	41.199	34.098	40.364	35.419	25.194	13.312																		
97	47.961	43.523	37.136	25.862	37.163	27.421	15.012	6.488	52.082	43.697	37.162	25.859	36.525	27.307	15.018	6.501																		
99	46.797	40.902	32.154	21.482	32.998	21.278	10.516	3.438	46.740	41.045	32.040	21.453	32.864	21.311	10.477	3.444																		
101	45.550	37.899	29.873	18.548	32.136	20.223	10.015	3.369	46.610	38.091	29.798	18.546	31.824	20.414	10.037	3.376																		
103	45.226	37.348	26.285	14.410	30.750	18.105	8.629	2.393	44.842	37.372	26.346	14.417	30.723	18.200	8.631	2.397																		
105	41.593	33.581	23.653	10.229	27.562	15.514	6.712	1.624	42.038	32.559	20.890	10.234	27.484	15.558	6.713	1.630																		
107	37.102	27.117	16.047	6.311	25.903	15.201	6.938	2.245	37.040	27.095	16.128	6.295	25.475	15.002	6.892	2.253																		
109	37.985	22.097	12.228	5.939	25.053	14.437	6.292	2.503	37.662	22.209	12.257	5.919	24.638	14.323	6.239	2.502																		
111	32.394	20.315	10.557	4.605	25.105	14.402	6.490	1.922	31.452	20.427	10.598	4.600	25.234	14.501	6.492	1.929																		
113	32.720	19.452	9.815	3.717	25.822	14.841	5.902	1.515	31.224	19.303	9.817	3.726	25.536	14.998	5.902	1.488																		

Columns 1

Columns 1 2 3 4 5 6 7 8 9 10 11 12 13 14 15 16

Figure 6.2. Output of averaging program. Run information followed by average amplitudes.

- D. ● Number of records processed (in this case, all records in the file).
- Selected screening threshold values; 10 for MAX 1 and 5 for MAX2.
- Parity check . . . The number of records read from the tape without parity error. Since this number here equals the number of records used, there were no parity errors.
- E. Reference information from the tape identifying the particular mode of system operation (normal operating mode, in this case).
- F. Average amplitudes, arranged in 16 columns, with rows holding results from 55 km to 113 km (as per the left-most column). Columns 1 through 8 (see numbers below the columns) contain the 240 averages for MAX1 screening, while columns 9 through 16 contain the averages for MAX2 screening. Column-sets 1-8 and 9-16 each follow the basic 8-pulse pattern: amplitudes for ordinary mode with 0, 1, 2, and 3 units of attenuation; followed by amplitudes for extraordinary mode with 0, 1, 2, and 3 units of attenuation. (The attenuation unit here is 6 dB.)

There is, in the receiver, a delay corresponding to an altitude increment of 5 km. This delay is not taken into account in the timing circuits that set (via operator selection) the starting height. The delay is taken into account in the data processing that follows. Thus the data in Figure 6.2 spans a true altitude interval of 50 km to 108 km, rather than the indicated interval 55 km to 113 km. The operator takes note of this delay. For example, if he wants to start sampling at 50 km, he will select a value indicated as 55 km on his control unit. We have found it less confusing to use the indicated value within the averaging program.

Counts accumulated by N1(J), N2(J), and N3(J,H) (see Figure 6.1) are printed on a separate page of computer output. For example, in the run of Figure 6.2, N1 showed that 1035, 1466, 1726, 2744, 1099, 1436, 1719, and 1744 values were included in the averages for columns 1-8, respectively. All data was thus used in the averages for columns 4 and 8, as indicated by $N1=1744=2 \cdot 872$, 872 records having been considered. The N3 counter showed that only a relatively few saturated values were included in the averages of columns 3, 4, 7, and 8,

and only at some upper altitudes. Columns 1, 2, 5, and 6, however, contain an excessive number of saturated values at many altitudes, and should not be used.

For any run, the amplitudes $A_o(h)$ and $A_x(h)$ obtained from the averaging program (Appendix II) are used to obtain the electron density profile $N(h)$ for the run. The procedure here requires the amplitude ratio A_x/A_o , to be used as in Equation (1.5).

The first step is to compute by hand an A_x/A_o vs. altitude profile using average amplitude values such as found in Figure 6.2. Because of the fact that data were recorded at four different values of receiver attenuation, and that raw data were screened using both MAX1 and MAX2 thresholds, the analyst must decide which of several possible values are to be used to compute A_x/A_o at each altitude. Judgements here must be based on experience with similar data. Because of the subjective nature of the decision process, we have not attempted to automate this step.

The following comments are based on the example run of Figure 6.2, and are intended to provide some insight:

- "Amplitudes" below 67 km (indicated altitude) are simply noise, and contain no useful information. In fact, we use no data below 75 km. As noted, an indicated altitude of 75 km on the listing represents a true altitude of 70 km, etc.
- A_x values at 105 km (listed altitude) and above are simply noise and cannot be used. In fact, we use no data above 89 km (84 km true).
- There is little difference between the averages in columns 1-8 and 9-16, showing that MAX1 and MAX2 thresholds are nearly equivalent. But since more values are included, generally, under the MAX1 screening, we will use only columns 1-8.
- The "best" data seems to be in columns 3 and 7. Amplitudes in columns 1, 2, 5, and 6 tend to be too large, indicating receiver saturation, while those in columns 4 and 8 tend to be too small. (Receiver attenuation is stepped so that choices such as this are possible!)

The A_x/A_o calculation then proceeds as shown in Table 6.1:

TABLE 6.1. AMPLITUDE CALCULATIONS FOR DATA IN FIGURE 6.2.

true altitude, km	A_o	A_x	A_x/A_o
70	6.732	10.371	1.54
72	14.724	19.832	1.35
74	20.925	24.783	1.18
76	25.767	28.617	1.11
78	28.554	29.391	1.03
80	29.963	20.425	0.68
82	32.877	17.700	0.42
84	31.699	13.152	0.41

The data used in obtaining the averages in columns 3 and 7, Figure 6.2, were all obtained at the same receiver attenuation, and so the averages can be combined directly to obtain A_x/A_o . If one wishes to use values from non-paired columns, compensation must be made. For example, say we choose to use $A_x = 12.401$ from column 8 at 74 km (true) rather than 24.783 from column 7. Then $A_x/A_o = 12.401/20.925 = 0.593$. For this run, the level of stepped attenuation was set at 6dB, so the amplitudes in column 8 are low, relative to columns 3 and 7, by 6dB, or a factor of 1.995. Thus, the preceding value of 0.593 must be increased by this factor: $A_x/A_o = 0.593 \cdot 1.995 = 1.18$.

Accordingly, one might expect all values in column 7, say, to be essentially twice the corresponding values in column 8. This relationship does hold, approximately, for mid-value amplitudes, but is clearly not the case for low amplitudes (due to noise effects) and high amplitudes (due to saturation effects).

The A_x/A_o profile in Table 6.1 above is typical in that, with increasing altitude, it drops quite smoothly from values above 1 to values below 1. In some runs, the ratio falls to values of 0.1 or less at high altitude, rather than the limit of about 0.4 in this run. Also, some profiles show a maximum near the low-altitude end. In this run, if a maximum does exist, it falls short of the range of useful data. It should be noted that our decision to limit the data interval to between 70 km and 84 km was based primarily on the A_x/A_o

profile, as results outside this interval seem unrealistic (i.e., non physical). Our computer program that changes the 8 values of A_x/A_0 in Table 6.1 (1.54 to 0.41) into an electron density profile is shown in Figure 6.3. The program name is RLTIM3 and the language is APL. As per Equation (1.5), the program must access tables R(h) and G(h). Examples of such tables are shown in Table 6.2, with Version C appropriate to the run we are considering. The particular tables to be used by RLTIM3 are to be named RTEST and GTEST.

The call of RLTIM3 includes arguments A and AXAO. AXAO is the list of values of A_x/A_0 , namely the 8 values from Table 6.1 for the example at hand. Argument A consists of 3 integers:

- A(1) is the altitude in kilometers of the first entry in AXAO (70 here);
- A(2) is the altitude of the first value of AXAO to be utilized (again, 70 here);
- A(3) is the degree of the polynomial to be fit to the values of

$$y(h) \equiv \ln R/AXAO$$

(y values are computed at line 8 of the program). In our example run, a value A(3) = 4 was found to provide good results. Generally, the value should be about equal to half the number of data points (8 here).

At line 11 of the program, a procedure GO* is called to perform the least-squares evaluation of the polynomial coefficients a_i . These coefficients provide "best" values (\bar{y}) of y at each altitude (x) over the range considered:

$$\bar{y} = a_0 + a_1x + a_2x^2 + a_3x^3.$$

Although the altitude interval between data samples is 2 km, we compute results at 1 km intervals using the preceding equation.

*GO, in turn, calls procedure ITER which calls procedure FUN. Listings of GO, ITER, and FUN are included in Figure 6.3.

```

      VRLTIM3[ ]V
    ▽ A RLTIM3 AXAO
[1] SEQ← 0 1 2 3 4 5
[2] N←ρAXAO
[3] NN←ρ((A[2]-A[1])÷2)+AXAO
[4] N0←A[2]
[5] N1←A[1]
[6] N3←A[3]
[7] N2←N1+2×(N-1)
[8] Y←●RTEST[(N0-50)+2×0,1(NN-1)]÷((A[2]-A[1])÷2)+AXAO
[9] X←2×0,12×(NN-1)÷2
[10] A←N3ρ0
[11] GO
[12] A←6ρA,0,0,0,0
[13] X←0,12×NN-1
[14] EDEN←A[2]+(2×A[3]×X)+(3×A[4]×X×X)+(4×A[5]×X×X×X)+5×A[6]×X×X×X×X
[15] EDEN←EDEN÷GTEST[(N0-50)+X]
[16] EDEN←EDEN+0.5
    ▽

      VGO[ ]V
    ▽ GO
[1] A LSQ CURVE FIT PROCEDURE
[2] COUNT←1
[3] FI1:(ρA) ITER(ρY)
[4] COUNT←COUNT+1
[5] →(COUNT<3)/FI1
[6] ERR
[7] 0.01×[0.5+100×FF]
    ▽

      VITER[ ]V
    ▽ K ITER N;P
[1] A LSQ CURVE FIT PROCEDURE
[2] FF←0ρ0
[3] J←ERR←0
[4] P←(K,K)ρ0
[5] M←(K,1)ρ0
[6] IT1:J←J+1
[7] A FUN X[J]
[8] F←G-Y[J]
[9] FF←FF,F
[10] ERR←ERR+F×F
[11] DH←(1,K)ρV
[12] DV←(K,1)ρV
[13] P←P+DV+.×DH
[14] M←M+F×DV
[15] →(J<N)/IT1
[16] P←⊗P
[17] AA←P+.×M
[18] AA←KρAA
[19] A←A-AA
[20] ERR←(ERR÷(ρX)-(ρA))×0.5
    ▽

      VFUN[ ]V
    ▽ A FUN X;N
[1] N←ρA
[2] V←6ρ0
[3] A←6ρA,0,0,0,0
[4] V←X×SEQ
[5] G←+/A×V
[6] V←NρV
[7] A←NρA
    ▽

```

Figure 6.3. Procedures used in standard data processing.

TABLE 6.2. TABULATED FUNCTIONS R(h) AND G(h) USED IN THE STANDARD DATA PROCESSING. VERSIONS A, B, AND C WERE COMPUTED USING THE CONDITIONS DEFINED IN TABLE 6.3

Altitude	R(h)			G(h)		
h, km	A	B	C	A	B	C
51	1.1458	1.1435	1.1933	2.2568E-5	2.1942E-5	2.8810E-5
52	1.1679	1.1645	1.2223	2.9385E-5	2.8295E-5	3.7186E-5
53	1.1880	1.1835	1.2488	3.6247E-5	3.4608E-5	4.5523E-5
54	1.2135	1.2074	1.2823	4.5710E-5	4.3196E-5	5.6886E-5
55	1.2394	1.2315	1.3162	5.6109E-5	5.2492E-5	6.9213E-5
56	1.2733	1.2628	1.3607	7.0852E-5	6.5440E-5	8.6435E-5
57	1.3085	1.2950	1.4069	8.7286E-5	7.9581E-5	1.0532E-4
58	1.3472	1.3300	1.4575	1.0647E-4	9.5726E-5	1.2698E-4
59	1.3904	1.3685	1.5137	1.2894E-4	1.1418E-4	1.5189E-4
60	1.4378	1.4103	1.5754	1.5471E-4	1.3478E-4	1.7990E-4
61	1.4866	1.4526	1.6386	1.8198E-4	1.5594E-4	2.0892E-4
62	1.5453	1.5027	1.7145	2.1548E-4	1.8107E-4	2.4376E-4
63	1.6107	1.5575	1.7987	2.5310E-4	2.0820E-4	2.8187E-4
64	1.6816	1.6159	1.8897	2.9368E-4	2.3614E-4	3.2180E-4
65	1.7594	1.6786	1.9890	3.3720E-4	2.6458E-4	3.6327E-4
66	1.8442	1.7456	2.0967	3.8287E-4	2.9264E-4	4.0552E-4
67	1.9393	1.8191	2.2165	4.3108E-4	3.2012E-4	4.4763E-4
68	2.0457	1.8990	2.3491	4.8052E-4	3.4566E-4	4.8886E-4
69	2.1574	1.9805	2.4865	5.2662E-4	3.6654E-4	5.2478E-4
70	2.2731	2.0621	2.6270	5.6756E-4	3.8186E-4	5.5389E-4
71	2.3908	2.1421	2.7673	6.0155E-4	3.9102E-4	5.7499E-4
72	2.5103	2.2202	2.9071	6.2773E-4	3.9393E-4	5.8765E-4
73	2.6323	2.2963	3.0468	6.4530E-4	3.9049E-4	5.9142E-4
74	2.7546	2.3692	3.1835	6.5303E-4	3.8071E-4	5.8580E-4
75	2.8757	2.4376	3.3153	6.5012E-4	3.6490E-4	5.7071E-4
76	2.9949	2.5014	3.4414	6.3585E-4	3.4334E-4	5.4606E-4
77	3.1077	2.5586	3.5573	6.1042E-4	3.1727E-4	5.1302E-4
78	3.2128	2.6091	3.6620	5.7437E-4	2.8766E-4	4.7265E-4
79	3.3044	2.6507	3.7505	5.3106E-4	2.5714E-4	4.2865E-4
80	3.3850	2.6855	3.8262	4.8139E-4	2.2600E-4	3.8170E-4
81	3.4513	2.7128	3.8867	4.2984E-4	1.9655E-4	3.3563E-4
82	3.5055	2.7340	3.9350	3.7799E-4	1.6904E-4	2.9131E-4
83	3.5477	2.7499	3.9716	3.2906E-4	1.4456E-4	2.5094E-4
84	3.5801	2.7615	3.9991	2.8398E-4	1.2302E-4	2.1475E-4
85	3.6048	2.7701	4.0196	2.4295E-4	1.0410E-4	1.8252E-4
86	3.6229	2.7762	4.0343	2.0711E-4	8.8022E-5	1.5482E-4
87	3.6361	2.7804	4.0448	1.7599E-4	7.4341E-5	1.3107E-4
88	3.6456	2.7834	4.0523	1.4908E-4	6.2687E-5	1.1072E-4
89	3.6522	2.7855	4.0574	1.2638E-4	5.2969E-5	9.3672E-5
90	3.6569	2.7869	4.0610	1.0715E-4	4.4801E-5	7.9298E-5
91	3.6603	2.7879	4.0636	9.0626E-5	3.7827E-5	6.6999E-5
92	3.6626	2.7886	4.0654	7.6561E-5	3.1916E-5	5.6557E-5
93	3.6643	2.7891	4.0666	6.4433E-5	2.6835E-5	4.7570E-5
94	3.6654	2.7895	4.0675	5.3816E-5	2.2398E-5	3.9715E-5
95	3.6663	2.7897	4.0681	4.4792E-5	1.8633E-5	3.3045E-5
96	3.6668	2.7899	4.0685	3.7234E-5	1.5484E-5	2.7464E-5
97	3.6672	2.7900	4.0688	3.0923E-5	1.2857E-5	2.2806E-5
98	3.6674	2.7901	4.0690	2.6192E-5	1.0888E-5	1.9315E-5
99	3.6676	2.7901	4.0691	2.1434E-5	8.9093E-5	1.5805E-5
100	3.667	2.7902	4.0692	1.7863E-5	7.4247E-5	1.3172E-5

TABLE 6.3. SPECIFICATIONS USED IN COMPUTING THE FUNCTIONS OF TABLE 6.2

All functions were computed using the Flood approximation, Equations 1.3A and 1.4A, and the collision frequency profile from Table 7.1.

VERSION	A	B	C
For station located at . . .	WSMR	WSMR	Balmertown, Ontario, Canada
Transmitter frequency, megahertz*	2.2375	2.6667	2.6667
Gyromagnetic frequency, megahertz*	1.404	1.404	1.638
Propagation/field line angle ϕ , degrees	30.0	30.0	12.2

* Convert to radians per second for use in the computations.

The polynomial is readily differentiated to obtain values of \bar{dy}/dx (at line 14), and division by $G(x)$ at line 15 completes the determination of the electron densities over the considered interval, in units of electrons per cubic centimeter.

Results for the example run are plotted in Figure 6.4, which shows altitude in kilometers on the vertical axis, and the logarithm of electron density (electrons per cubic centimeter) on the horizontal axis, which is scaled from 10^1 to 10^4 . Numerical values of electron density appear to the right of the altitude values.

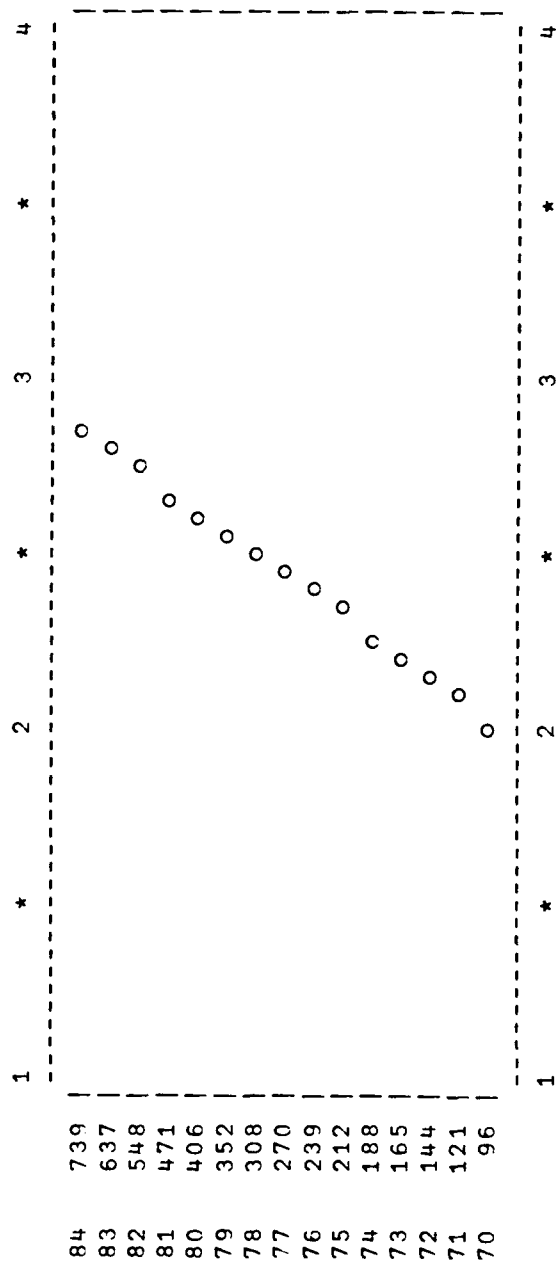


Figure 6.4. Example result, standard data processing.

SECTION 7

An Alternate Procedure for Data Processing

The data reduction procedure based on Equation (1.5), and implemented in the program RLTIM3 described in Section 6, is what we shall now call the standard procedure for reducing partial-reflection data. We have developed another procedure that provides benefits not otherwise obtained, and this non-standard procedure is the subject for discussion here.

Several investigators (5, 6) have noted a strong correlation between electron-density profiles $N(h)$ and the profile of ordinary amplitude $A_o(h)$. The correlation is most pronounced at low altitude. Belrose and Burke (5) used A_o profiles to extrapolate their electron density profiles to altitudes below which results were otherwise suspect. They drew theoretical support for this technique from a paper by Booker (7).

Our non-standard method is designed to obtain the electron-density profile more or less directly from the $A_o(h)$ profile. First, we use the standard method to obtain an electron density profile $N(h)$ that is restricted to mid-altitudes (70-80 km range) only, where the results tend to have maximum validity. We then adjust constants C_1 and C_2 in this expression,

$$N'(h) = C_2 \cdot h \cdot A_o(h) \cdot (E(h))^{C_1}, \quad (7.1)$$

until N' agrees as closely as practical with N over the altitude range of N . Then N' is taken as the profile of electron density for the run.

Kissick (8) has developed another procedure, more elaborate than ours, for obtaining electron densities from only the $A_o(h)$ profile. His work lends strong support to the idea that the ordinary echoes alone are rich in information.

The rationale for Equation (7.1) will now be explained.

The function $E(h)$ is empirical, and is given in Table 7.1. It has unit value at low altitude and increases in exponential fashion at high altitude. The purpose of $E(h)$ is to compensate for the fact that $A_0(h)$ is reduced at high altitude by the reflection and absorption of radio waves at lower altitude.

Multiplication of A_0 by altitude h in Equation (7.1) is done for this reason: In the well-known radar equation, echo intensity is proportional to the back-scattering cross section of the target, and inversely proportional to the fourth power of target distance ($I \propto \sigma/h^4$). The cross section for partial reflections should be proportional to the area of the radar beam, which varies as h^2 ($\sigma \propto h^2$). The combining of these relationships gives $I \propto 1/h^2$ for echo intensity, and, correspondingly, $A_0 \propto 1/h$ for echo amplitude. Multiplication of A_0 by h in Equation (7.1) is thus compensation for the altitude effect.

Constants C_1 and C_2 in Equation (7.1) are, as noted, adjustable, and should be selected to make N' follow the trend of N . In effect, C_1 controls the "slope" of N' , since increasing C_1 increases the value of N' at high altitude but does not change the value at low altitude. Constant C_2 simply scales the overall result.

An example from the non-standard reduction is given in Figure 7.1. The A_0 values here were taken from column 3 of Figure 6.2, and the constants were chosen for good agreement with the corresponding standard result of Figure 6.4. Constant values were $C_1 = 3.0$, $C_2 = 0.14$.

What are the advantages of the non-standard method? In the first place, $N'(h)$ provides electron density at altitudes lower than $N(h)$ can reasonably be extended, which is the same extrapolation of results used by Belrose and Burke. In the second place, $N'(h)$ can show a "fine structure" not found in $N(h)$. At best, the standard method can provide only gross changes in electron density with altitude. Any interesting features that cover only a few kilometers will be lost. However, any features in the $A_0(h)$ profile will still be present in the $N'(h)$ profile.

Results are given in Section 8. In all cases, results were obtained using the alternate, non-standard method.

TABLE 7.1. TABULATIONS OF $E(h)$. $E(h)$ IS THE EMPIRICAL EXPONENTIAL FUNCTION USED IN THE NON-STANDARD DATA REDUCTION. $\nu(h)$ IS ELECTRON COLLISION FREQUENCY OBTAINED FROM MEASUREMENTS AT WSMR MADE VIA THE ROBIN SPHERE PROGRAM, AND USED IN THE STANDARD DATA REDUCTION

Altitude h, km	$E(h)$	$\nu(h)$
51	1.0000	5.2000E7
52	1.0001	4.5000E7
53	1.0001	4.0000E7
54	1.0002	3.5000E7
55	1.0003	3.1000E7
56	1.0005	2.6880E7
57	1.0007	2.3550E7
58	1.0010	2.0660E7
59	1.0015	1.8110E7
60	1.0020	1.5880E7
61	1.0028	1.4040E7
62	1.0037	1.2260E7
63	1.0049	1.0680E7
64	1.0065	9.3100E6
65	1.0085	8.1050E6
66	1.0109	7.0460E6
67	1.0139	6.0890E6
68	1.0175	5.2270E6
69	1.0218	4.4940E6
70	1.0268	3.8700E6
71	1.0328	3.3410E6
72	1.0396	2.8860E6
73	1.0474	2.4870E6
74	1.0564	2.1380E6
75	1.0664	1.8320E6
76	1.0777	1.5600E6
77	1.0904	1.3230E6
78	1.1045	1.1150E6
79	1.1202	9.4000E5
80	1.1377	7.8770E5
81	1.1570	6.6040E5
82	1.1785	5.5220E5
83	1.2023	4.6250E5
84	1.2288	3.8760E5
85	1.2582	3.2430E5
86	1.2910	2.7200E5
87	1.3276	2.2840E5
88	1.3684	1.9180E5
89	1.4142	1.6160E5
90	1.4655	1.3640E5
91	1.5234	1.1500E5
92	1.5887	9.6930E4
93	1.6627	8.1440E4
94	1.7468	6.7940E4
95	1.8429	5.6500E4
96	1.9531	4.6940E4
97	2.0800	3.8970E4
98	2.2270	3.3000E4
99	2.3982	2.7000E4
100	2.5987	2.2500E4

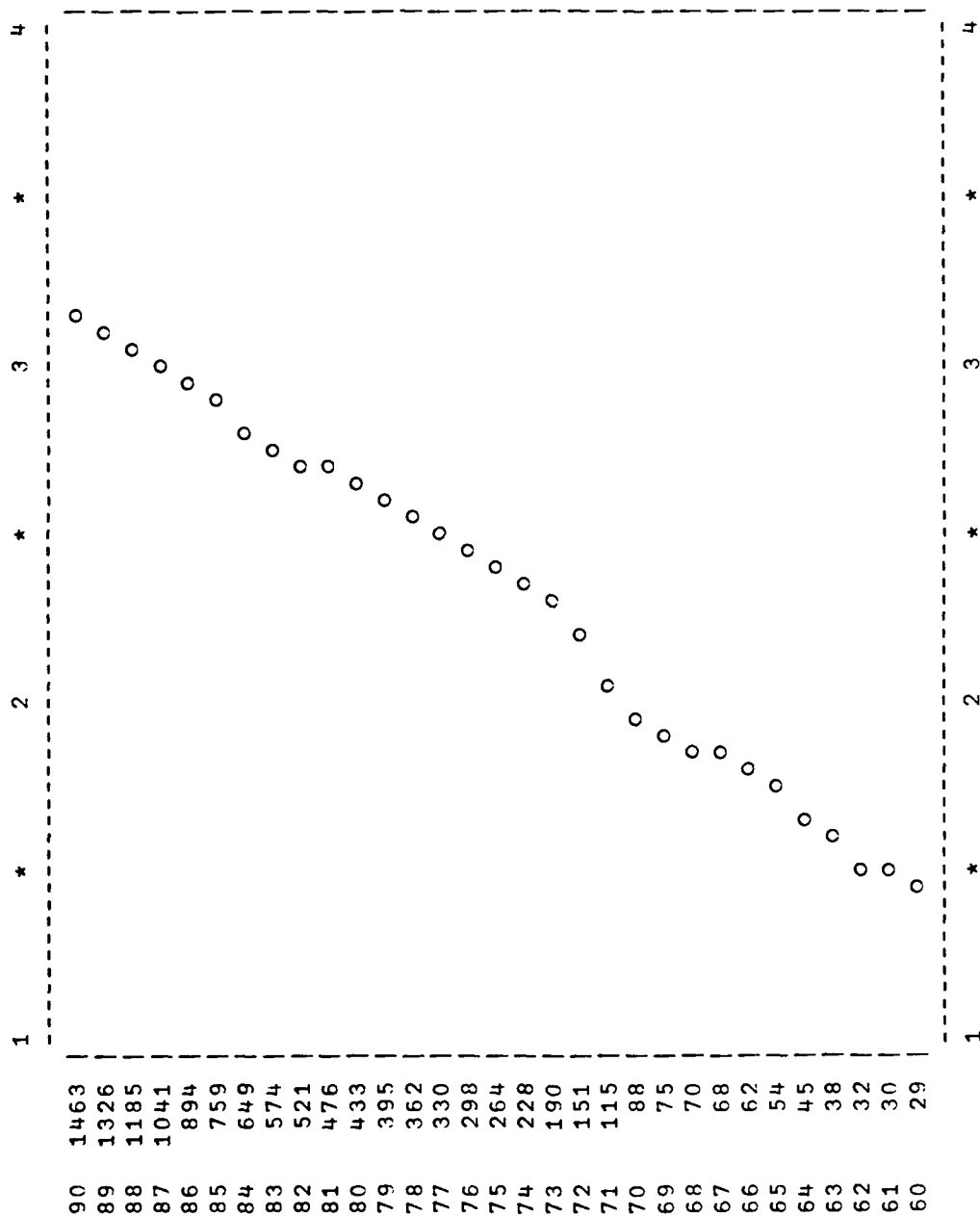


Figure 7.1. Example result, non-standard data processing.

SECTION 8

Results

From this partial reflection experiment, 682 electron density profiles have been produced. Because this number is so large, the profiles are contained in a separate volume. Figure 8.1 shows the format we have used to present the profiles determined from the individual runs. In each case there is a tabulation of electron density at 1-kilometer increments, and a semilogarithmic plot of electron density vs. altitude. Recall that the time duration of a run is on the order of 10 minutes, and that results are based on a time average of the several hundred measurements of echo amplitude made during the run.

Tables 8.1, 8.2, and 8.3 list the date and start-times of the runs.

The 41 runs in Table 8.1 were made at WSMR in 1975 by Mr. Glenn D. Falcon of the Institute for Telecommunication Sciences, Office of Telecommunications, U. S. Department of Commerce, Boulder, Colorado. These data were taken prior to PSL participation in the experiment. However, data reduction for these runs was performed by PSL.

Table 8.2 lists 413 runs made by PSL at WSMR between September 1977 and August 1979.

Table 8.3 lists 198 runs made by PSL at Balmertown, Ontario, Canada, in February 1979. The station was moved to Canada as part of the Atmospheric Sciences Laboratory scientific program for the solar eclipse of 26 February 1979.

Data from the eclipse program spanning totality were also processed in 30 1-minute segments, extending from 1045 to 1115 local time. (Totality was from approximately 1053 to 1055.) These 30 profiles are included in the results volume.

Figures 8.2 - 8.11 contain averages of results for the WSMR data on a monthly basis. In forming the averages, we used only data recorded during the midday

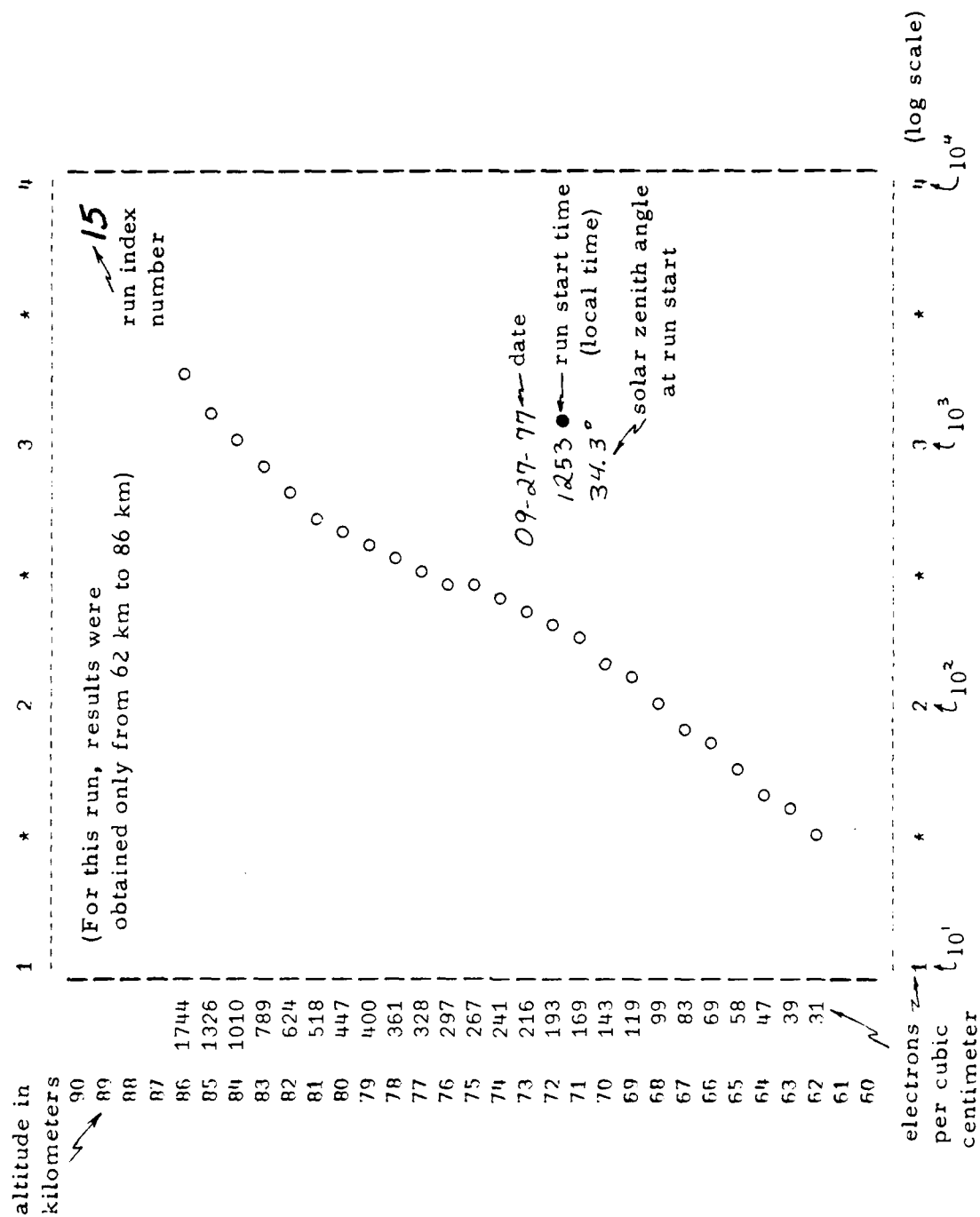


Figure 8.1. Key to electron density profiles.

hours of 1000 to 1400 MST, and only covered those months for which a significant number of midday runs were available. Within the plots, 'o' marks the average value, while the '*' marks are separated from the average by one standard deviation.

In regard to the eclipse data, solar photons are the primary agent for ionization of the atmosphere in the D region, and a total solar eclipse can allow measurements showing the dynamics of the ionization process. However, the sun was very active during February 1979, and, apparently, particles in the solar wind were a major factor in D-region ionization. Thus changes in ionization during the eclipse were not pronounced. Figure 8.12 shows time variation in electron density obtained from partial reflections during the eclipse, at altitudes of 60, 65, 70, 75 km. A small decrease of electron density at the lower two altitudes is seen, but, at the higher two altitudes, there appears to be an increase in electron density. Interpretation of these results is still pending.

TABLE 8.1. RUN INDEX FOR WSMR, 1975

<u>Date</u>	<u>Time, Mtn. Daylight</u>	<u>Solar Zenith Angle</u>	<u>Sequence No.</u>
09-26-75	0557	-	1
	0622	98.6 °	2
	0633	96.3	3
	0649	92.9	4
	0659	90.8	5
	0718	86.8	6
	0735	83.2	7
	0747	80.7	8
	0810	75.9	9
	0836	70.6	10
10-01-75	1330	36.3	11
	1355	37.9	12
	1415	39.8	13
	1445	43.4	14
	1520	48.7	15
	1545	52.9	16
	1635	62.1	17
	1713	69.6	18
	1800	79.2	19
	1840	87.5	20
10-02-75	1955	-	21
	1205	38.3	22
	1231	36.6	23
	1311	36.1	24
	1410	39.6	25
	1435	42.5	26
	1455	45.2	27
	1516	48.3	28
	1531	50.8	29
	1550	54.0	30
10-03-75	1613	58.2	31
	1700	67.2	32
	1800	79.4	33
	1900	92.0	34
	2010	-	35
	1040	49.2	36
	1140	41.0	37
	1210	38.2	38
	1237	36.8	39
	1412	40.2	40
	1436	42.9	41

TABLE 8.2. RUN INDEX FOR WSMR, 1977-1979

Date	Local Time*	Solar Zenith Angle	Sequence No.				
09-20-77	1135	37.3°	1	10-12-77	1230	40.6°	41
09-23-77	1135	38.3	2		1300	40.0	42
	1205	35.1	3		1315	40.2	43
	1713	67.8	4		1331	40.7	44
	1735	72.4	5		1400	42.5	45
09-26-77	0830	71.9	6		1426	45.0	46
	0930	59.9	7		1443	46.9	47
	1030	49.0	8		1505	49.9	48
	1130	39.9	9		1525	52.9	49
	1230	34.6	10		1549	56.8	50
	1330	34.6	11	10-19-77	0930	65.7	51
	1430	40.0	12		1030	55.6	52
	1515	46.5	13		1130	47.7	53
09-27-77	1015	51.8	14		1230	43.2	54
	1253	34.3	15		1330	43.2	55
09-28-77	1253	34.6	16		1430	47.7	56
09-29-77	0755	79.8	17	10-25-77	1253	44.7	57
	0845	69.6	18	10-26-77	0953	63.4	58
	0953	56.4	19		1053	54.3	59
	1053	46.1	20		1153	47.8	60
	1153	38.4	21		1253	45.0	61
	1253	35.0	22		1353	46.8	62
	1400	37.8	23		1705	73.8	63
	1415	39.3	24	10-31-77	1155	46.7	64
	1430	41.0	25	11-01-77	1153	47.0	65
	1445	43.0	26	11-02-77	0855	64.7	66
	1500	45.1	27		0930	59.3	67
	1535	50.7	28		1000	55.3	68
	1551	53.5	29		1030	51.9	69
	1609	56.8	30		1100	49.4	70
09-30-77	1255	35.4	31		1130	47.8	71
10-05-77	1253	37.4	32		1200	47.3	72
10-10-77	1253	39.3	33		1230	47.8	73
10-11-77	1253	39.7	34		1300	49.4	74
	1320	39.9	35		1330	52.0	75
10-12-77	0833	74.9	36		1403	55.7	76
	0930	63.9	37		1430	59.4	77
	1115	47.2	38		1500	64.0	78
	1130	45.4	39	11-03-77	0900	64.1	79
	1215	41.4	40		0930	59.6	80

* Mountain daylight time thru 10-26-77,
Mountain standard time from 10-31-77.

Note: Mountain daylight times on the data plots are marked with a '●'.

Table 8.2 (cont)

<u>Date</u>	<u>Local Time*</u>	<u>Solar Zenith Angle</u>	<u>Sequence No.</u>				
11-03-77	1001	55.4°	81	11-05-77	0615	95.3°	121
	1030	52.2	82		0645	89.2	122
	1100	49.7	83		0715	83.3	123
	1131	48.1	84		0745	77.6	124
	1200	47.6	85		0815	72.2	125
	1230	48.1	86		0831	69.4	126
	1300	49.7	87		0900	64.6	127
	1330	52.2	88		0930	60.1	128
	1400	55.6	89		1000	56.1	129
	1430	59.6	90		1030	52.8	130
	1500	64.2	91		1100	50.3	131
	1530	69.2	92		1130	48.7	132
11-04-77	1225	48.3	93		1200	48.2	133
	1300	50.0	94		1230	48.7	134
	1330	52.5	95		1300	50.3	135
	1400	55.9	96		1330	52.8	136
	1430	59.9	97		1400	56.1	137
	1500	64.4	98	11-09-77	0930	61.0	138
	1530	69.4	99		1000	57.1	139
	1600	74.7	100		1030	53.8	140
	1630	80.3	101		1100	51.4	141
	1645	83.2	102		1130	49.9	142
	1700	86.2	103		1200	49.3	143
	1715	89.1	104		1230	49.9	144
	1730	92.1	105		1300	51.4	145
	1745	95.2	106		1330	53.9	146
	1830	-	107		1400	57.1	147
	1900	-	108		1430	61.0	148
	2000	-	109		1500	65.5	149
	2100	-	110	11-22-77	0945	61.7	150
	2200	-	111	11-23-77	1130	53.2	151
	2300	-	112		1200	52.8	152
11-05-77	0000	-	113		1230	53.3	153
	0100	-	114		1300	54.7	154
	0200	-	115		1345	58.5	155
	0300	-	116		1415	61.9	156
	0400	-	117		1445	65.9	157
	0500	-	118		1520	71.2	158
	0545	-	119	12-07-77	0930	65.6	159
	0600	98.3	120		1000	62.0	160

* Mountain standard time.

Table 8.2 (cont)

Date	Local Time*	Solar Zenith Angle	Sequence No.				
12-07-77	1030	59.1*	161	01-04-78	1245	56.4	201
	1100	56.8	162		1315	58.2	202
	1130	55.5	163		1345	60.8	203
	1200	55.0	164		1415	64.0	204
	1230	55.5	165		1445	67.9	205
	1300	56.9	166	01-11-78	1015	60.1	206
	1330	59.1	167		1045	57.4	207
	1400	62.0	168		1115	55.6	208
	1430	65.7	169		1145	54.7	209
	1500	69.8	170		1215	54.7	210
12-14-77	1015	61.0	171	01-18-78	1345	60.0	211
	1045	58.4	172		1415	63.4	212
	1115	56.7	173		1445	67.3	213
	1145	55.7	174		0935	63.7	214
	1215	55.7	175		1000	60.6	215
	1245	56.7	176		1100	55.3	216
	1300	57.4	177		1130	53.9	217
	1315	58.4	178		1230	53.9	218
	1330	59.6	179		1300	55.3	219
	1400	62.6	180		1330	57.6	220
12-21-77	1015	61.3	181	01-25-78	1400	60.6	221
	1044	58.8	182		1430	64.3	222
	1115	56.9	183		1500	68.6	223
	1145	56.0	184		0930	63.2	224
	1215	56.0	185		1000	59.4	225
	1245	56.9	186		1030	56.3	226
	1315	58.7	187		1100	53.9	227
	1345	61.3	188		1130	52.5	228
	1415	64.5	189		1200	52.0	229
	1445	68.4	190		1230	52.5	230
12-28-77	1130	56.3	191	02-01-78	1300	53.9	231
	1200	55.8	192		1330	56.2	232
	1230	56.3	193		1400	59.4	233
01-04-78	0915	67.9	194		1430	63.1	234
	0945	64.1	195		0900	66.2	235
	1015	60.8	196		0930	61.8	236
	1045	58.2	197		1000	57.9	237
	1115	56.4	198		1030	54.7	238
	1145	55.5	199		1100	52.3	239
	1215	55.5	200		1130	50.8	240

* Mountain standard time.

Table 8.2 (cont)

Date	Local Time*	Solar Zenith Angle	Sequence No.				
02-01-78	1200	50.3°	241	03-22-78	1245	34.8°	281
	1230	50.8	242		1315	37.6	282
	1300	52.3	243		1345	41.4	283
	1330	54.7	244		1415	46.0	284
	1400	57.9	245		1445	51.1	285
	1430	61.7	246	03-29-78	1000	41.5	286
	1520	69.3	247		1030	37.1	287
02-08-78	0920	61.6	248		1100	33.6	288
	1000	56.2	249		1130	31.2	289
	1030	52.9	250		1200	30.4	290
	1100	50.4	251		1230	31.2	291
	1345	54.4	252		1300	33.5	292
	1415	58.1	253		1330	37.0	293
	1445	62.3	254		1400	41.5	294
02-15-78	0900	63.1	255		1430	46.5	295
	1000	54.3	256	04-05-78	1000	39.4	296
	1030	50.9	257		1030	34.8	297
	1100	48.3	258		1100	31.1	298
	1225	46.5	259		1130	28.6	299
	1335	51.4	260		1200	27.7	300
	1415	56.3	261		1230	28.6	301
	1445	60.6	262		1300	31.0	302
02-22-78	1045	47.3	263		1330	34.8	303
	1115	45.1	264		1400	39.4	304
	1145	43.9	265		1430	44.6	305
	1215	43.9	266	04-13-78	1445	45.5	306
	1245	45.0	267		1515	51.4	307
03-01-78	1240	42.3	268		1545	57.5	308
	1310	44.5	269		1615	63.7	309
	1330	46.5	270		1645	70.0	310
	1355	49.5	271	04-14-78	1043	30.2	311
03-15-78	1210	36.0	272		1115	26.5	312
	1230	36.6	273		1145	24.5	313
	1300	38.6	274		1215	24.5	314
	1330	41.8	275		1245	26.4	315
	1400	45.8	276		1315	29.9	316
03-22-78	1045	37.6	277		1345	34.4	317
	1115	34.9	278		1415	39.6	318
	1145	33.4	279		1445	45.2	319
	1215	33.4	280		1515	51.2	320

* Mountain standard time.

Table 8.2 (cont)

Date	Local Time *	Solar Zenith Angle	Sequence No.				
07-19-78	1315	11.8°	321	08-18-78	0955	46.3°	361
	1400	17.5	322		1025	40.2	362
	1430	23.0	323		1055	34.3	363
	1500	28.9	324		1125	28.9	364
07-21-78	1445	26.1	325		1155	24.2	365
08-07-78	1100	31.3	326		1225	20.7	366
	1130	25.7	327		1255	19.2	367
	1200	21.2	328		1325	20.0	368
	1250	15.9	329		1400	23.6	369
	1310	15.9	330	12-21-78	1125	56.5	370
08-14-78	1030	38.5	331		1150	55.9	371
	1100	32.6	332	01-22-79	1200	52.7	372
	1200	22.5	333		1215	52.8	373
	1230	20.0	334		1230	53.2	374
	1300	17.9	335	05-25-79	1130	23.4	375
	1330	19.1	336		1200	18.0	376
	1400	22.5	337		1230	13.8	377
	1430	27.2	338		1300	12.0	378
08-16-78	0900	57.4	339		1330	13.7	379
	0930	51.1	340	06-29-79	1000	40.5	380
	1000	44.9	341		1030	34.2	381
	1030	38.8	342		1100	27.9	382
	1100	33.0	343		1130	21.8	383
	1130	27.6	344		1200	16.0	384
	1200	23.0	345		1230	11.2	385
	1230	19.7	346		1300	9.0	386
	1300	18.5	347		1330	11.2	387
	1330	19.7	348		1400	16.0	388
	1400	23.0	349	07-09-79	1150	18.3	389
08-17-78	0900	57.5	350		1230	11.8	390
	0925	52.3	351		1320	11.8	391
	0950	47.1	352		1400	16.5	392
	1025	40.0	353		1424	21.0	393
	1055	34.1	354		1445	25.2	394
	1125	28.7	355	07-10-79	1120	24.2	395
	1155	24.0	356		1153	17.8	396
	1225	20.4	357		1240	10.8	397
	1250	19.0	358		1400	16.6	398
	1330	20.0	359		1430	22.2	399
08-18-78	0935	50.4	360	07-11-79	1000	40.9	400

* All times are mountain daylight, except on 12-21-78 and 01-22-79, which are mountain standard.

Table 8.2 (cont)

<u>Date</u>	<u>Local Time*</u>	<u>Solar Zenith Angle</u>	<u>Sequence No.</u>
07-11-79	1030	34.6°	401
	1100	28.3	402
	1130	22.3	403
	1200	16.6	404
	1230	12.0	405
	1315	10.5	406
	1345	14.1	407
	1430	22.3	408
	1625	47.9	409
08-01-79	1700	55.3	410
	1740	63.7	411
	1815	71.1	412
	1845	77.3	413

* Mountain daylight time

TABLE 8.3. RUN INDEX FOR BALMERTOWN, CANADA, 1979

Date	Time, Central Std.	Solar Zenith Angle	Sequence No.				
02-08-79	1100	68.3	1				
	1155	67.1	2	02-17-79	1730	95.5	51
	1320	69.3	3		1740	97.0	52
	1355	71.6	4		1815	-	53
	1455	77.1	5	02-18-79	0845	76.7	54
	1645	91.1	6		0905	74.4	55
02-09-79	0850	78.6	7		0950	69.9	56
	1130	67.1	8		1050	65.7	57
	1700	93.0	9		1150	63.9	58
02-10-79	1305	67.9	10		1250	64.8	59
	1355	71.0	11		1350	68.2	60
	1510	78.3	12	02-19-79	1425	71.2	61
02-11-79	0930	73.8	13		0830	78.2	62
	1000	71.2	14		0905	74.1	63
	1050	67.9	15		0950	69.6	64
	1200	66.1	16		1050	65.4	65
	1300	67.4	17		1150	63.6	66
02-12-79	0800	84.0	18		1250	64.5	67
	0900	76.7	19		1350	67.9	68
	2215	-	20		1415	70.0	69
02-13-79	0820	81.1	21		1450	73.5	70
	0900	76.4	22		1550	80.6	71
	1000	70.6	23	02-20-79	1650	89.0	72
	1050	67.3	24		0630	94.8	73
	1150	65.6	25		0700	90.3	74
	1335	68.7	26		0730	85.9	75
	1400	70.5	27		0850	75.5	76
	1500	76.3	28		0910	73.2	77
	1520	78.6	29		0950	69.3	78
	1600	83.6	30		1050	65.0	79
02-16-79	1050	66.3	31		1150	63.3	80
	1150	64.6	32		1250	64.1	81
	1210	64.6	33		1350	67.6	82
	1250	65.5	34		1450	73.1	83
	1350	68.8	35		1550	80.4	84
	1450	74.3	36	02-21-79	1645	88.0	85
	1600	82.8	37		0630	94.6	86
	1700	91.3	38		0700	90.0	87
	1720	94.3	39		0730	85.7	88
	1810	-	40		0850	75.2	89
02-17-79	0850	76.4	41		0950	68.9	90
	0910	74.1	42		1010	67.3	91
	0950	70.2	43		1050	64.7	92
	1050	66.0	44		1150	62.9	93
	1150	64.3	45		1250	63.8	94
	1350	68.5	46		1350	67.2	95
	1410	70.2	47		1450	72.8	96
	1450	74.1	48		1550	80.1	97
	1550	81.2	49	02-22-79	0530	-	98
	1650	89.5	50		0600	98.9	99
					0630	94.3	100

Table 8.3 (cont)

Date	Time, Central Std.	Solar Zenith Angle	Sequence No.				
02-22-79	0700	89.8	101	02-25-79	1115	62.2	151
	0730	85.4	102		1130	61.8	152
	0850	74.9	103		1145	61.6	153
	0950	68.6	104		1200	61.5	154
	1020	66.2	105		1215	61.5	155
	1050	64.3	106		1300	62.8	156
	1150	62.6	107	02-26-79	0540	-	157
	1250	63.4	108		0600	97.9	158
02-23-79	1350	66.9	109		0630	93.2	159
	0530	-	110		0645	90.9	160
	0600	98.7	111		0700	88.6	161
	0630	94.0	112		0716	86.3	162
	0700	89.5	113		0800	80.0	163
	0730	85.1	114		0830	76.1	164
	0850	74.6	115		0900	72.5	165
	0950	68.3	116		0930	69.2	166
02-24-79	1020	65.9	117	02-27-79	1000	66.4	167
	1050	64.0	118		1035	63.8	168
	1120	62.8	119		1045	63.3	169
	1150	62.2	120		1103	62.4	170
	1250	63.1	121		1127	61.5	171
	1350	66.6	122		1150	61.1	172
	1450	72.2	123		1233	61.5	173
	1550	79.5	124		1300	62.5	174
02-25-79	0805	80.0	125		1330	64.1	175
	0830	76.7	126		2100	-	176
	0900	73.1	127		2115	-	177
	0930	69.9	128		2130	-	178
	1000	67.1	129		2145	-	179
	1015	65.9	130		2200	-	180
	1030	64.9	131		2215	-	181
	1045	63.9	132		2230	-	182
02-25-79	1100	63.2	133		2245	-	183
	1115	62.6	134		0530	-	184
	1130	62.2	135		0545	99.9	185
	1145	61.9	136		0552	98.8	186
	1230	62.2	137		0615	95.2	187
	1250	62.8	138		0634	92.3	188
	1350	66.2	139		0645	90.6	189
	1450	71.9	140		0704	87.8	190
02-25-79	1550	79.2	141		0745	81.8	191
	0600	98.1	142		0803	79.3	192
	0800	80.3	143		0825	76.4	193
	0840	75.2	144		0844	74.0	194
	0900	72.8	145		0930	68.9	195
	0930	69.5	146		1000	66.1	196
	1000	66.8	147		1030	63.8	197
	1030	64.5	148		1100	62.1	198
02-25-79	1045	63.6	149				
	1100	62.8	150				

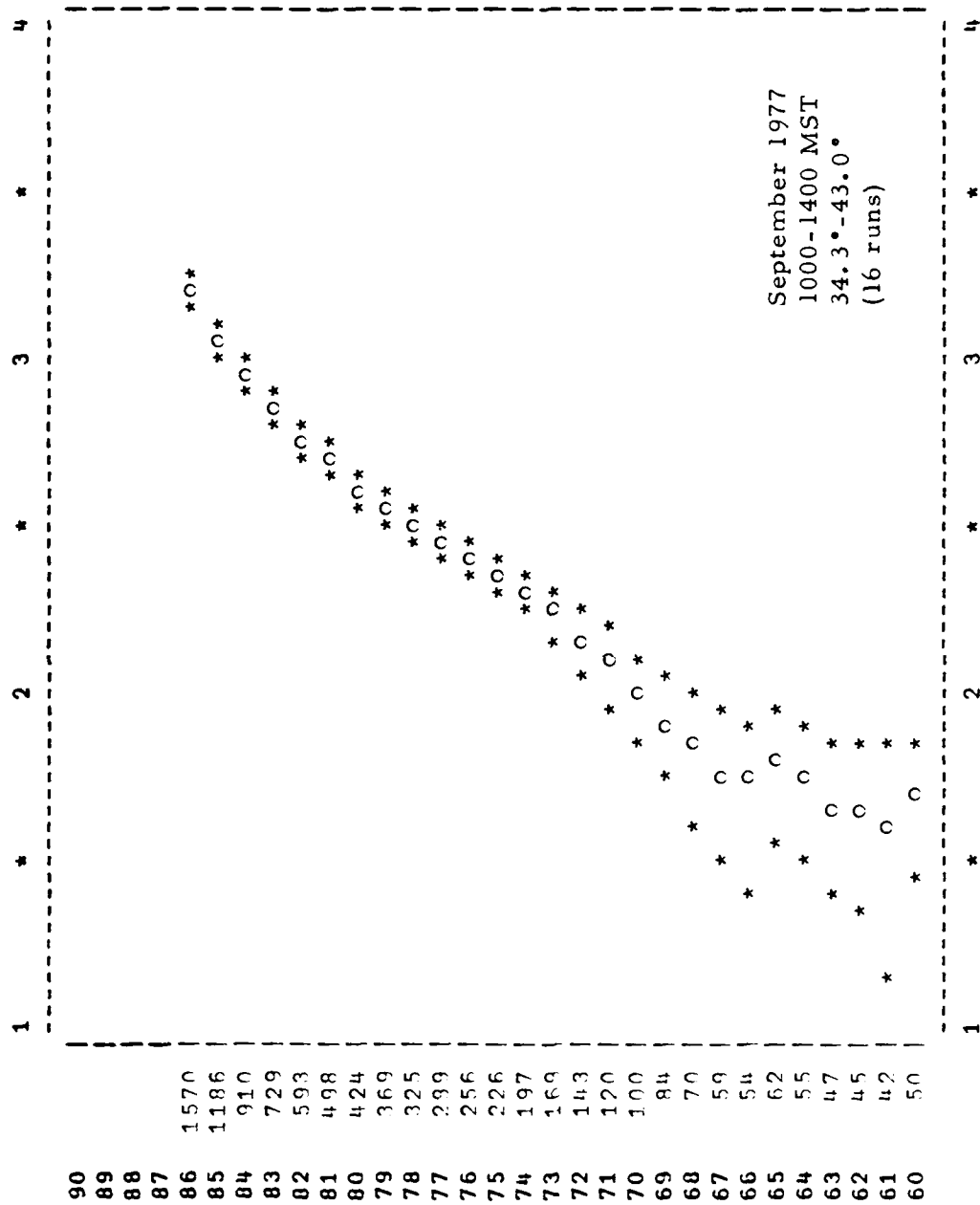


Figure 8.2. Mean and standard deviation electron density profile for September 1977.

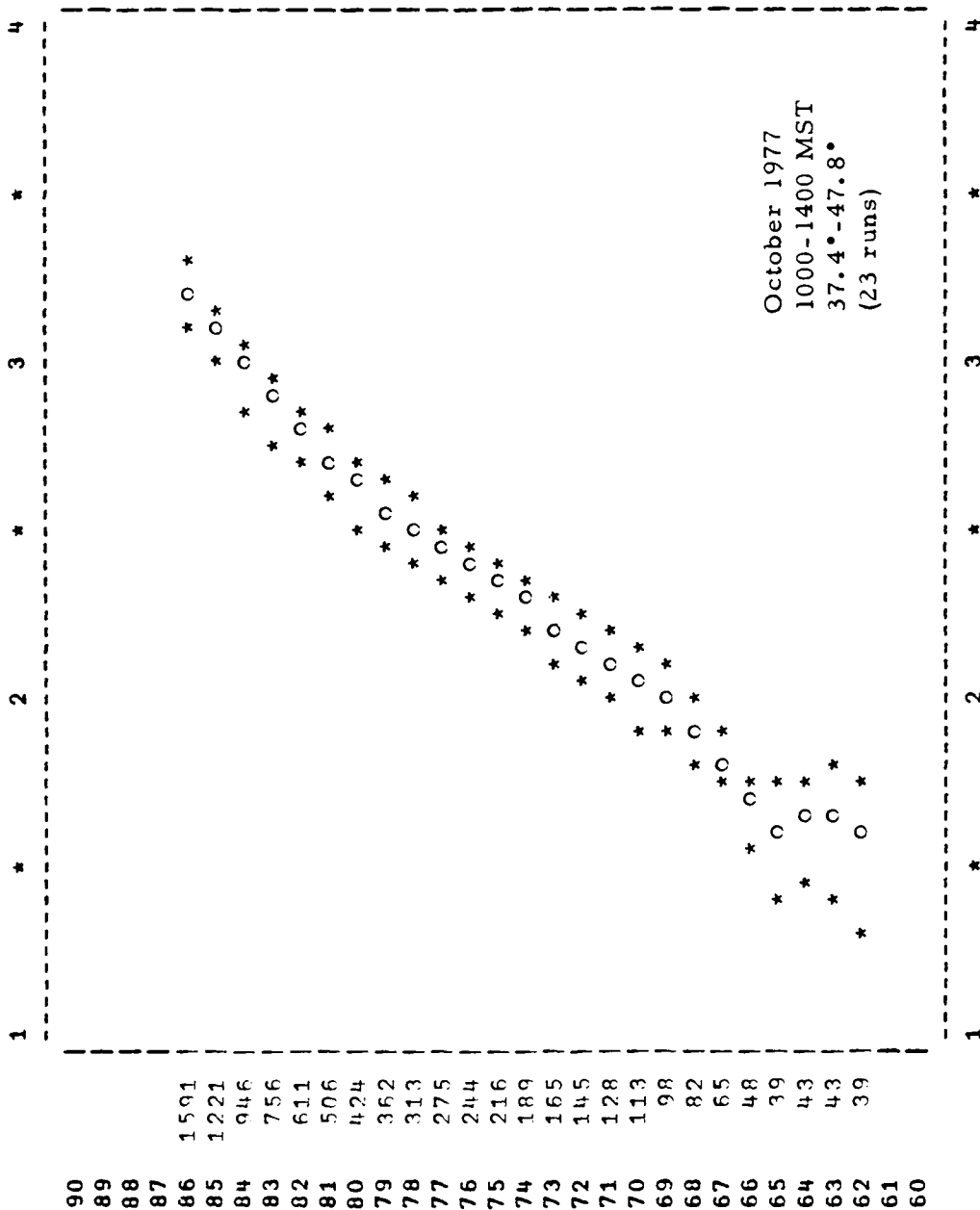


Figure 8.3. Mean and standard deviation electron density profile for October 1977.

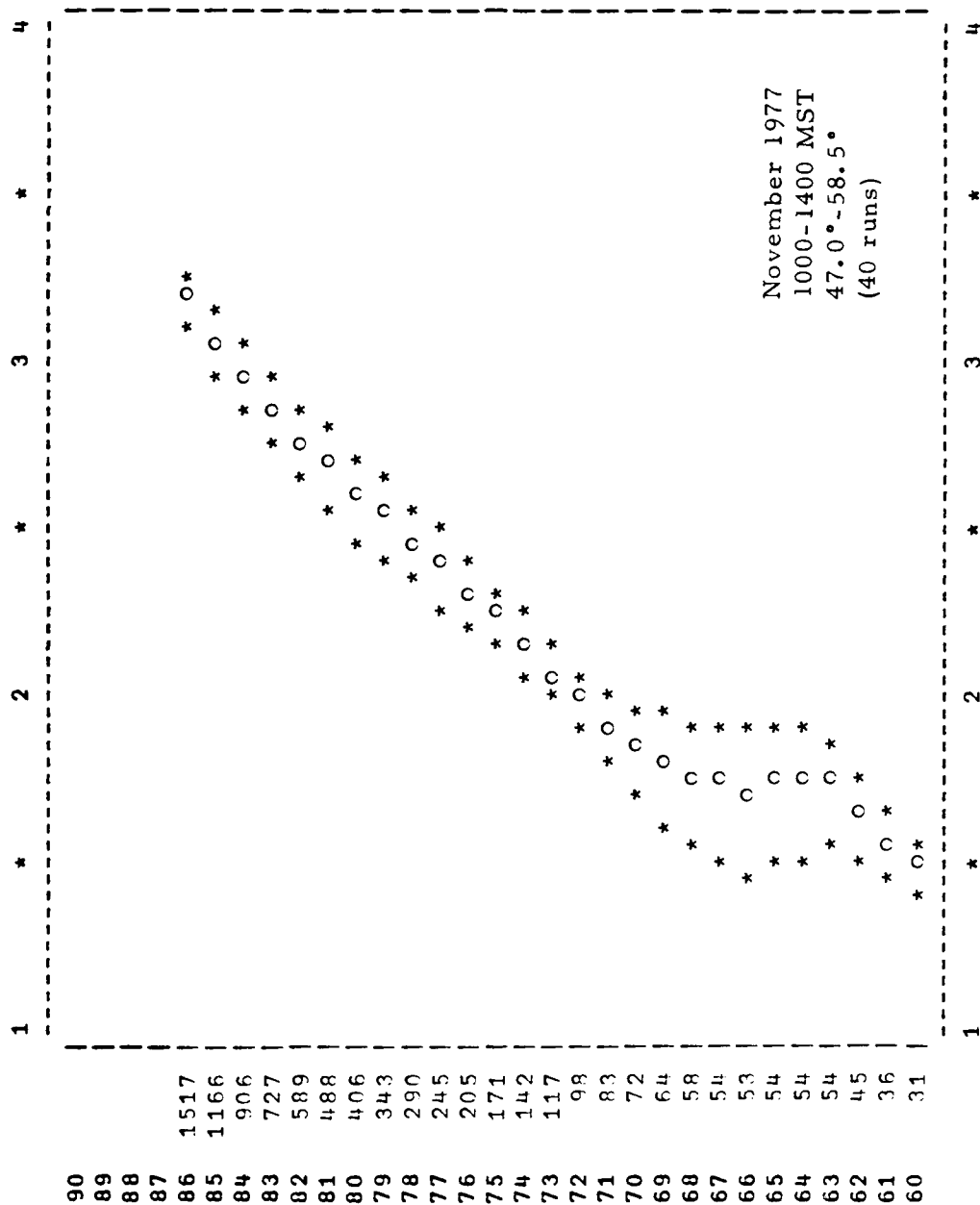


Figure 8.4. Mean and standard deviation electron density profile for November 1977.

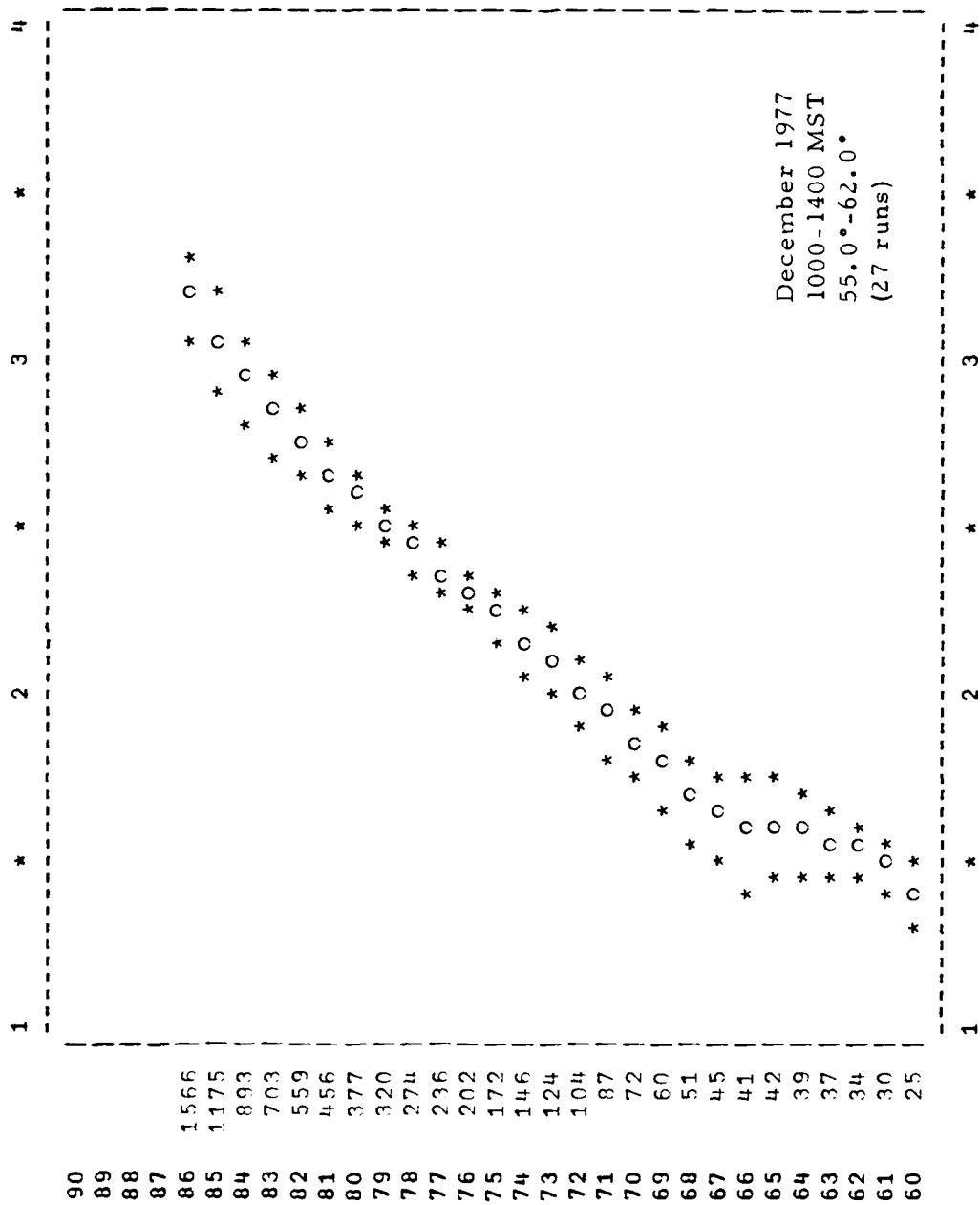


Figure 8.5. Mean and standard deviation electron density profile for December 1977.

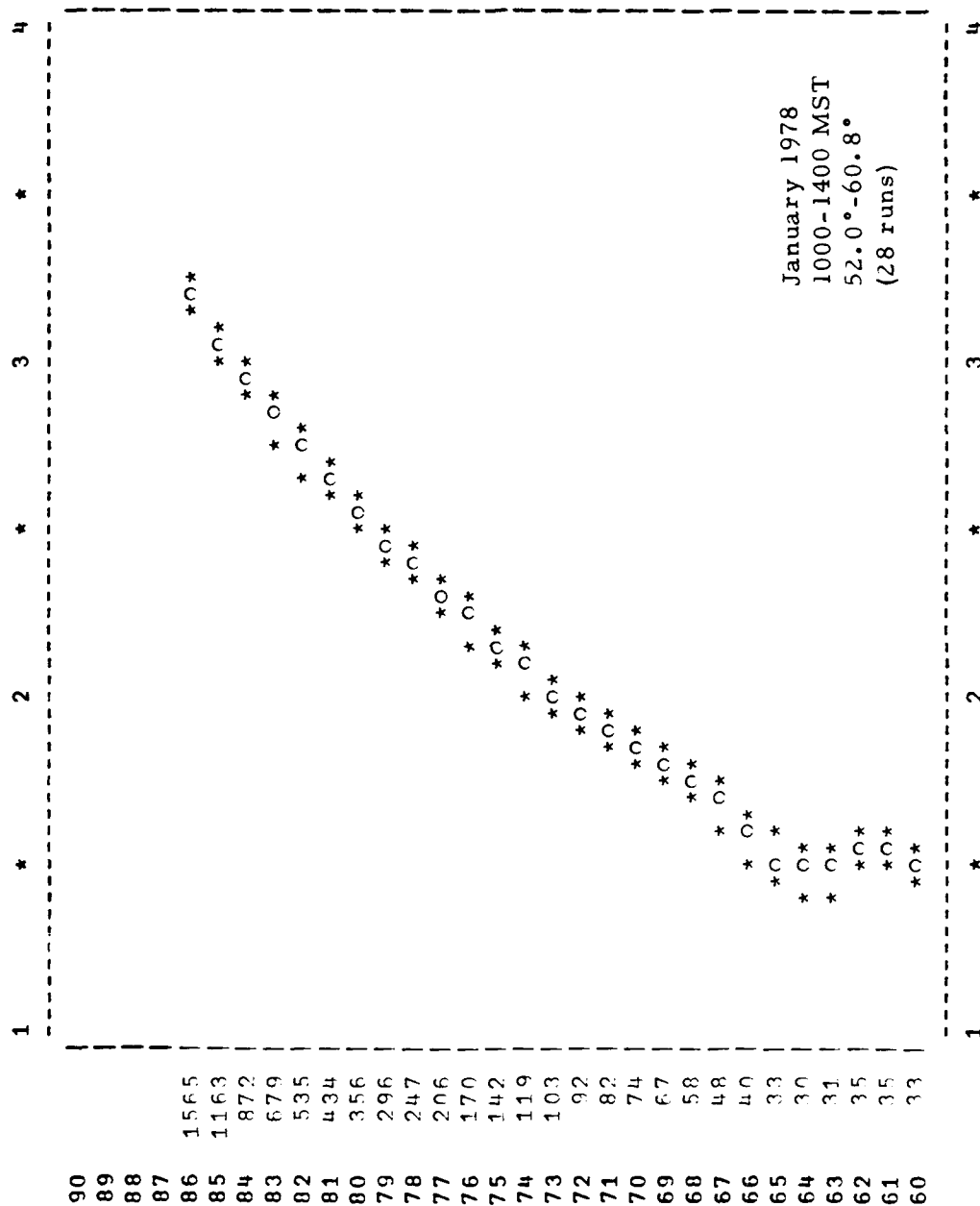


Figure 8.6. Mean and standard deviation electron density profile for January 1977.

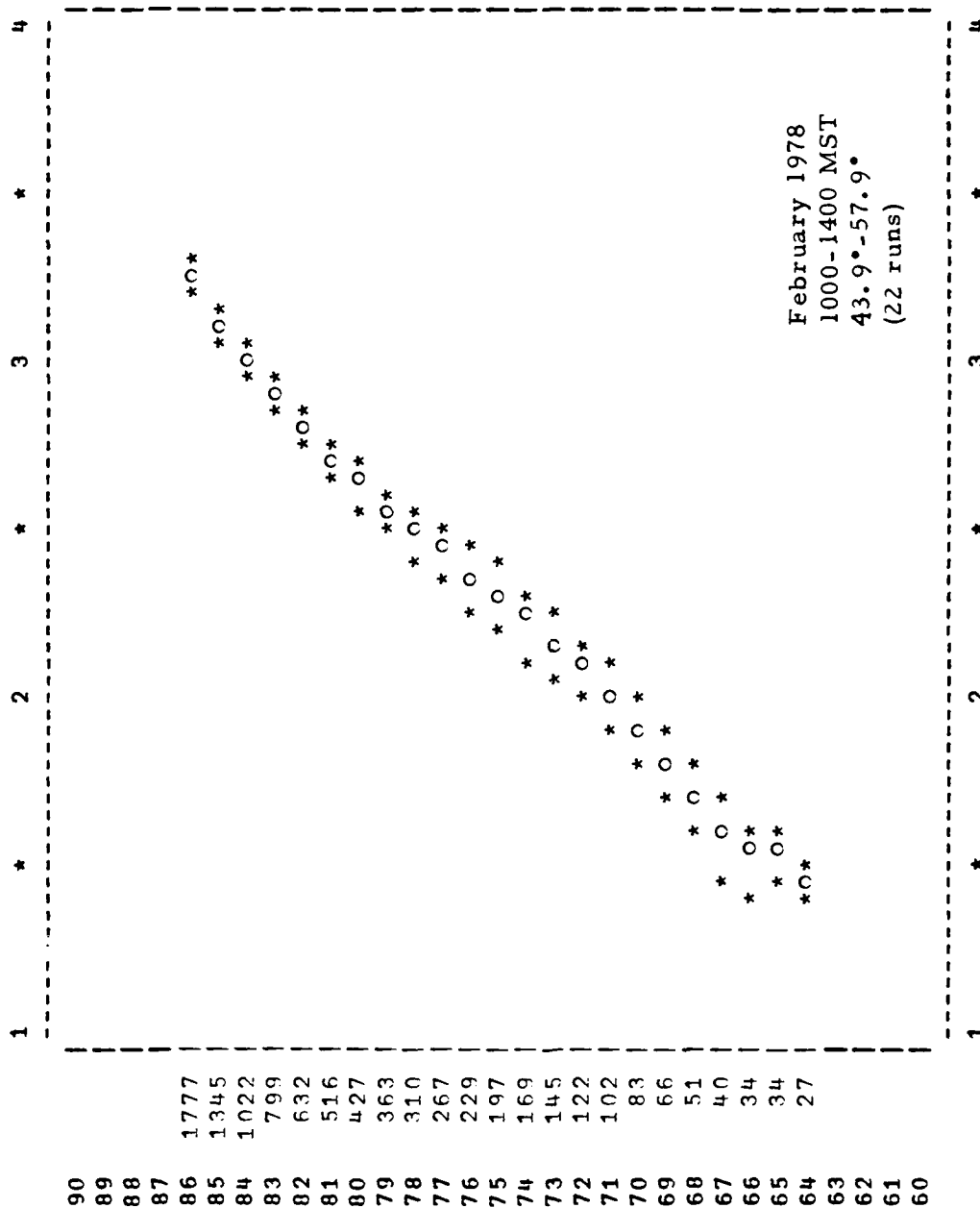


Figure 8.7. Mean and standard deviation electron density profile for February 1977.

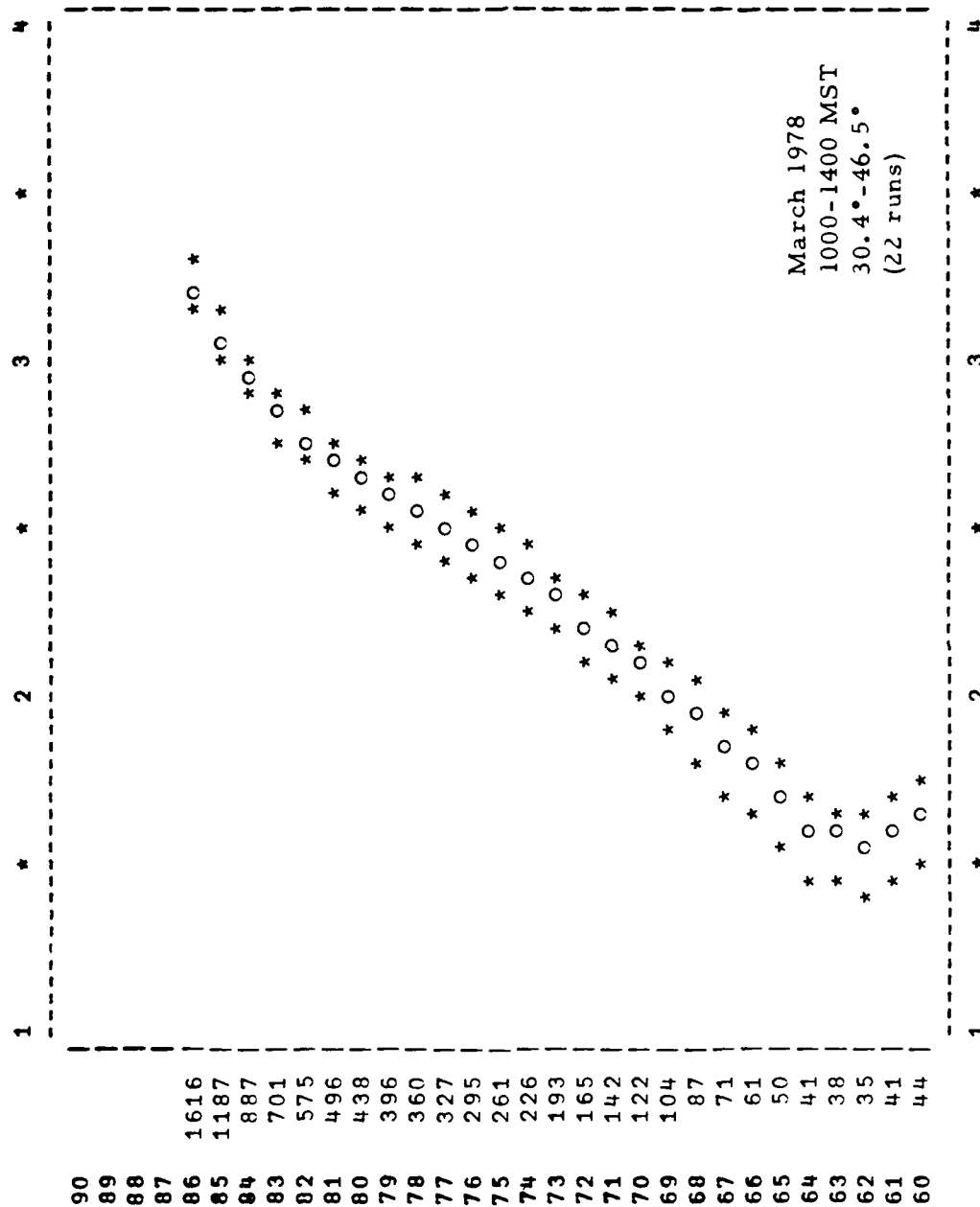


Figure 8.8. Mean and standard deviation electron density profile for March 1977.

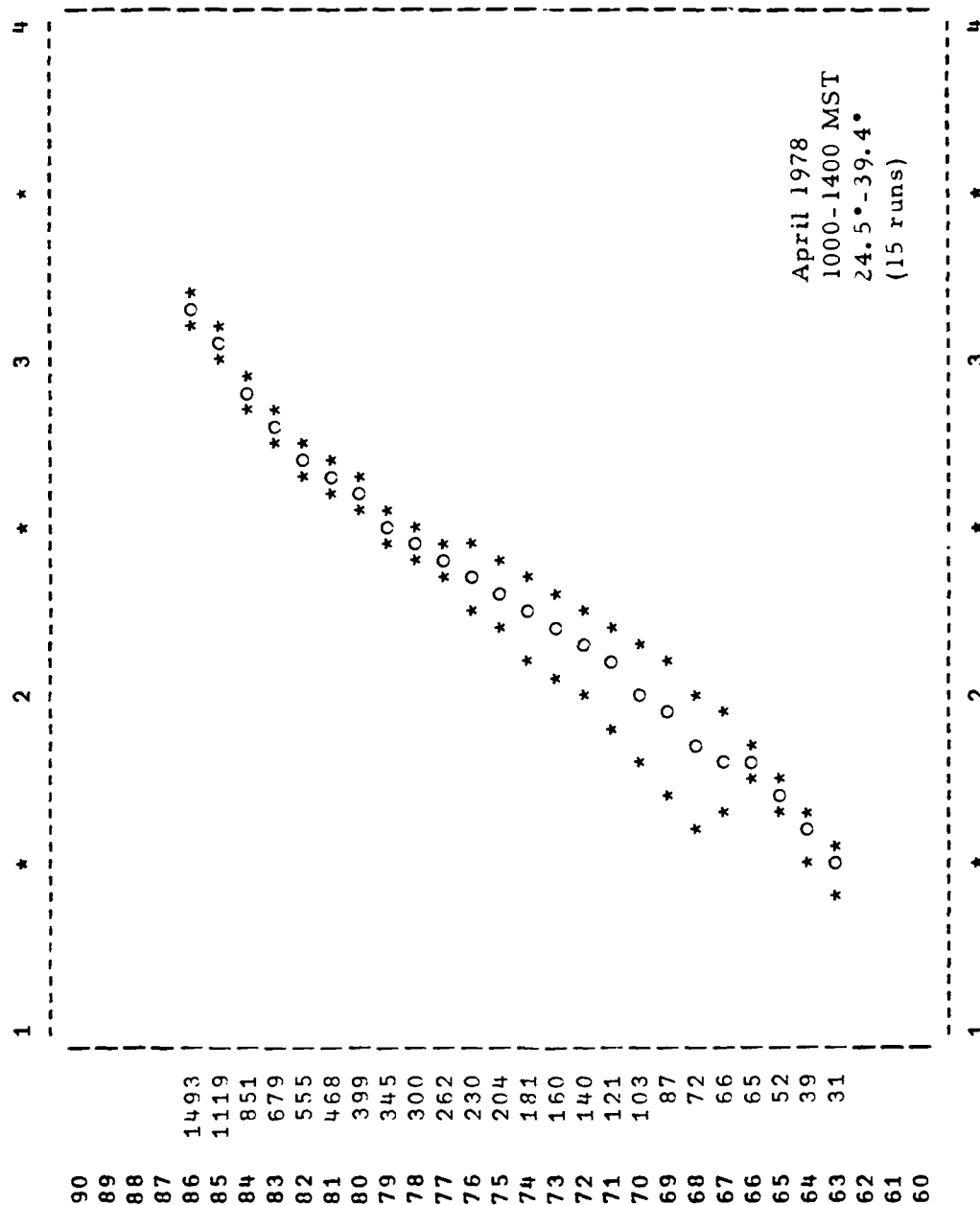


Figure 8.9. Mean and standard deviation electron density profile for April 1977.

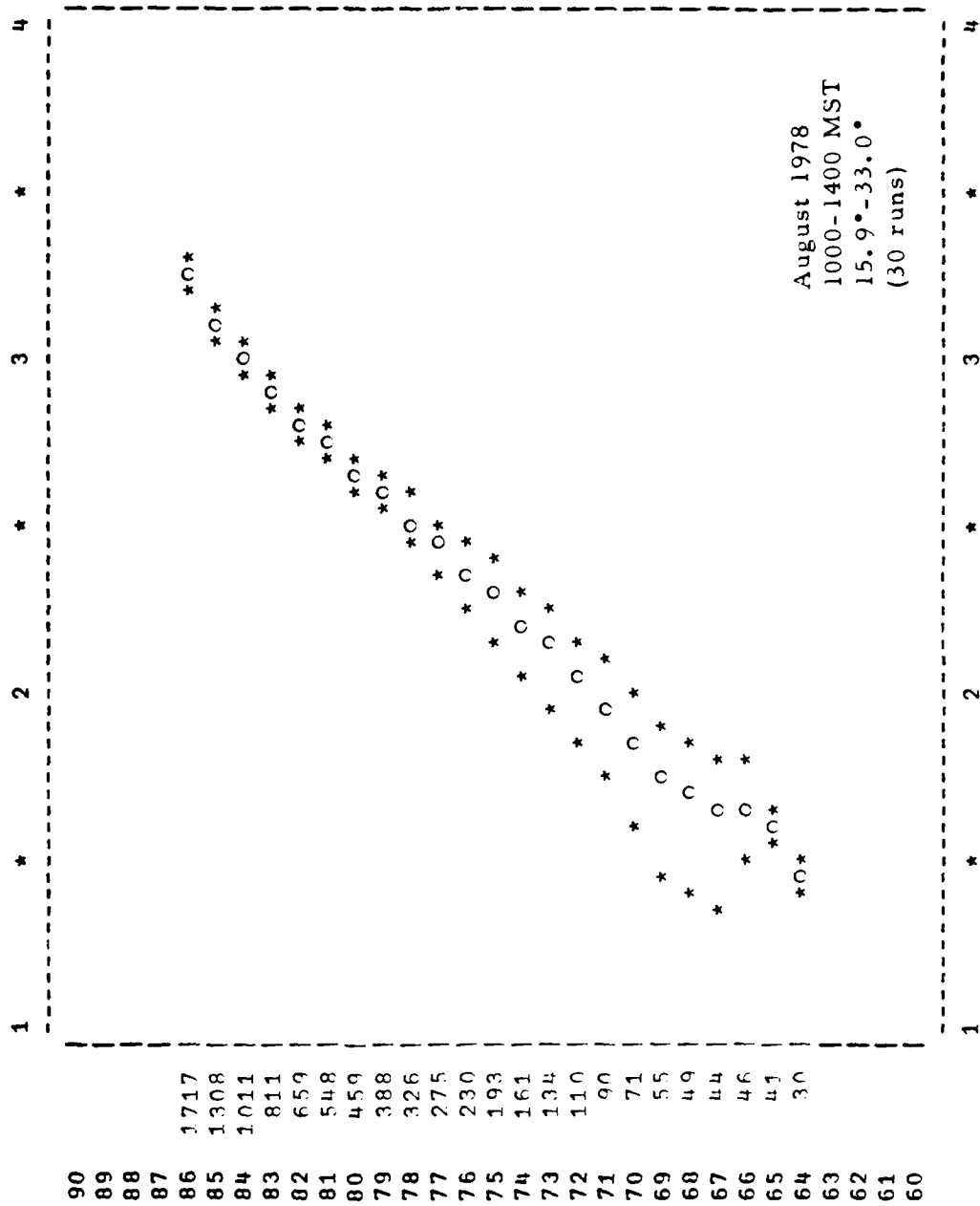


Figure 8.10. Mean and standard deviation electron density profile for May 1977.

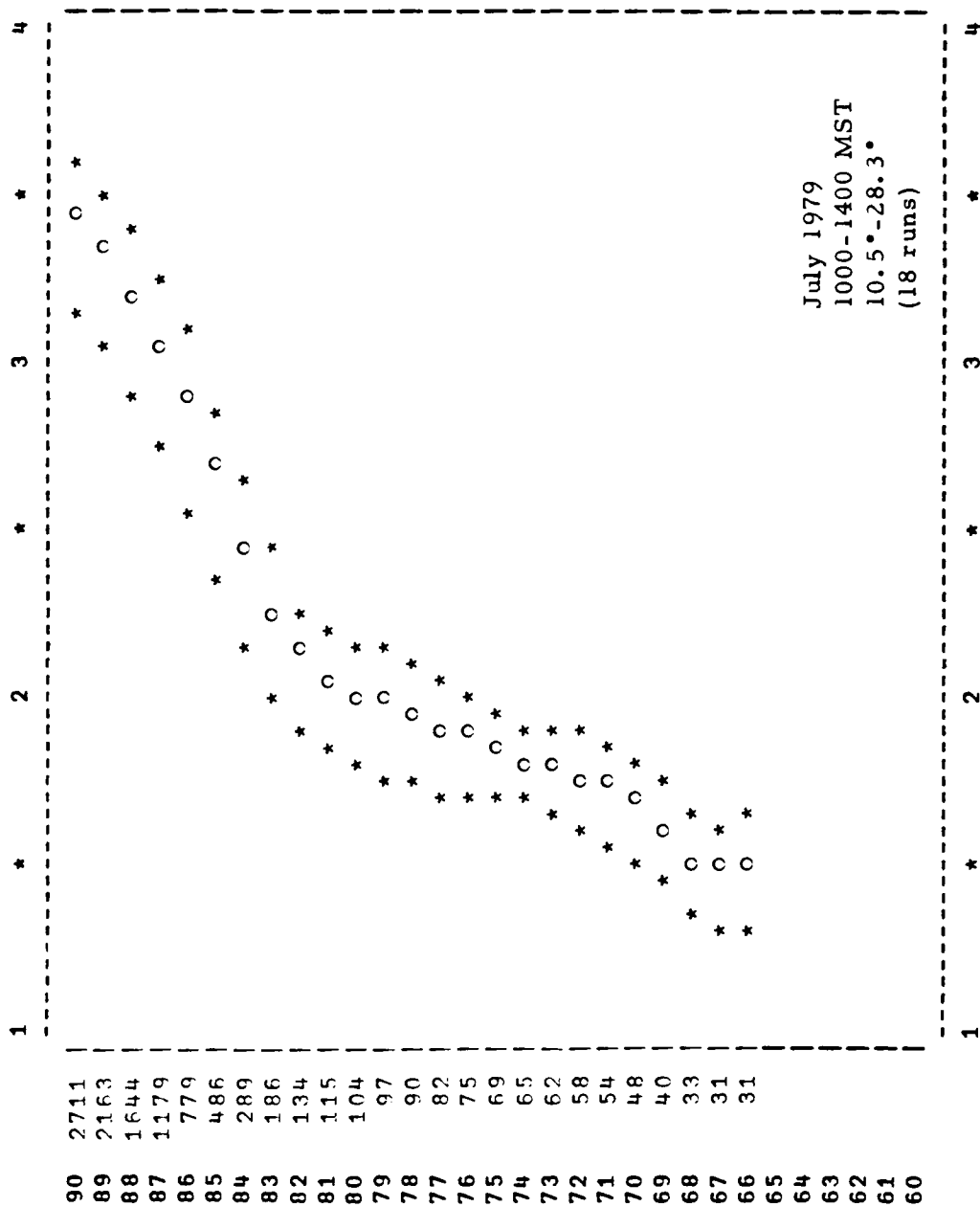


Figure 8.11. Mean and standard deviation electron density profile for June 1977.

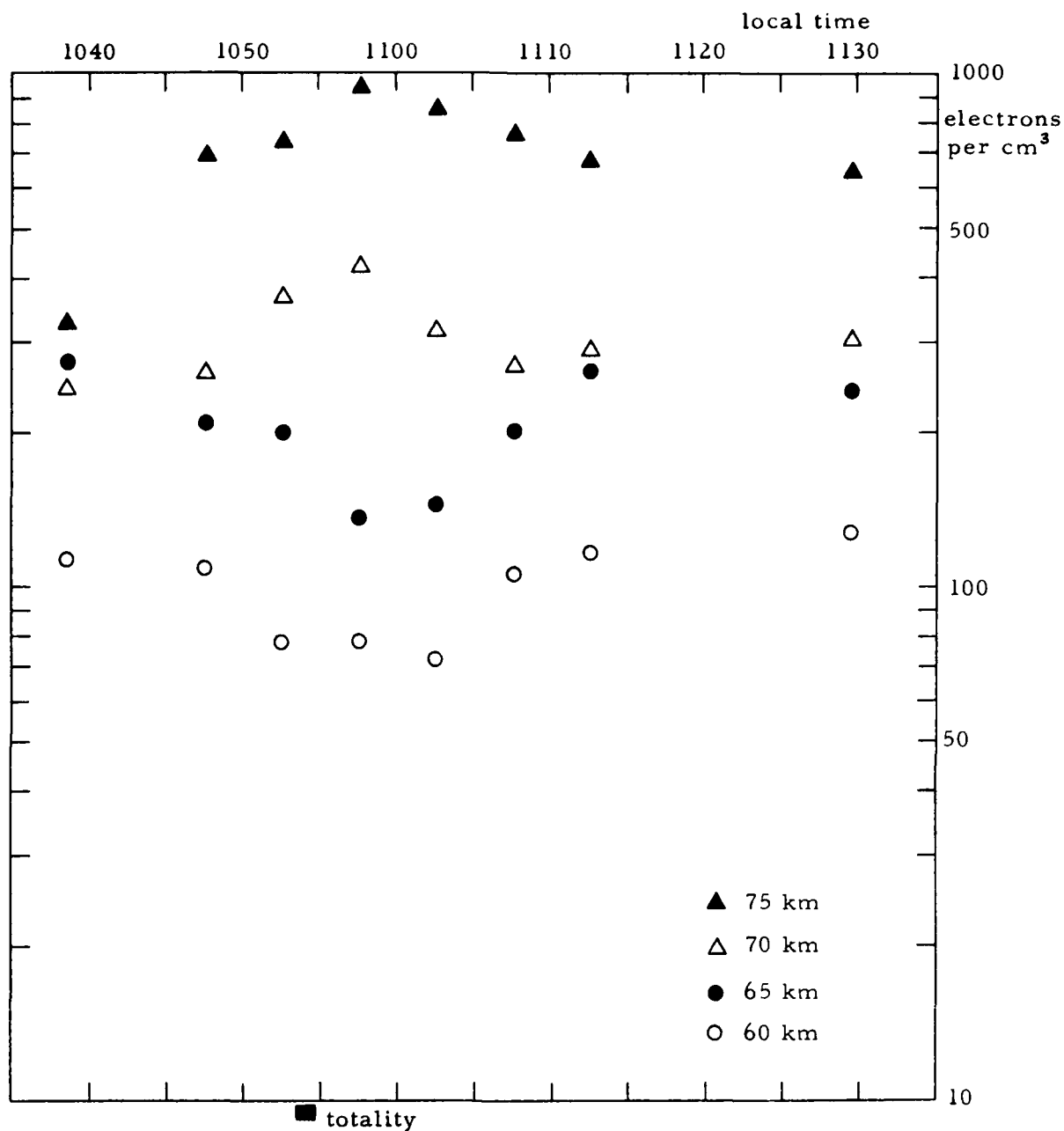


Figure 8.12. Electron density vs. time measured at Balmertroun, Ontario, Canada, during the solar eclipse of 26 February 1979. Data, time averaged over 5-minute intervals, is given for altitudes of 60, 65, 70, and 75 kilometers. Measurements were made by partial reflection.

REFERENCES

1. J.B. Gregory and A.H. Manson, "Seasonal variations of electron densities below 100 km at mid-latitudes-I, differential absorption measurements," J. Atmosph. Terr. Phys., vol. 31, pp. 683-701, 1969.
2. H.K. Sen and A.A. Wyller, "On the generalization of the Appelton-Hartree magneto-ionic formulas," J. Geophys. Res., vol. 65, pp. 3931-3950, 1960.
3. W.A. Flood, "A D-region mid- and high-latitude approximation to the Sen Wyller refractive index equations," to be published. Dr. Flood is with the dept. of electrical engineering, NC State U., Raleigh, NC.
4. H.A. Von Biel, "Amplitude distributions of D-region partial reflections," J. Geophys. Res., vol. 76, pp. 8365-8367, 1971.
5. J.S. Belrose and M.J. Burke, "Study of the lower ionosphere using partial reflections," J. Geophys. Res., vol. 69, pp. 2799-2818, 1964.
6. F.F. Gardner and J.L. Pawsey, "Study of the ionospheric D-region using partial reflections," J. Atmosph. Terr. Phys., vol. 3, pp. 321-344, 1953.
7. H.G. Booker, "Radio scattering in the lower ionosphere," J. Geophys. Res., vol. 64, pp. 2164-2177, 1959.
8. W.A. Kissick, "The effects of artificial ionospheric heating on partial reflections," Scientific report 422, Ionospheric research laboratory, Penn. State Univ., 1 April 1974.
9. M.J. Burke and E.H. Hara, "Tables of the semiconductor integrals $C(x)$ and their approximations for use with the generalized Appelton-Hartree magneto-ionic formulas," Defense Research Telecommunications Establishment Report 113, Ottawa, Canada, 1963.

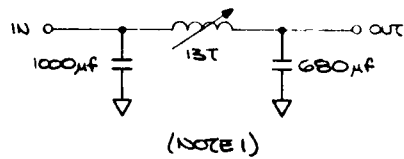
APPENDIX I

Schematic Diagrams

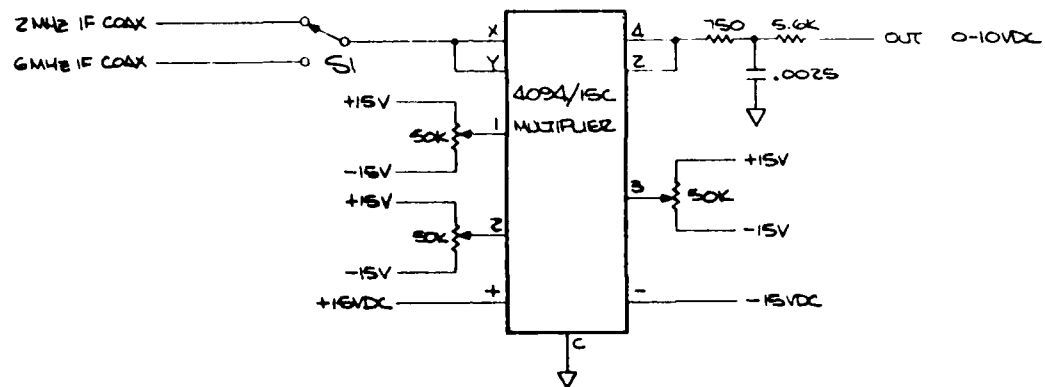
The following schematics for the partial reflection sounder are contained in this Appendix:

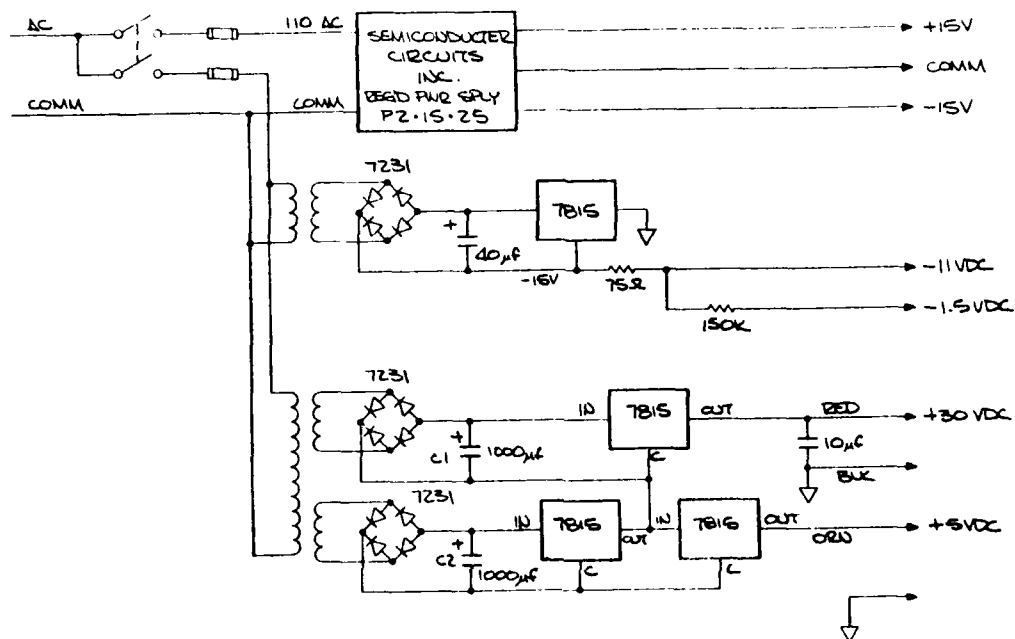
PSL Drawing

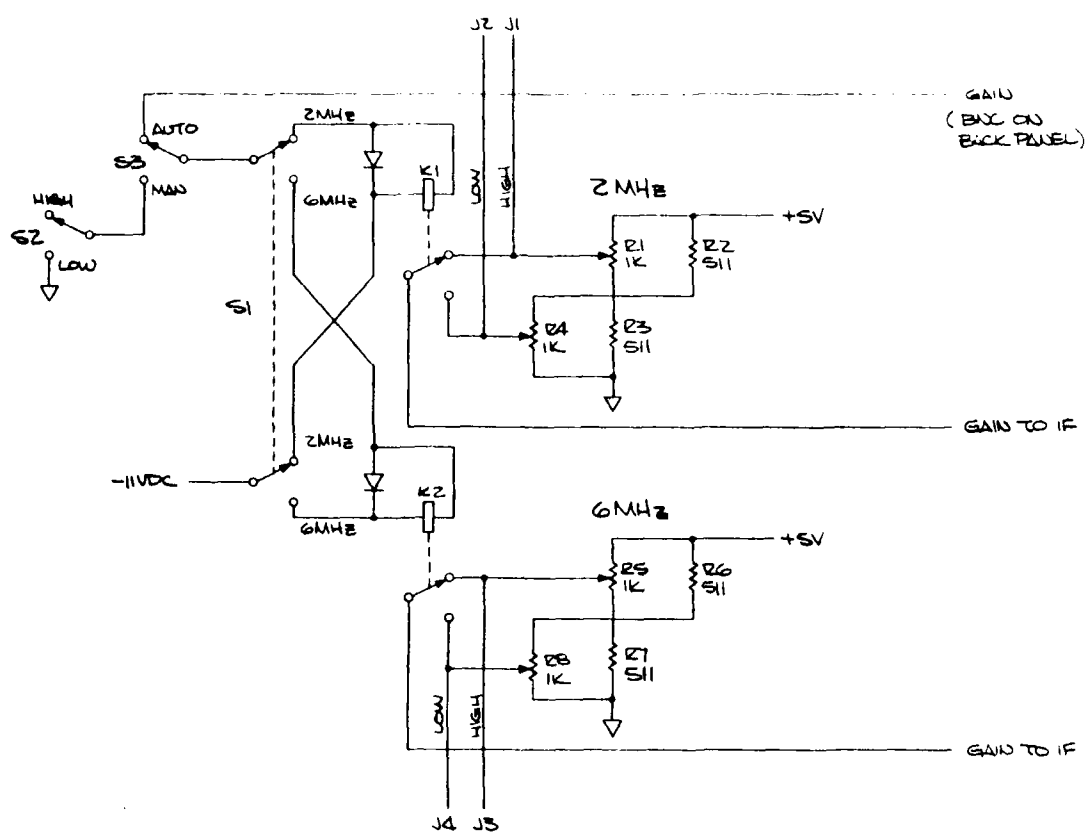
<u>Number</u>	<u>Title</u>	<u>Appendix-I Page No.</u>
012328	Phase Shifter, 2.666 MHz	2
012329	Receiver detector	3
012330	Receiver power supplies	4
012331	IF gain control	5
012332	Scope trigger control	6
012333	Logic control FPB-1, socket 3	7
012334	System control	8
012335	Program control unit detector amplifier, board 7	9
012336	Data converter, card 8	10
012337	Board 10 (sheet 1)	11
012337	Board 10 (sheet 2)	12
012338	Boards 14 and 18	13
012339	Board 13	14
012340	Pulse width	15
012341	Status and control FPB-3 (sheet 1)	16
012341	Status and control FPB-3 (sheet 2)	17
012342	Function control, board 6	18
012343	Clock divider, board 2	19
012344	Record counter FPB-1	20
012345	Over voltage cutoff, board 1	21
012346	Board 19	22
012347	Status logic, board 4	23
012348	Board 16 (sheet 1)	24
012348	Board 16 (sheet 2)	25
012349	Board 12	26
012360	Receiver attenuator section	27
012361	Receiver polarization selector	28
012363	IF amplifier (6 MHz)	29
012363	IF amplifier (2 MHz)	30

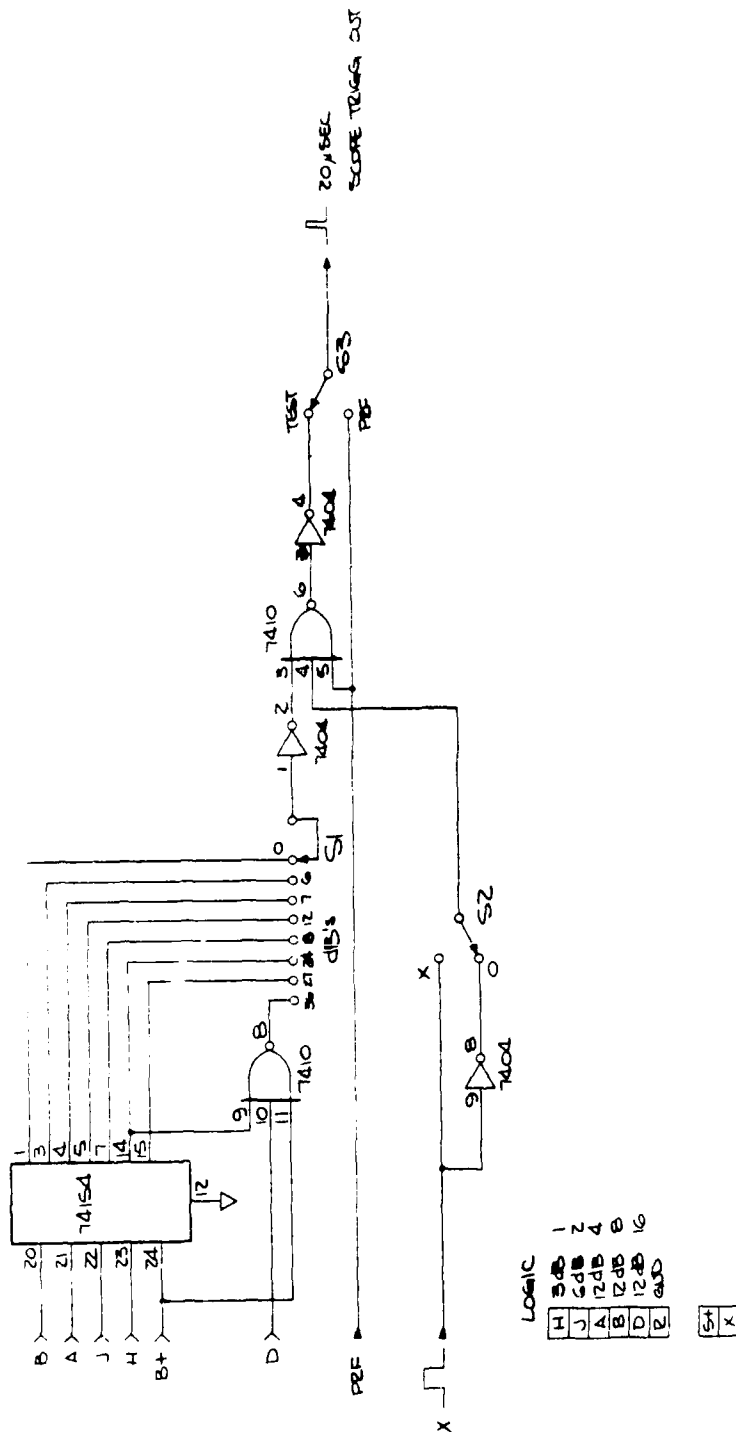


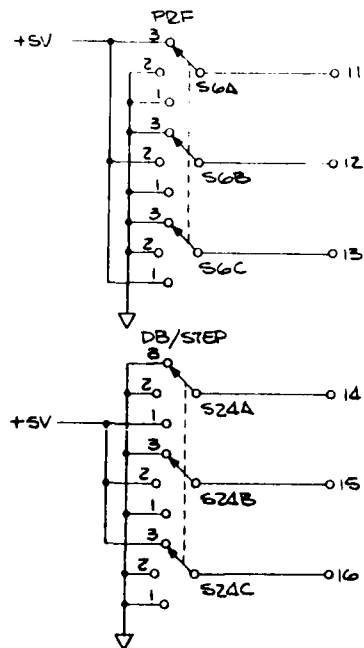
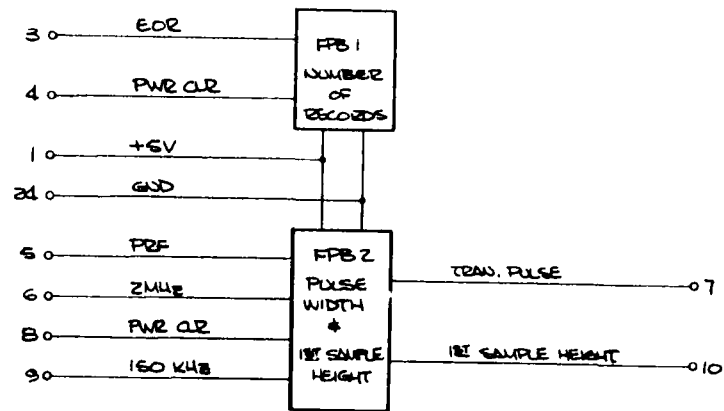
1. BECAUSE OF OUTPUT-INPUT π , THE CAPACITORS ARE NOT EQUAL. THESE VALUES WERE PICKED TO GET 90° SHIFT WITH MINIMAL SIGNAL LOSS.

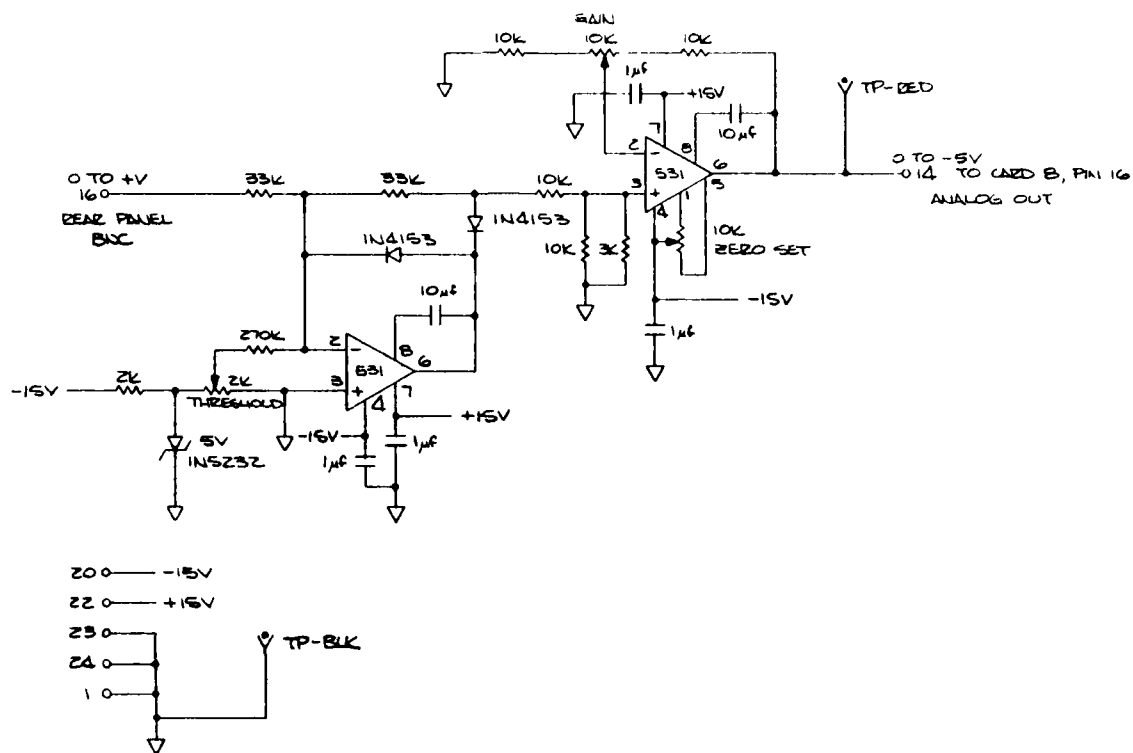


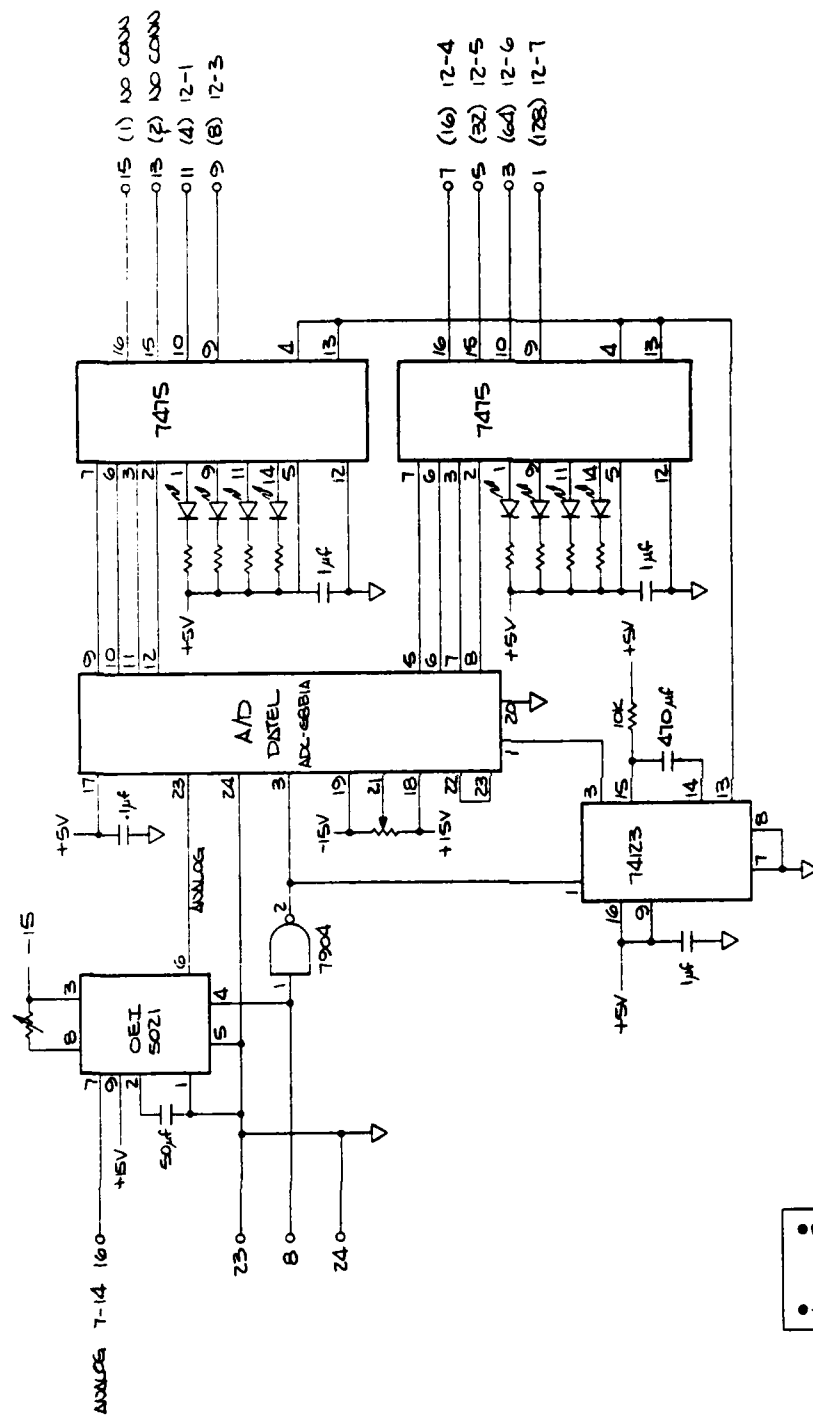






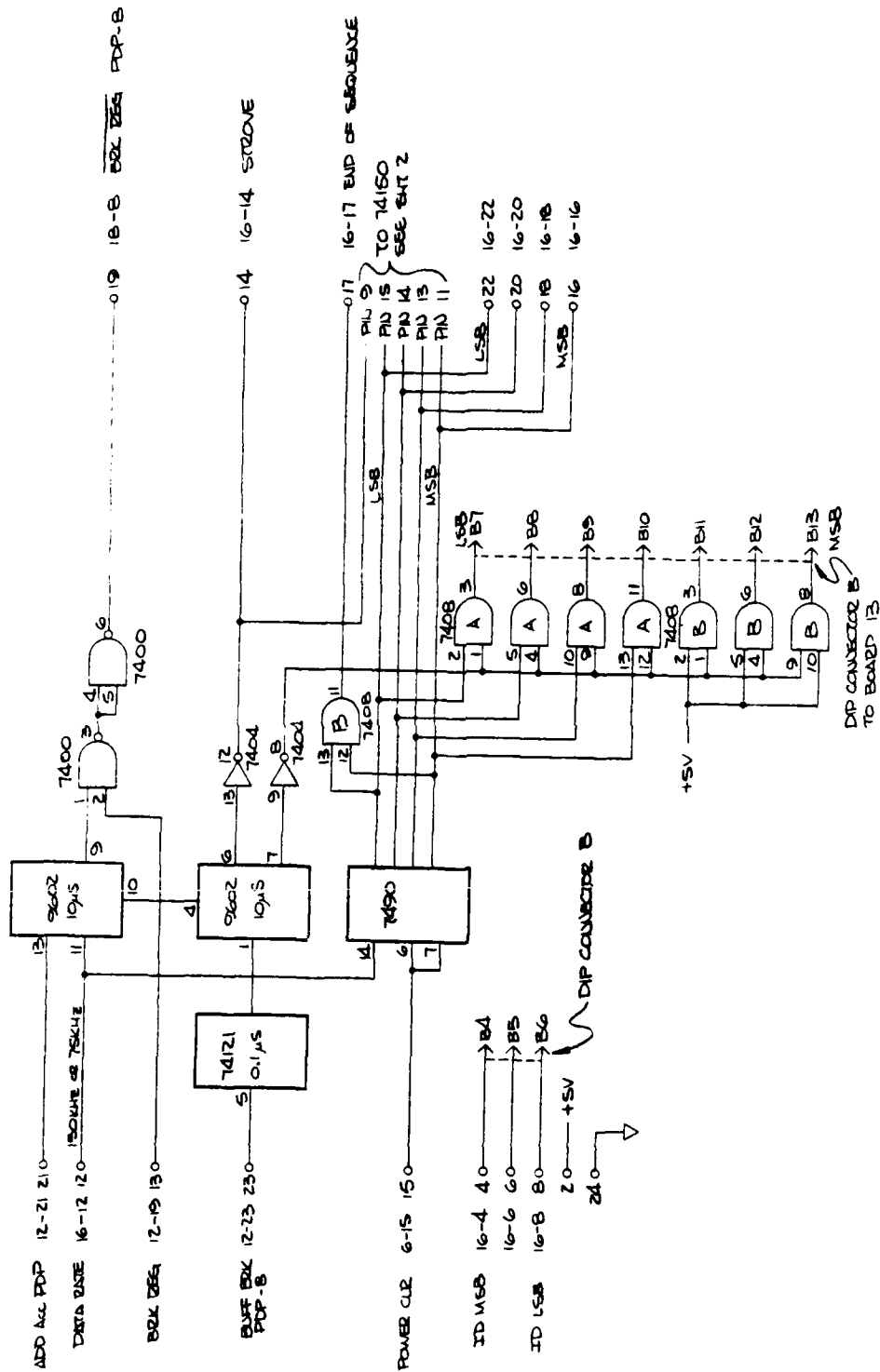






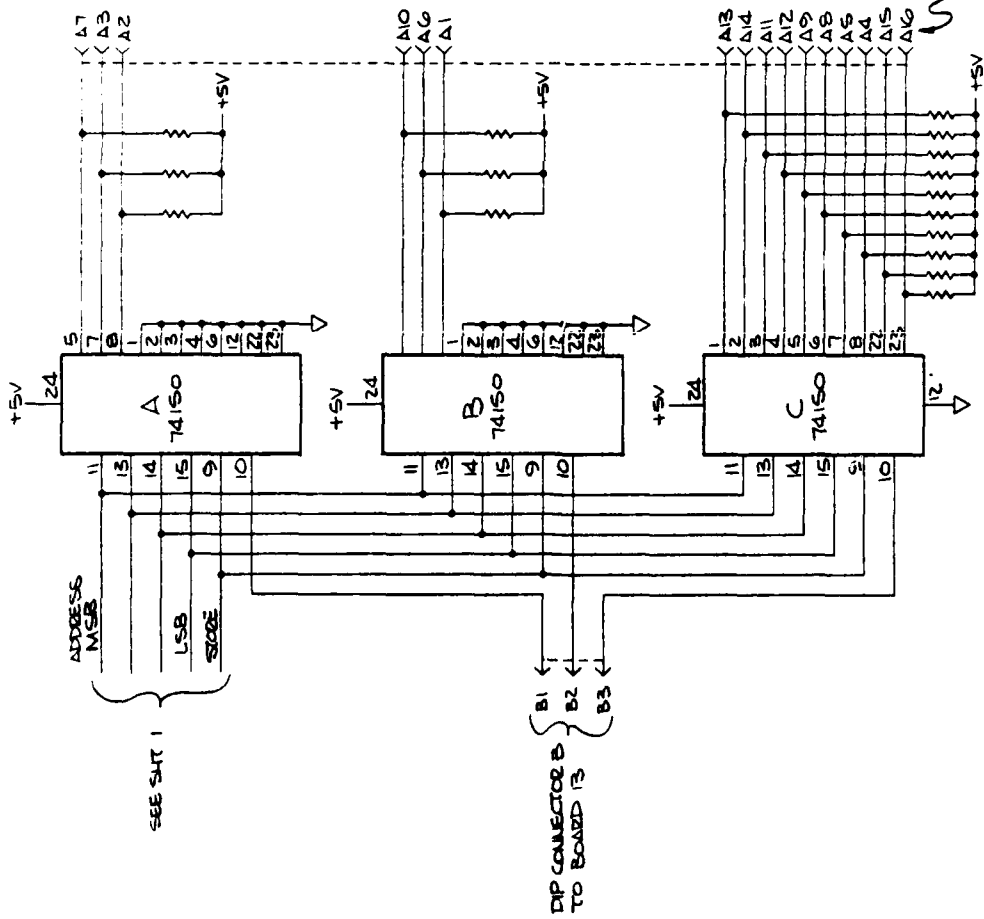
PIN ASSIGNMENT
FOR OEI 5021

1	7	13	19
2	8	14	20
3	9	15	21
4	10	16	22
5	11	17	23
6	12	18	24



FRONT PANEL SWITCH DESIGNATION

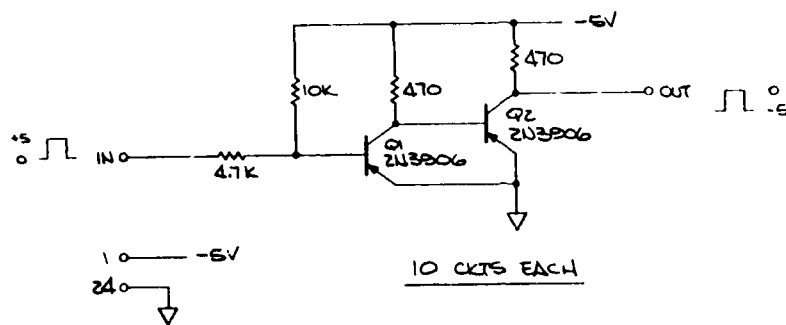
4A-3
2A-3
1A-3



FRONT PANEL SWITCHES

MOON	DAY	YEAR	MOON	WIND	WAVE	WAVE	WAVE
10	15	9	16	41	09	64	910
1A1B	2A2B	3	4A4B	516	71B		

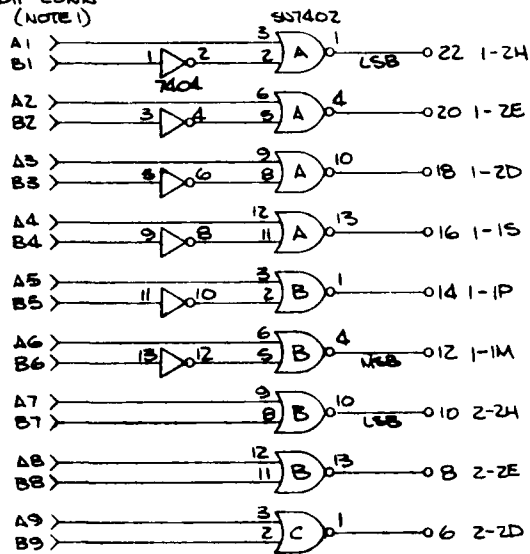
1. ALL RESISTORS 5.1K.



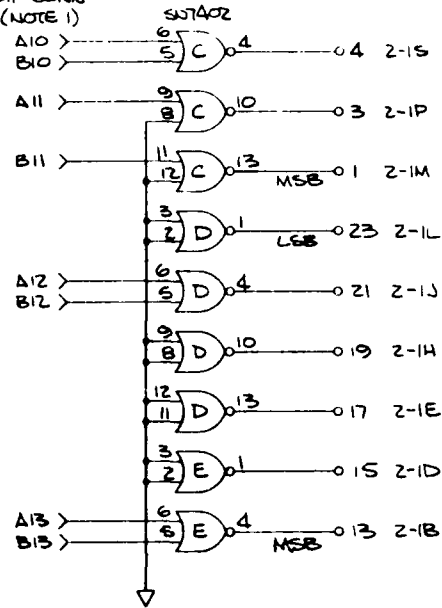
PINS

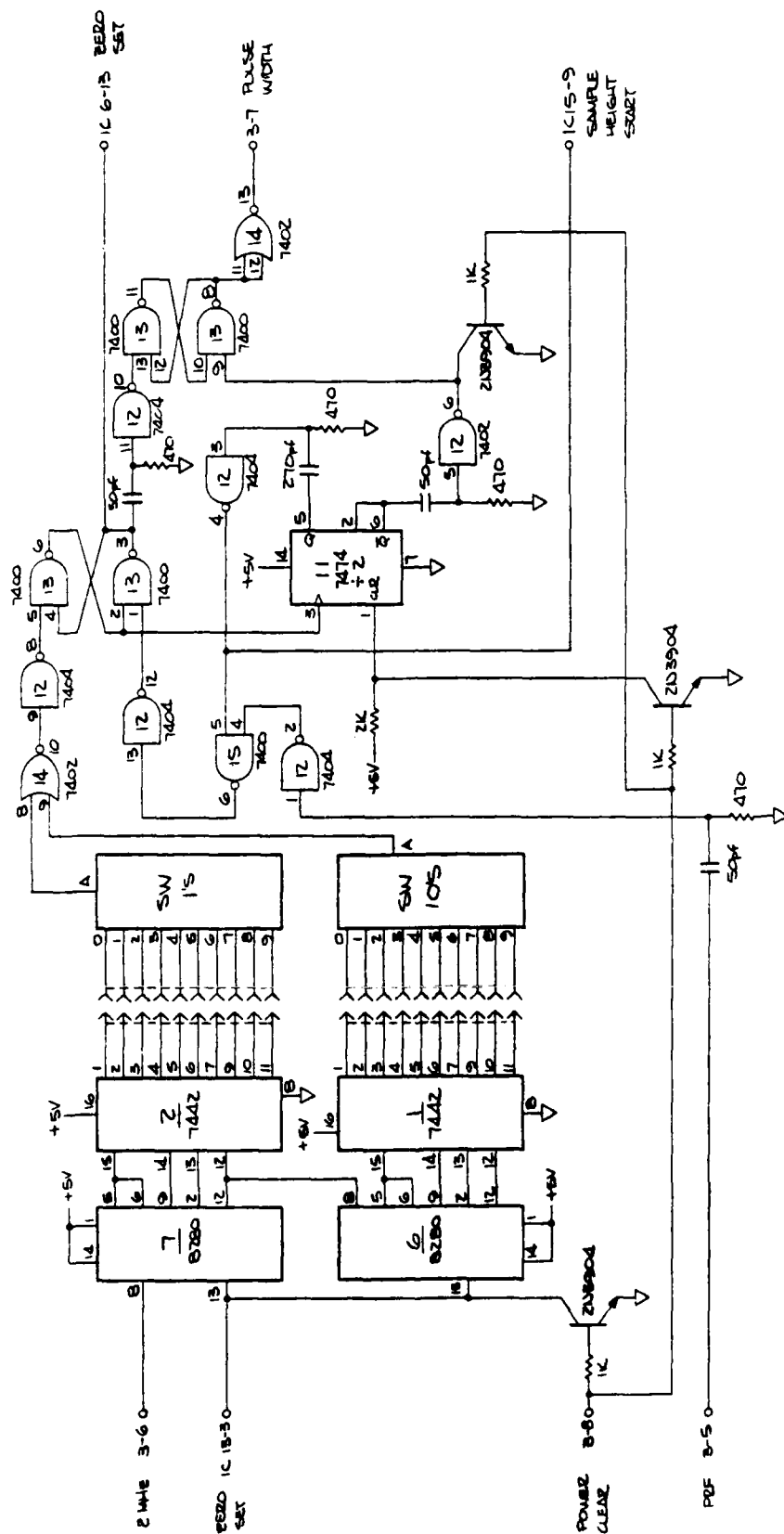
IN	OUT
+	2
+	4
+	6
+	8
+	10
+	12
+	14
+	16
+	18
+	20

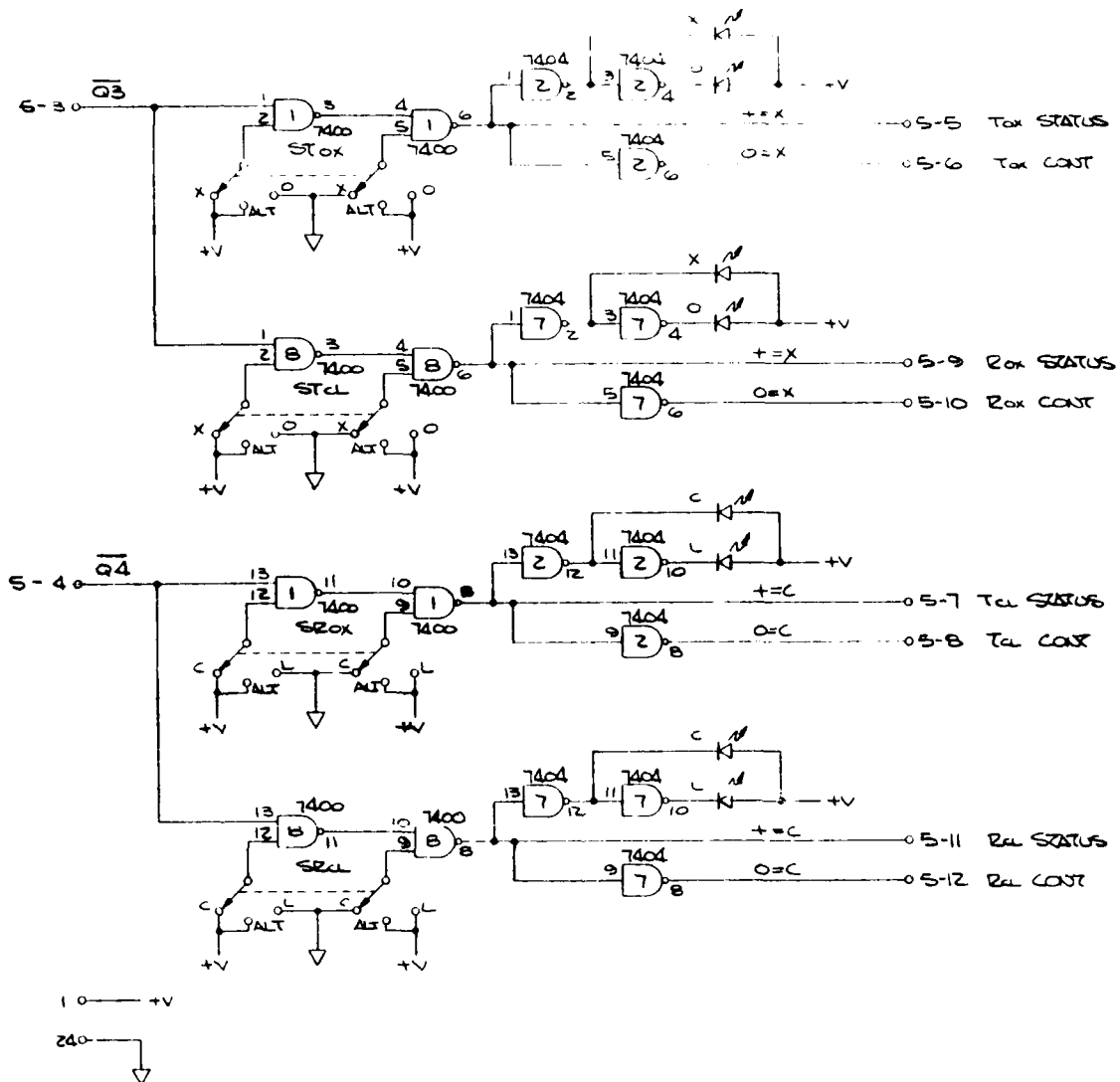
DIP CONN
(NOTE 1)

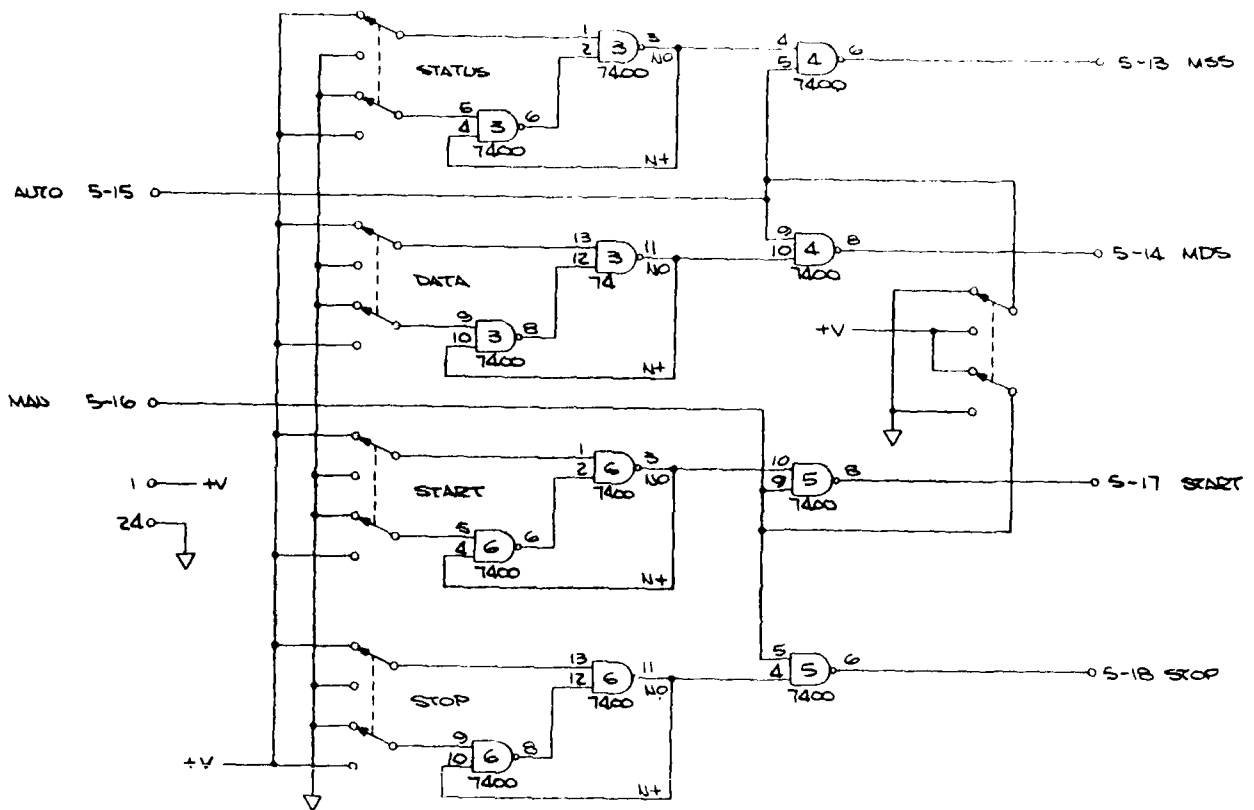


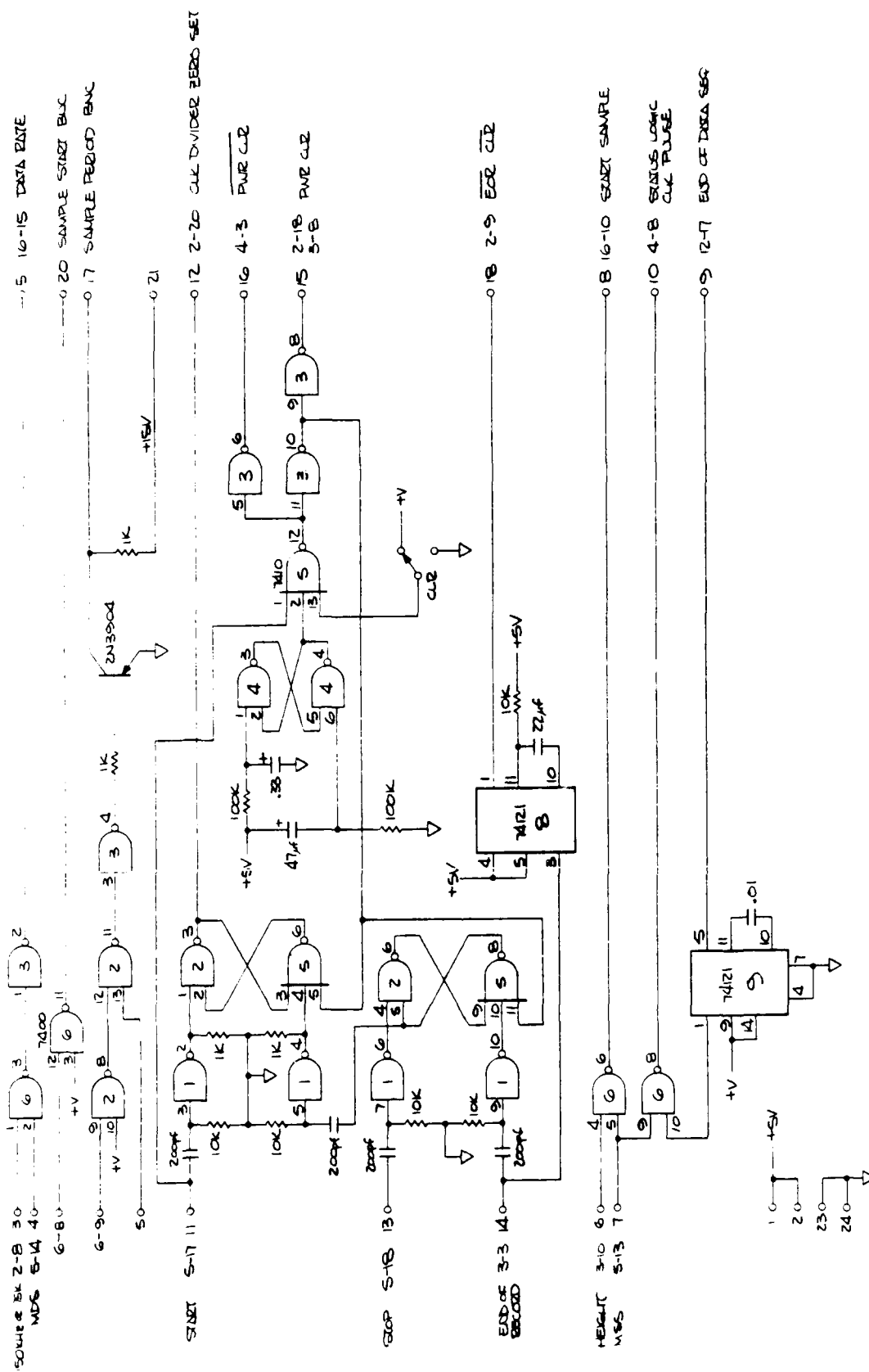
DIP CONN
(NOTE 1)













AD-A095 566

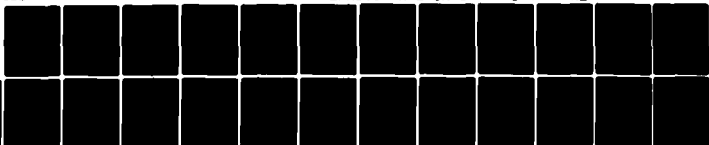
NEW MEXICO STATE UNIV LAS CRUCES PHYSICAL SCIENCE LAB F/G 4/1
D-REGION ELECTRON DENSITY MEASUREMENTS OBTAINED BY PARTIAL REFL--ETC(U)
NOV 80 D MOTT, W GAMMILL, R VALDEZ DAAD07-79-C-0008

UNCLASSIFIED

ERADCOM/ASL-CR-80-0008-4

NL

2 of 2
80-90-01



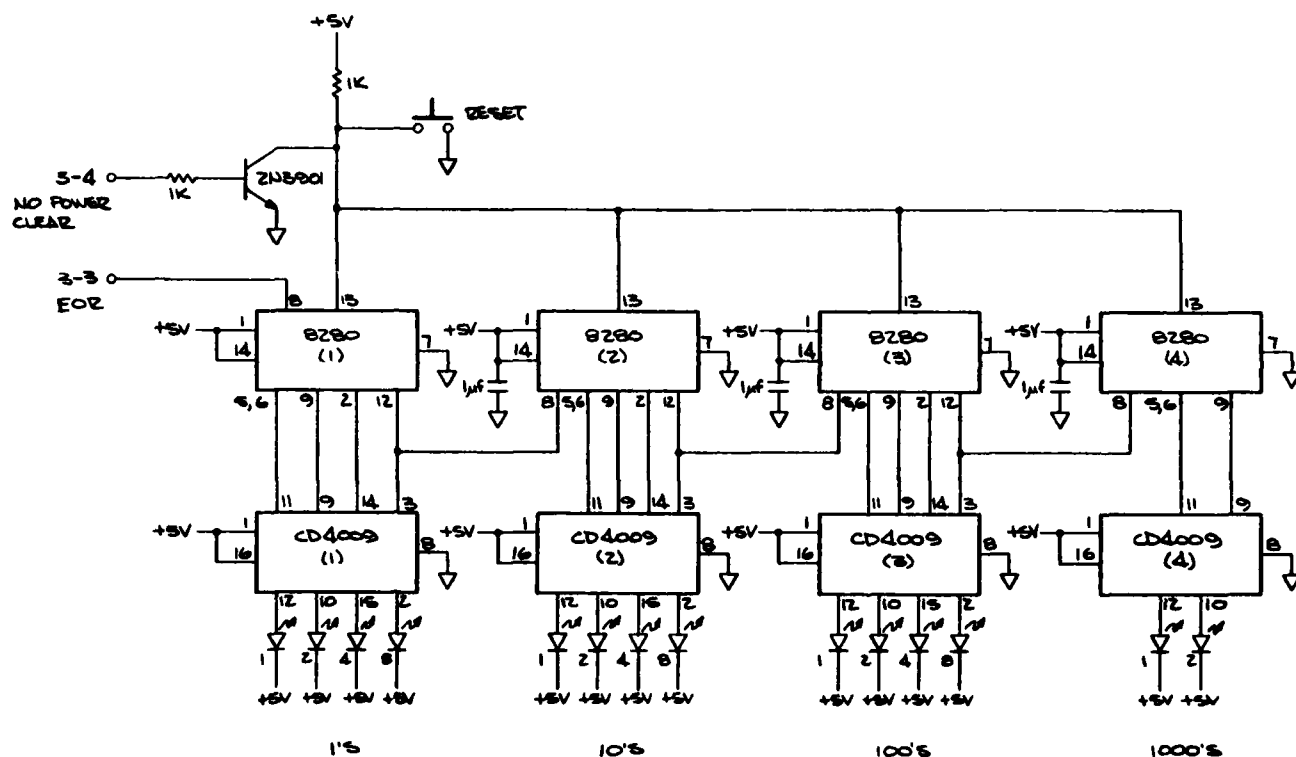
END

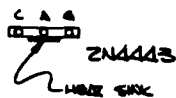
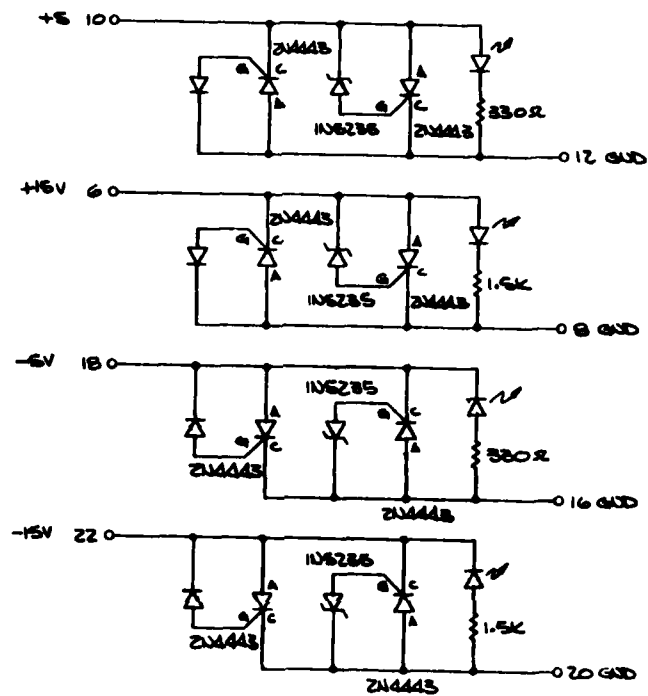
DATE

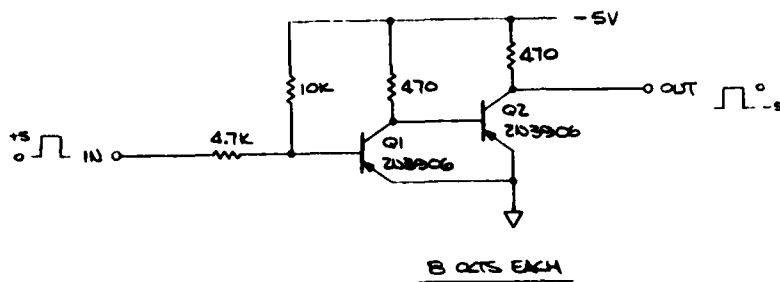
FILED

13-11

DTIC

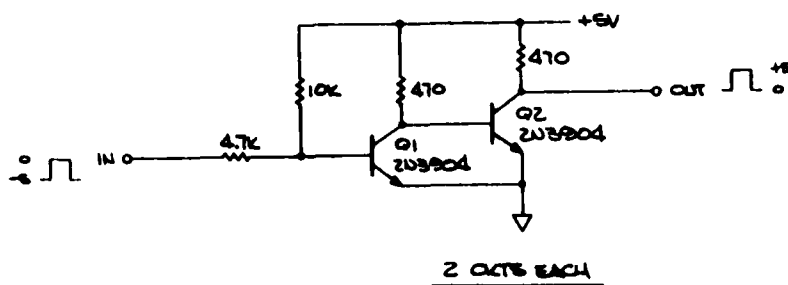




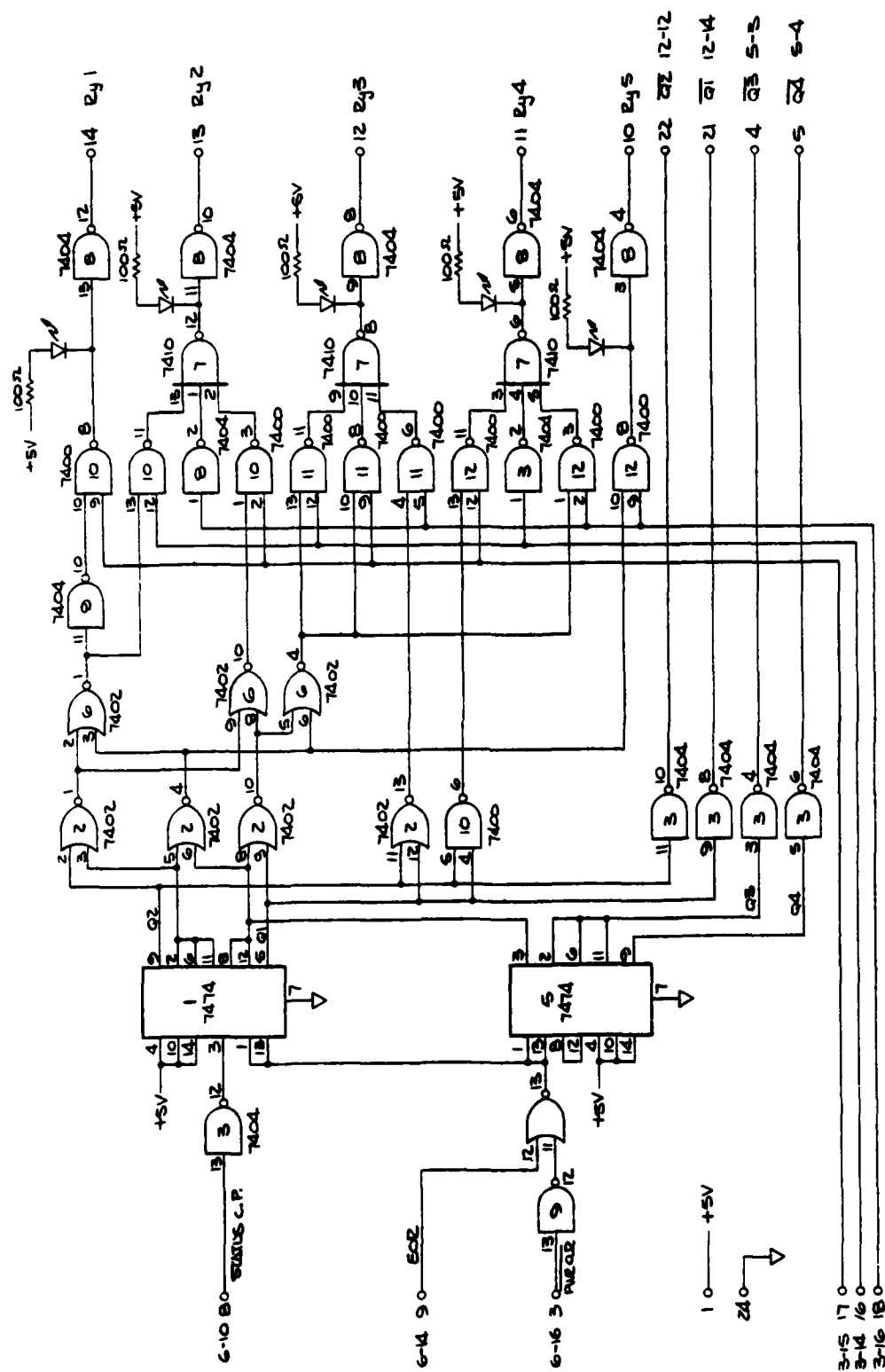


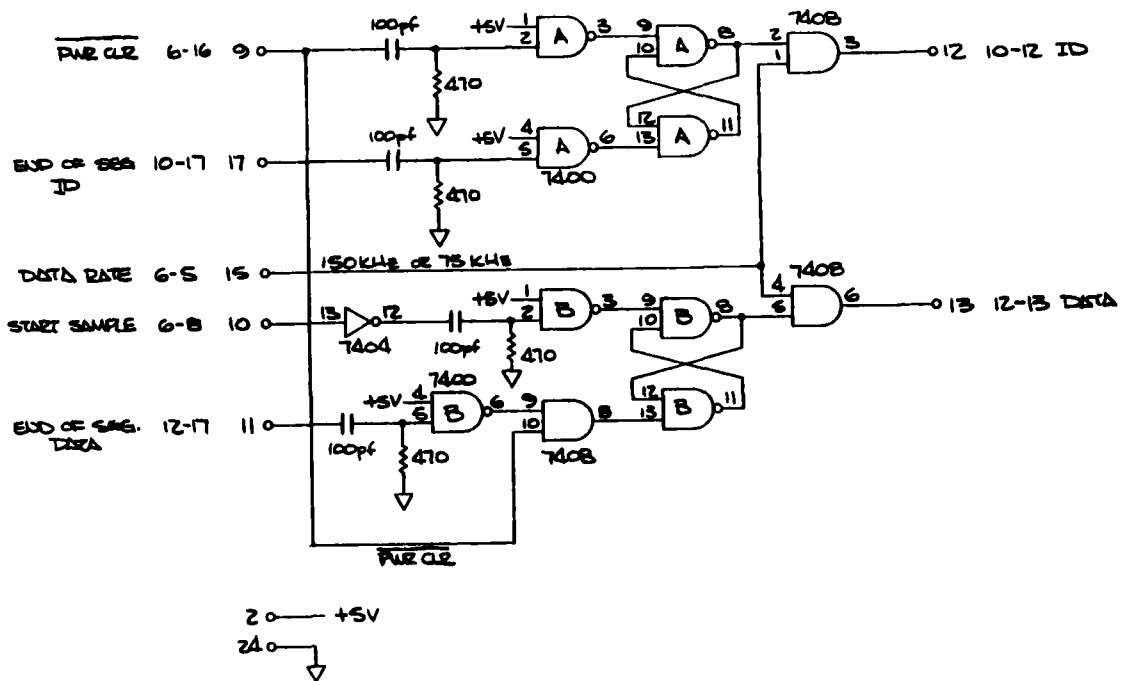
PINS

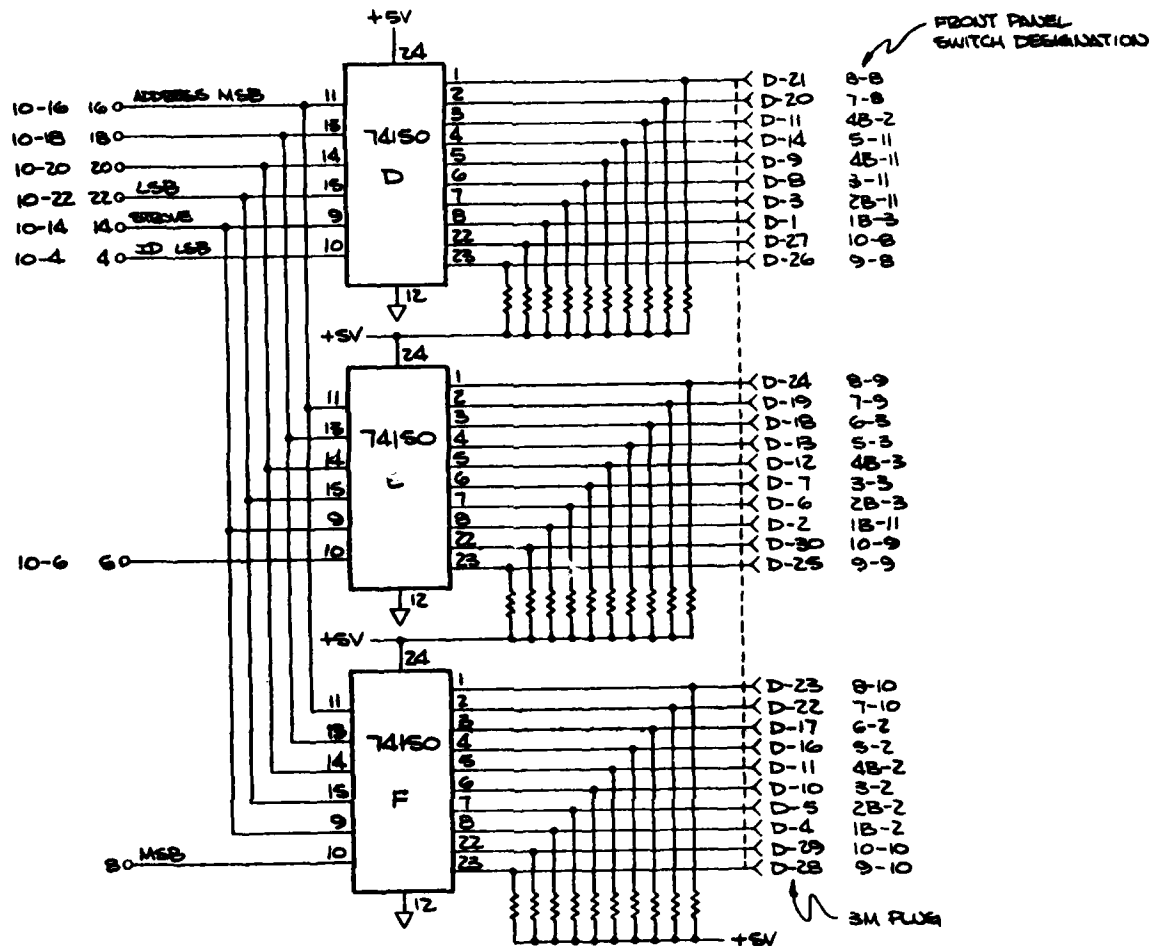
IN	OUT
+	2
+	4
+	6
+	8
+	10
+	12
+	14
+	16
-	18
-	20



1 0 — -5V
 23 0 — +5V
 24 0 —



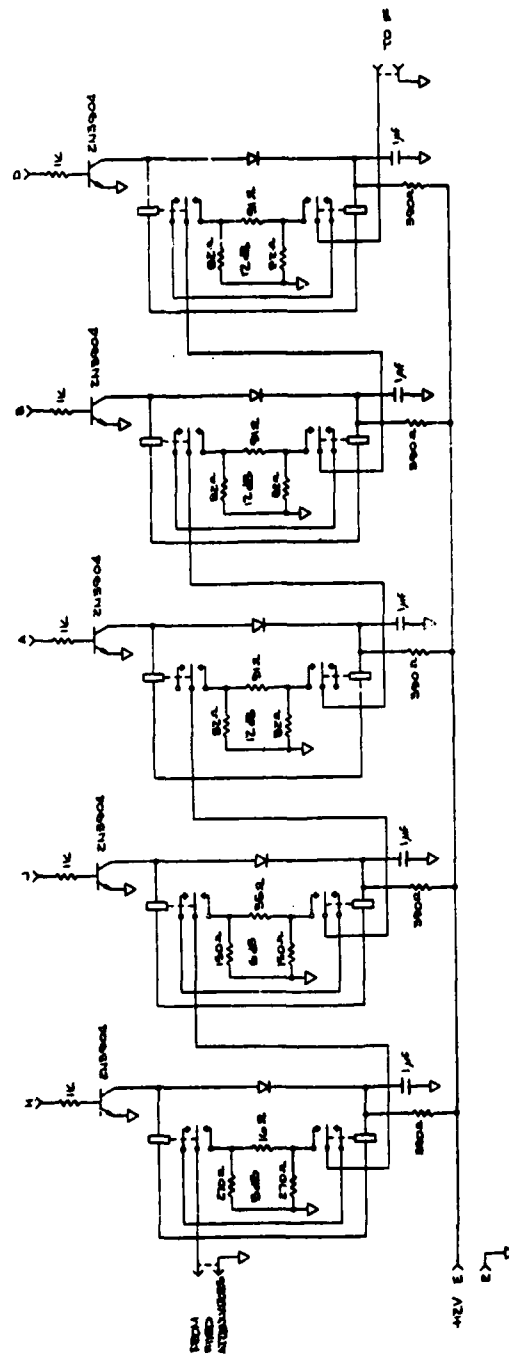




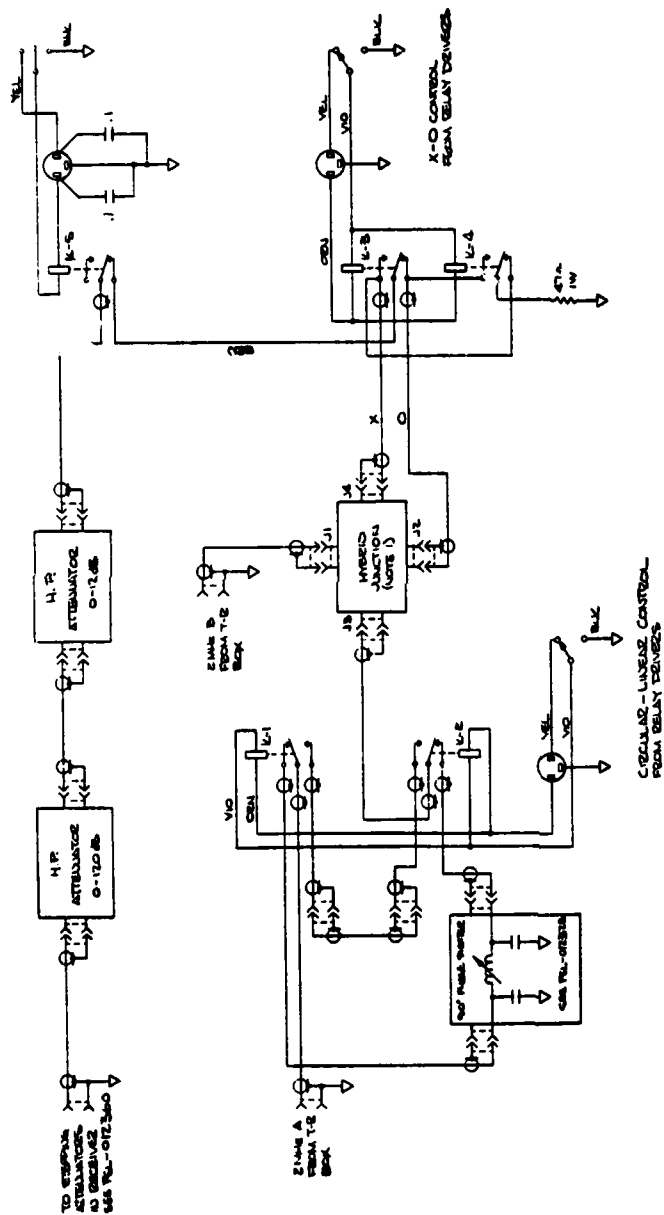
1. ALL RESISTORS 5.1K.

FRONT PANEL SWITCHES

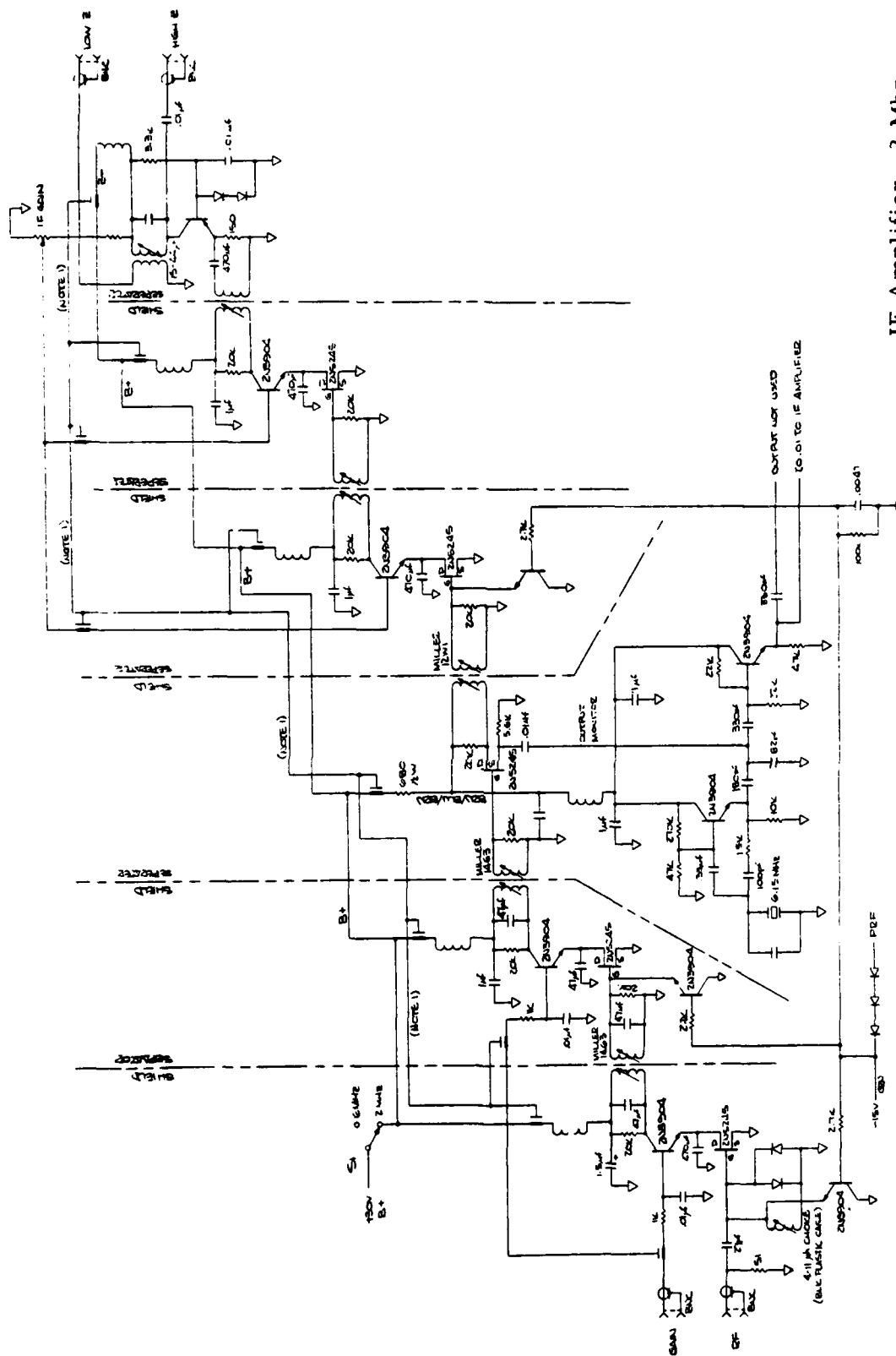
MON	DAY	YEAR	MOSE	MIN	FILE	TAPE
10	15	9	16	41	09	64
1A/1B	2A/2B	3	4A/4B	5/6	7/8	9/10



Receiver Attenuation Section
012360



Receiver Polarization Selector
012361



IF Amplifier, 2 Mhz
012363

2. SAME 'IF' FOR 2.25Mhz. EXCEPT CHANGE RIAL ONE AND RESUME.
1. TAP OFF FEED THRU CAPACITORS ARE COMMON TO ENVELOPE TOP.

APPENDIX II

Averaging Program

This appendix contains a listing of the FORTRAN program used to time-average the data. The program is run at White Sands Missile Range on the UNIVAC 1108 system.

Pages 2-5 contain the main program, named FLOOD. Subroutines INDATA3 and UNPACK are found on pages 6 and 7. Page 8 contains information regarding input cards.

```

C MAIN PROGRAM FLOOD
  INTEGER H
  COMMON MON,MDAY,NHOUR,NMIN
  COMMON/APLO(4,3),JPLO(3,2),KPP,JPP,LPL0(2,2),LPP,ANT(60),WPP,
  IMPOL(3,5),RHT(40),NPOL(3,2)
  COMMON/DATE1,DATE2,DATE3,DATE4,DATE5,DATE6,DATE7
  COMMON/ELD/JFILE,ISTMT,NDHT,JFI
  COMMON/INPUT/IDATA(16,30),NOPAR,ISTAT(16,2),N,ID(12)
  REAL Y
  DIMENSION A(18,30),A2(8,30),S(18,30),S2(8,30),NI(8),NZ(8),NJ(8,30)
  X,NH(30),RX(64),IFILE(30)
  DATA KPL0/6HALL VA,6HLUES ,6H
  1 6HVALUES,6H IN RA,6HNGE ,6H
  2 6HTRE-C,6HORRELA,6HTED VA,6HLUES /
  3 JPLO /6HNOISE ,6HFROM M,6HIN 2
  4 6HNOISE ,6HFROM F,6HIRST 2/
  5 LPL0 /6H(UNSMO,6HOTHFD),6H(SHOOT,6HHED) /
  DATA MPOL/6HSIGNAL,6H PLUS ,6HNOISE
  1 6HSIGNAL,6H PLUS ,6HNOISE
  2 6HSIGNAL,6H
  3 6HSIGNAL,6H AMPLI,6HTUDE
  4 6HSIGNAL,6H AMPLI,6HTUDE /
  DATA NPOL/6HORDINA,6HRY WAV,6HME
  1 6HETRAO,6HORDINA,6HRY WAVE/
  1040 FORMAT (1,FILE',12)
  1502 FORMAT (215,3011)
  1504 FORMAT (813X,F7.4)
  1506 FORMAT (7712X,'NO OF RECORDS USED =',18,9X'MAXI VALUE =',13,9X
  X 'MAX2 VALUE =',12,5X'PARITY CHECK =',18)
  1508 FORMAT (7)
  1509 FORMAT (12X,'COUNTS',//)
  1510 FORMAT (12X,'STANDARD DEVIATIONS',//)
  1511 FORMAT (1//12X,'SHORT RECORD')
  1512 FORMAT (7712X,'ERROR IN RECORD COUNT')
  1514 FORMAT (1//12X,'NO USEABLE RECORDS')
  1516 FORMAT (772X,'AVERAGES USING MAXI',18X'AVERAGES USING MAX2',//)
  1518 FORMAT (14X'RECORD',5X'MONTH',7X'DAY',6X'YEAR',6X'HOUR',14X
  X 'MINUTE',16X'FILE',18X'TAPE')
  1520 FORMAT (1X'RECEIVER CALIBRATION, REL. AMPLITUDE FOR COUNTS
  X 0 TO 63',//)
  1522 FORMAT (1818)
  1524 FORMAT (11X,13,2X,R1F7,3,2X,R1F7,3,11)
  1525 FORMAT (811X,F7.3)
  1544 FORMAT (41S,744,11,215,12)
  1546 FORMAT (11X,' FILE NO. =',13,5X,'STARTING HEIGHT =',13,5X,
  X 'SEGMENT NO. =',13,5X,'RECORDS PER SEGMENT =',19,9X,
  X 'REF. HEIGHT INDEX =',13,12X,'TIME,DATE,COMMENTS:',7A6,
  X 'SOLAR ZENITH ANGLE =',16,6,3,9 RADIANS, OR',17,3,9 DEGREES')
  1547 FORMAT (16,14,24,42,14,'SOLAR ZENITH ANGLE=FR,3,
  X 9H RADIANS 3H0R F8.3,4H DEGREES)
  1548 FORMAT (1//12X,'NO STARTING OR ENDING HEIGHT')
  1599 FORMAT (12X,12(118,2X))
  1605 FORMAT (111)
  1610 FORMAT (12X,'NT',2X,R1F7,1//)
  1611 FORMAT (2X,'N2',2X,R1F7,1//)
  1612 FORMAT (11X,13,2X,R117)

```


1 0152:00Y4 FLOOD

20 JUN 79 PAGE 3

```

115 C      START OF LOOP FOR DATA ACCUMULATION
116 C
117 C      175 CALL IDATA3(ILFILE,NOWORD)
118 C      TEST FOR TAPE EOF: IF YES/NO, (LFILE=1/D
119 C      IF (LFILE.NE.0) GOTO 245
120 C      IF (NOWORD.LT.88) GOTO 520
121 C      NOREC=NOREC+1
122 C      IF (NOREC.EQ.1) PRINT 1599, (ID(1),I=1,12)
123 C      DO 210 J=1,4
124 C      R=J
125 C      195 KI=1
126 C      K2=1
127 C      IF (IDATA(K,IJ,KHT).GT.MAX1) KI=0
128 C      M1J=INT(J/KI)
129 C      IF (IDATA(K,IJ,KHT).GT.MAX2) K2=0
130 C      NZ(J)=NZ(J)+K2
131 C      DO 205 M=1,MM
132 C      IF (INSEG.EQ.1) GOTO 197
133 C      IF (IDATA(K,M).GT.MAX3) N3(J,M)=N3(J,M)+1
134 C      I=IDATA(K,M)+1
135 C      A1(J,M)=A1(J,M)+K1*RX(I)
136 C      A2(J,M)=A2(J,M)+K2*RX(I)
137 C      GOTO 200
138 C      197 A1(J,M)=IDATA(J,M)
139 C      A2(J,M)=IDATA(J,M)
140 C      200 CONTINUE
141 C      205 CONTINUE
142 C      KER=8
143 C      IF ((K.LE.16).AND.(INSEG.NE.1)) GOTO 195
144 C      210 CONTINUE
145 C
146 C      IF (NOREC.LT.NSEG) GOTO 175
147 C
148 C      END OF ACCUMULATION
149 C
150 C      265 PRINT 1506, NOREC,MAX1,MAX2,NOPAR
151 C      PRINT 1508
152 C      PRINT 1522, (ISTAT(K,I),K=1,8)
153 C      PRINT 1522, (TSTAT(K,I),K=9,16)
154 C      IF (NOREC) 525,530,270
155 C      DO 285 M=1,MM
156 C      MH(M)=JSTMT+2*(M-1)
157 C      DO 280 K=1,8
158 C      IF (M1(K).GT.0) A1(K,M)=A1(K,M)/M1(K)
159 C      IF (M2(K).GT.0) A2(K,M)=A2(K,M)/M2(K)
160 C      280 CONTINUE
161 C      285 CONTINUE
162 C      PRINT 1516
163 C      PRINT 1524, (MM,M1,M2,TAT(K,M),K=1,8), (A2(K,M),K=1,8), (H=1,MM)
164 C      IF (IPUN.GT.0) GOTO 400
165 C      PUNCH 1547, (DATE1, IDATE2, IDATE3, Y, DEG
166 C      PUNCH 1525, ((A1(K,M),K=1,8), M=1,MM)
167 C      PUNCH 1547, (DATE1, IDATE2, IDATE3, Y, DEG
168 C      PUNCH 1525, ((A2(K,M),K=1,8), M=1,MM)
169 C      400 CONTINUE
170 C      IF (INSEG.LT.5) GO TO 410
171 C      PRINT 1605

```

```

172 PRINT 1610,(N1(K),K=1,8)
173 PRINT 1611,(N2(K),K=1,8)
174 PRINT 1612,((N1(K),N2(K),K=1,8)),M=1,M=8
175 910 CONTINUE
176 IF (MODREC.EQ.NSEC) GOTO 155
177 NULY = 10
178 DO 590 I=1,90
179   8RT(I)=TSYH*ZRT-2
180   590 ANT(I)=ISTAT+1-1
181   C INITIALIZE PLOTTING
182   IF (IPLT.GT.0) GOTO 591
183   CALL ERTANT9,DAY,DUH)
184   IFL=150
185   KPP=2
186   JPP=1
187   LPP=1
188   MPP=1
189   CALL FPLOT(A2,B,J0)
190   C 591 CONTINUE
191   C
192   C
193   C
194   C
195   GOTO 535
196   520 PRINT 1511
197   GOTO 175
198   525 PRINT 1512
199   GOTO 535
200   530 PRINT 1514
201   535 KFILE=KFILE+1
202   NFILE=NFILE+1
203   IF (IPLT.EQ.0) GOTO 540
204   IF (KFILE.EQ.0) GOTO 999
205   GOTO 145
206   C
207   C
208   C
209   540 CALL MTRANT9,B,IT
210   GOTO 535
211   546 PRINT 1548
212   999 CONTINUE
213   IF (IPLT.EQ.0) CALL MSTR(3)
214   CALL EXIT
215   END

```

S 8152800174 INDATA

```

1 SUBROUTINE IDATA3(LFILE, NOWORD)
2 COMMON /INPUT/IDATA(16, 30), NOPAR, ISTAT(16, 21, N, ID(1,21)
3 DIMENSION JDATA(88)
4 DIMENSION INOLD(1,30)
5 INTEGER MT
6 READ NEW RECORD
7 C
8 CALL NTRAN(1,2,88,JDATA,LSTAT)
9 CALL NTRAN(1,22)
9 C TEST IF EOF OR PARITY ERROR WAS ENCOUNTERED ON TAPE
10 IF (LSTAT(2,11),180,115)
11 110 NOPAR=NOPAR+1
12 115 LFILE = 0
13 DO 120 K = 1, 16
14 DO 120 MT(1:30)
15 120 IDATA(K, MT) = 0
16 NOWORD = 88
17 CALL UNPACK (JDATA, INOLD, 88)
18 DO 150 L=1,12
19 150 ID(L)=INOLD(L)
20 L = 13
21 DO 300 K=1,16
22 DO 200 MT = 1,30
23 IDATA(K,MT)=INOLD(L)
24 L=L+1
25 DO 250 M=1,2
26 ISTAT(K,M)=INOLD(1)
27 L=L+1
28 CONTINUE
29 RETURN
30 LFILE = 1
31 NOWORD = 0
32 KFC = 0
33 RETURN
34 END

```

```

1  SUBROUTINE UNPACK(JDATA,IMOLD,NUM)
2  DIMENSION JDATA(1),IMOLD(1)
3  IC=0
4  DO 100 JMT,NUM
5      IS=0
6      DO 100 I=1,6
7          IC=IC+1
8          IMOLD(IC)=JDATA(I)
9          IS=IS+6
10     CONTINUE
11     RETURN
12     END

```

```

00000100
00000200
00000300
00000400
00000500
00000600
00000700
00000800
00000900
00001000
00001100
00001200

```

Cards inputs to the averaging program

I. Tape control. One card, format 2I5,30I1

<u>Column</u>	<u>Format</u>	<u>Name</u>	<u>Description</u>
1-5	I5	NOFILE	Number of files (N) to skip on the front end of the data tape. Note: the first file contains no data, so "file 1" of data is actually the second file on the tape.
6-10	I5	KFILE	Number of files (M), after the N skipped files, to be considered for processing (including any files <u>not</u> to be processed via flags in the following M columns).
11-40	30I1	IFILE	One digit for each of the M files to be considered; column 11 for the first, column 10+M for the last. Files flagged with a 0 (or blank) will be processed, those with a 1 will be skipped over.

II. Receiver calibration array RX; 64 values on 8 cards, 8 numbers per card, each of format 8(3X,F7.4).

III. Information relating to the files to be processed. One card per file of format 4I5,7A6,I3,2I5,I2.

<u>Column</u>	<u>Format</u>	<u>Name</u>	<u>Description</u>
1-5	I5	JFILE	File number to be printed on the listing.
6-10	I5	ISTHT	Starting height of echo samples.
11-15	I5	NSEG	Number of records per segment.
16-20	I5	IJKHT	Reference height index for noise thresholds.
21-62	7A6	IDATE1 through IDATE7	Date, time, and comments to be printed on listing. Date and time are also used to compute solar zenith angle.
63-65	I3	IPLT	● Plot flag; 0 for plots, 1 for no plots of average amplitudes.
66-70	I5	MAX1	First noise threshold for screening raw data.
71-75	I5	MAX2	Second noise threshold for screening raw data.
76-77	I2	IPUN	● Punch flag; 0 for cards, 1 for no cards containing the average amplitudes. ● Note: we generally do <u>not</u> call for cards or plots.

APPENDIX III

Solar Zenith Angle

Solar zenith angle, which is the angular distance of the sun away from the local vertical, is of importance in this project because of the fact that changes in this angle are generally well correlated with changes in electron density in the D region.

We describe here the simple procedure we have used to estimate solar zenith angle as a function of time and date. (Accuracy of the estimate is sufficient for our purpose.) Parameters required are the latitude of the station site, and a factor based on the time of the most recent autumnal equinox. The computer program ZEN in Figure 2, which is written in APL, performs the required computations. Comments follow that are keyed by number to the line numbers in Figure 2.

The basic calculation involves the spherical triangle on the celestial sphere shown in Figure 1.

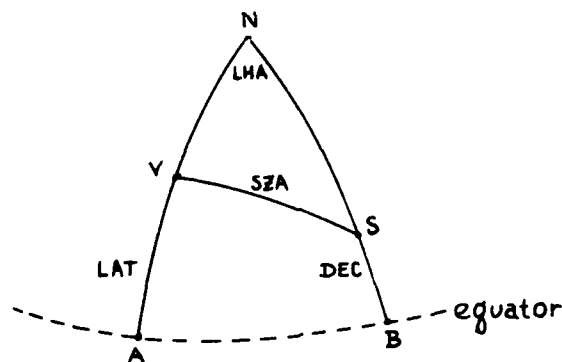


Figure 1. Solar Zenith Angle Triangle.

Vertices N, V, and S of the triangle correspond respectively to projections of the earth's spin axis, local vertical at the station site, and the line from earth to sun. The dotted line is the projection of the earth's equatorial plane.

Angle LAT (between points A and V) is the station latitude, LHA (between sides NV and NS) is the local hour angle, DEC (between points S and B) is the solar declination, and SZA (between points V and S) is the desired solar zenith angle.

Angle LHA grows uniformly with time at the rate of 360° per day, and is zero at local noon. Small uncertainties exist here because of the fact that $LHA = 0$ does not generally occur at precisely noon local time, and may occur as much as 10 or 15 minutes before or after noon. However, the corresponding uncertainty in solar zenith angle is, for our purpose, negligible. Note that one should always employ local standard time and not daylight-savings time!

Angle DEC is a sinusoidal function of time, with an amplitude of 23.5° and a period of one year. It is zero at the equinoxes, and changes from negative to positive at the autumnal equinox. (Figure 1 shows a positive DEC.)

Angle SZA is found using this standard equation of spherical trigonometry:

$$\cos SZA = \sin LAT \cdot \sin DEC + \cos LAT \cdot \cos DEC \cdot \cos LHA. \quad (1)$$

Program comments (for Figure 2)

6. As described in the comments of line 1-5, BASE is to be set to the time interval in hours between the autumnal equinox preceding the time of interest and 00:00 of the subsequent 1 October (all times local standard time). The value of BASE given here is for the autumnal equinox of 1977 which occurred at 20:30 mountain standard time on 22 September 1977. From this event to 00:00 hours of 23 September is 3.50 hours, and from 00:00 of 23 September to 00:00 hours of 1 October is $24 \cdot 8 = 192$ hours: Thus, $BASE = 3.50 + 192 = 195.5$ hours. (See Table 1 for other BASE values.)

7. Our station, at WSMR, is located at $32^\circ 24'$ north latitude. (At the Ontario, Canada site, the latitude was $51^\circ 5'$.)

8. Days per month from October 1977 through September 1978, inclusive. The time of interest must occur in one of these months.

9. Conversion of latitude in degrees, minutes, and seconds to radians.

10.-13. Month, day, hour, and minute of the time of interest. Note that these 4 values are entered into the argument of the call-statement for program ZEN.

14. This statement converts the month value from the calendar scale in which 1 = January to the "fiscal" scale in which 1 = October.

15. Month is converted into total elapsed days; 0 for October, 31 for November, 61 for December, 92 for January, etc.

16. Using the result from line 15, the time of interest is converted into the number of hours (Δt) from the autumnal equinox to the time of interest.

17. SUN is an angle proportional to Δt :

$$\text{SUN} = 2\pi \cdot (\Delta t \text{ hours}) \div (\text{number of hours in one year}) \quad \text{radians}$$

18. Local hour angle LHA:

$$\text{LHA} = 2\pi \cdot (\text{hour of day} - 12 \text{ hours}) \div 24 \text{ hours} \quad \text{radians}$$

19. The solar declination (DEC) is 23.5° times the sine of angle SUN (from line 17). SDEC is the sine of DEC.

20. CDEC is the cosine of DEC.

21. Solar zenith angle computed via Eq. (1) above.

22. Printout of solar zenith angle.

Table 1. Base values for zenith angle calculations.

Values applicable for WSMR; mountain standard time.

<u>from</u>	<u>to</u>	<u>base</u>
Oct 1974	Sept 1975	189.00 hours
Oct 1975	Sept 1976	183.05
Oct 1976	Sept 1977	201.18
Oct 1977	Sept 1978	195.50
Oct 1978	Sept 1979	189.57
Oct 1979	Sept 1980	183.71

APPENDIX IV

Receiver Calibration

The receiver used in the partial reflection sounder is calibrated by applying the cw signal from an rf signal generator to the receiver input and observing the digitized values of output signal strength vs. input amplitude (see Section 5.5). The receiver should be calibrated following any adjustment that could influence its sensitivity, or after any period of time (weeks, typically) in which the sensitivity might drift.

In practice, digitized values obtained in the calibration show a small random fluctuation with time, and so the average of many values is used in each case. With constant input to the receiver, the digitized signal strength is recorded on magnetic tape for several minutes in the same format as reflection data, and the program used to average the reflection data is also used to average the calibration data. A "run" of calibration data is identified with a particular input level.

Table 1 shows typical results of input signal amplitude (in microvolts) vs. average counts. Each change in input voltage corresponded to a 1 dB change in input power. The dBm input values are included in the table only for reference, and play no part in the calibration procedure.

We assume that input amplitudes S_i from the signal generator can be expressed as a function of average counts C_i , with the relationship being of the polynomial form

$$S_i = \sum_{j=0}^3 A_j (C_i)^j, \quad (1)$$

where A_0 , A_1 , A_2 , and A_3 are constants. Best values of the (over determined) constants are found using the method of least squares. For the values in Table 1, best values are as follows:

TABLE 1. TYPICAL RECIEVER CALIPRATION DATA

<u>Power input to receiver from signal generator, dBm</u>	<u>Input amplitude (S), microvolts*</u>	<u>Average digitized count (C) at receiver output</u>
-97	3.158	57.97
-98	2.815	48.06
-99	2.509	39.51
-100	2.236	32.43
-101	1.993	26.23
-102	1.776	24.05
-103	1.583	19.63
-104	1.411	16.13
-105	1.257	13.74
-106	1.121	11.35
-107	0.998	9.63
-108	0.890	8.09
-109	0.793	7.05
-110	0.707	6.03
-111	0.630	5.14
-112	0.562	4.10
-113	0.500	3.38
-114	0.446	2.72
-115	0.398	2.09
-116	0.354	1.54
-117	0.316	0.99

*Input amplitude is computed from input power, and not measured.
It is the input power that is measured.

$$\begin{aligned}A_0 &= 0.21990 \\A_1 &= 0.088315 \\A_2 &= -0.0010286 \\A_3 &= 6.5537 \times 10^{-6}.\end{aligned}$$

When it comes to reducing the partial-reflection data, we require the ratio of received amplitudes; extraordinary-mode amplitude divided by ordinary-mode amplitude. It is by means of the receiver calibration "curve" that average digital counts, which constitute the data, are converted into corresponding signal amplitude. Any linear factor introduced into the calibration will cancel in the ratio. Thus, and only for convenience, we scale the constants so that a maximum count of 63 corresponds to an amplitude of 63 (units arbitrary). After each constant is multiplied by the appropriate scale factor, these values obtain:

$$\begin{aligned}A_0 &= 4.1480 \\A_1 &= 1.6659 \\A_2 &= -0.019404 \\A_3 &= 1.2362 \times 10^{-4}.\end{aligned}$$

If we use these constants in Equation (1), signal amplitude (S) as a function of count (C) is as shown in Table 2. To use this calibration, the 64 values in the "S"-columns of Table 2 are entered into the data reduction program (Appendix II) as the array RX.

TABLE 2. TABULATED RECEIVER CALIBRATION "CURVE" OBTAINED FROM CALIBRATION DATA OF TABLE 1

<u>Count (C)</u>	<u>Amplitude (S)</u>	<u>(C)</u>	<u>(S)</u>
0	0.0000	32	41.6391
1	5.7947	33	42.4355
2	7.4032	34	43.2176
3	8.9745	35	43.9862
4	10.5091	36	44.7419
5	12.0080	37	45.4855
6	13.4717	38	46.2177
7	14.9011	39	46.9393
8	16.2968	40	47.6510
9	17.6597	41	48.3536
10	18.9905	42	49.0478
11	20.2898	43	49.7343
12	21.5585	44	50.4139
13	22.7974	45	51.0874
14	24.0070	46	51.7554
15	25.1882	47	52.4187
16	26.3418	48	53.0781
17	27.4684	49	53.7343
18	28.5688	50	54.3881
19	29.6437	51	55.0401
20	30.6940	52	55.6911
21	31.7202	53	56.3419
22	32.7232	54	56.9932
23	33.7038	55	57.6457
24	34.6626	56	58.3003
25	35.6004	57	58.9575
26	36.5179	58	59.6183
27	37.4159	59	60.2832
28	38.2951	60	60.9531
29	39.1563	61	61.6287
30	40.0002	62	62.3108
31	40.8276	63	63.0000

APPENDIX V

Polynomial Approximations For $C_{3/2}(x)$ and $C_{5/2}(x)$

The functions are defined by this integral:

$$C_p(x) = \frac{1}{p!} \int_0^{\infty} \frac{\varepsilon^p}{\varepsilon^2 + x^2} \exp(-\varepsilon) d\varepsilon$$

The integral can be approximated by a polynomial with a high degree of accuracy, for the required range of x as shown by Burke and Hara (9). For the integral $C_{3/2}(x)$,

$$C_{3/2}(x) = \frac{x^4 + a_3 x^3 + a_2 x^2 + a_1 x + a_0}{x^6 + b_5 x^5 + b_4 x^4 + b_3 x^3 + b_2 x^2 + b_1 x + b_0}$$

where

$$\begin{aligned} a_0 &= 2.3983474 \times 10^{-2} \\ a_1 &= 1.1287513 \times 10 \\ a_2 &= 1.1394160 \times 10^2 \\ a_3 &= 2.4653115 \times 10 \\ b_0 &= 1.8064128 \times 10^{-2} \\ b_1 &= 9.3877372 \\ b_2 &= 1.4921254 \times 10^2 \\ b_3 &= 2.8958085 \times 10^2 \\ b_4 &= 1.2049512 \times 10^2 \\ b_5 &= 2.4656819 \times 10 \end{aligned}$$

For the integral $C_{5/2}(x)$,

$$C_{5/2}(x) = \frac{x^3 + a_2 x^2 + a_1 x + a_0}{x^5 + b_4 x^4 + b_3 x^3 + b_2 x^2 + b_1 x + b_0}$$

where

$$a_0 = 1.1630641$$

$$a_1 = 1.6901002 \times 10$$

$$a_2 = 6.6945939$$

$$b_0 = 4.3605732$$

$$b_1 = 6.4093464 \times 10$$

$$b_2 = 6.8920505 \times 10$$

$$b_3 = 3.5355257 \times 10$$

$$b_4 = 6.6314497$$

